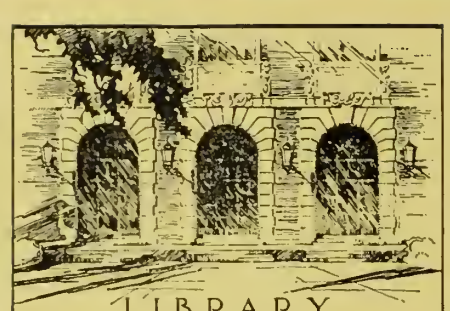

LIBRARY
OF THE
UNIVERSITY
OF ILLINOIS

510.84
Il6r
no. 243-249
cop. 2

The person charging this material is responsible for its return on or before the **Latest Date** stamped below.

Theft, mutilation, and underlining of books are reasons for disciplinary action and may result in dismissal from the University.

UNIVERSITY OF ILLINOIS LIBRARY AT URBANA-CHAMPAIGN

MAR 13 1972

FEB 16 RECD

L161— O-1096

Digitized by the Internet Archive
in 2013

http://archive.org/details/threeparticleeff248jord

510.84
I26N
.no.248

Report No. 248

Math.

THREE PARTICLE EFFECTS IN THE PAIR DISTRIBUTION FUNCTION FOR He^4 GAS

by

Harry F. Jordan

September 25, 1967

THE LIBRARY OF THE
AUG 15 1968
UNIVERSITY OF ILLINOIS

DEPARTMENT OF COMPUTER SCIENCE · UNIVERSITY OF ILLINOIS · URBANA, ILLINOIS

Report No. 248

THREE PARTICLE EFFECTS IN THE PAIR DISTRIBUTION FUNCTION FOR He^4 GAS*

by

Harry F. Jordan

September 25, 1967

Department of Computer Science
University of Illinois
Urbana, Illinois 61801

*This work was supported in part by the Atomic Energy Commission and was submitted in partial fulfillment of the requirements for the degree of Doctor of Philosophy in Physics, September 1967.

ACKNOWLEDGMENT

The author wishes to thank Professor Lloyd D. Fosdick whose professional guidance and encouragement were indispensable in preparing this work. Thanks for support in preparation of the manuscript is due to the Department of Computer Science and in particular to Mrs. Gayanne Carpenter and Mrs. Frieda Anderson who typed the text. The author also wishes to express gratitude to his wife whose personal support and encouragement did much to lighten the burden of preparation.

TABLE OF CONTENTS

		Page
ACKNOWLEDGEMENT		iii
LIST OF TABLES		v
LIST OF FIGURES		vi
1.	INTRODUCTION	1
2.	THEORY OF THE PAIR DISTRIBUTION FUNCTION	3
2.1	Definition of the Pair Distribution Function in Terms of the Density Matrix	3
2.2	The Effect of Spin and Statistics on the Density Matrix	6
2.3	Cluster Expansion for the Pair Distribution Function	9
3.	PATH INTEGRAL FORMULATION FOR THE DENSITY MATRIX	18
3.1	Expression of Density Matrix Elements in Terms of Wiener Integrals	18
3.2	Upper Bounds on Off-Diagonal Matrix Elements	23
3.3	Approximation of the Diagonal Matrix Element by a Multiple Riemann Integral	26
4.	EVALUATION OF $g_1(r_{12})$	37
4.1	The Multiple Integral Approximation for $g_1(r_{12})$	37
4.2	Monte Carlo Evaluation of the Multiple Integrals	49
4.3	Integration over the Position of the Third Particle	62
5.	NUMERICAL RESULTS	75
5.1	Results and Accuracy Considerations	75
5.2	Numerical Comparisons with Theory and Experiment	85
5.3	Conclusion	97
LIST OF REFERENCES		99
APPENDIX A		102
APPENDIX B		105
VITA		129

LIST OF TABLES

Table		Page
1.1	Numerical Values of $\lambda^{-3}g_c(r_{12};20,000)$, $\lambda^{-3}g_e(r_{12};20,000)$, and $W_2(r_{12})$ for T = 5°K.	110
1.2	Numerical Values of $\lambda^{-3}g_c(r_{12};20,000)$, $\lambda^{-3}g_e(r_{12};20,000)$, and $W_2(r_{12})$ for T = 10°K. . . .	111
1.3	Numerical Values of $\lambda^{-3}g_c(r_{12};20,000)$, $\lambda^{-3}g_e(r_{12};20,000)$, and $W_2(r_{12})$ for T = 20°K. . . .	112
1.4	Numerical Values of $\lambda^{-3}g_c(r_{12};20,000)$, $\lambda^{-3}g_e(r_{12};20,000)$, and $W_2(r_{12})$ for T = 30°K. . . .	113
1.5	Numerical Values of $\lambda^{-3}g_c(r_{12};20,000)$, $\lambda^{-3}g_e(r_{12};20,000)$, and $W_2(r_{12})$ for T = 40°K. . . .	114
1.6	Numerical Values of $\lambda^{-3}g_c(r_{12};20,000)$, $\lambda^{-3}g_e(r_{12};20,000)$, and $W_2(r_{12})$ for T = 50°K. . . .	115
1.7	Numerical Values of $\lambda^{-3}g_c(r_{12};20,000)$, $\lambda^{-3}g_e(r_{12};20,000)$, and $W_2(r_{12})$ for T = 75°K. . . .	116
1.8	Numerical Values of $\lambda^{-3}g_c(r_{12};20,000)$, $\lambda^{-3}g_e(r_{12};20,000)$, and $W_2(r_{12})$ for T = 100°K. . . .	117
1.9	Numerical Values of $\lambda^{-3}g_c(r_{12};20,000)$, $\lambda^{-3}g_e(r_{12};20,000)$, and $W_2(r_{12})$ for T = 273.18°K. .	118
2	Numerical Values of the Third Virial Coefficient C(T) and the Cluster Integral b_2	119

LIST OF FIGURES

Figure		Page
1	Center-of-mass and relative coordinates for 3 particles	38
2	$f_{13}(r_{12},\underset{\sim}{Q})\times f_{23}(r_{12},\underset{\sim}{Q})$ as a function of $\underset{\sim}{Q}$ for $r_{12} = 1.1\sigma$ and $T = 20^{\circ}K$.	66
3	$\lambda^{-3}g_1(r_{12};20,000)$ as a function of r_{12}/σ and T.	76
4	Computed third virial coefficient as a function of temperature	77
5	$\lambda^{-3}g_1$ and sampling error for $T = 5^{\circ}K$.	79
6	$\lambda^{-3}g_1$ and sampling error for $T = 20^{\circ}K$.	80
7	$\lambda^{-3}g_1$ and sampling error for $T = 75^{\circ}K$.	81
8	$\lambda^{-3}g_1$ and sampling error for $T = 273.18^{\circ}K$. . . .	82
9	Comparison of $\lambda^{-3}g_1$ with classical and semi-classical values for $T = 5^{\circ}K$.	87
10	Comparison of $\lambda^{-3}g_1$ with classical and semi-classical values for $T = 10^{\circ}K$.	88
11	Comparisons of $\lambda^{-3}g_1$ with classical and semi-classical values for $T = 20^{\circ}K$.	89
12	Comparison of $\lambda^{-3}g_1$ with classical and semi-classical values for $T = 50^{\circ}K$.	90
13	The pair distribution function for average density $\rho_o = .095$ gm/cc.	92
14	The pair distribution function for average density $\rho_o = .184$ gm/cc.	93
15	The pair distribution function as a function of temperature for $\rho_o = .184$ gm/cc.	94
16	Comparison of claculated third virial coefficient with classical and experimental values	96

LIST OF FIGURES (Continued)

Figure		Page
17	$\lambda^{-3}g_1$ and sampling error for T = 5°K.	120
18	$\lambda^{-3}g_1$ and sampling error for T = 10°K.	121
19	$\lambda^{-3}g_1$ and sampling error for T = 20°K.	122
20	$\lambda^{-3}g_1$ and sampling error for T = 30°K.	123
21	$\lambda^{-3}g_1$ and sampling error for T = 40°K.	124
22	$\lambda^{-3}g_1$ and sampling error for T = 50°K.	125
23	$\lambda^{-3}g_1$ and sampling error for T = 75°K.	126
24	$\lambda^{-3}g_1$ and sampling error for T = 100°K.	127
25	$\lambda^{-3}g_1$ and sampling error for T = 273.18°K. . . .	128

THREE PARTICLE EFFECTS IN THE PAIR DISTRIBUTION FUNCTION FOR He^4 GAS

Harry Frederick Jordan, Ph.D.
Department of Physics
University of Illinois, 1967

The diagonal elements of the 3-particle density matrix for He^4 have been formulated in terms of Wiener functional integrals in order to compute both that part of the pair distribution function linear in the density and the third virial coefficient. The 3-particle interaction energy was taken to be a sum of Lennard-Jones (12-6) potentials between pairs of particles. Evaluation of the Wiener integrals was carried out by a Monte Carlo sampling technique to yield the pair distribution function and third virial coefficient for temperatures from $273^{\circ}K$ to $5^{\circ}K$. Comparison of the linear portion of the density expansion of the pair distribution function gave qualitative agreement with experimental values for the pair distribution function in liquid He^4 measured by neutron diffraction. The values of the third virial coefficient calculated by this method are consistently smaller than the experimental values and consistently larger than the classical values of this quantity over the given temperature range.

1. INTRODUCTION

In the past helium gas has been a common substance for use in the comparison with experiment of the results of theoretical models and techniques in quantum statistical mechanics. At the time quantum theory began to be well understood the statistical mechanical theory of gases had developed further than the theory of either solids or liquids. The use of helium as a test substance arose due to the fact that of the monatomic gases, for which the application of statistical mechanics presents the least complexity, helium is the only one having small enough atomic weight to exhibit sizeable quantum effects in its thermodynamic properties at moderate experimental temperatures and pressures.

The second virial coefficient B(T) has received a great deal of attention, and calculations of B(T) have been made using several different forms of the intermolecular potential (for a survey of much of this work see Hirshfelder, Curtis, and Bird [1]). The two methods most frequently applied to the calculation of B(T) are the expression of B(T) in terms of the phase shifts of 2-particle collision theory and the expansion of B(T) about the classical limit as a power series in Planck's constant h (the Wigner-Kirkwood expansion). The latter method is useful only for high temperatures since the series converges slowly, if at all, for temperatures less than about $40^{\circ}K$ in He^4.

Few quantum mechanical calculations have been made for higher order virial coefficients. Larsen [2] and Pais and Uhlenbeck [3] have done work on the third virial coefficient. Both calculations have made use of the binary collision expansion of Lee and Yang [4], for which the convergence properties are not well understood. The Wigner-Kirkwood expansion is applicable to systems of more than two particles and can thus be used to compute higher order virial coefficients, but the calculations are more complex, and the convergence difficulties are the same as in the 2-particle case. The phase shift approach, of course, is only valid for quantities which may be expressed in terms of 2-body collision theory.

Recently two calculations of the trace of the 2-particle density matrix, a 2-body property more general than the second virial, have been made in ways which admit of generalization to the N-particle problem for $N > 2$. One of these [5] involves the numerical calculation of the eigenfunctions and eigenvalues of the Schrödinger equation for the relative coordinate and explicit evaluation of the sum over states involved in the density matrix. The other [6] makes use of a path integral formulation for the quantum mechanical density matrix and a Monte Carlo evaluation of the multiple integrals which arise in the evaluation of these path integrals. This thesis concerns the application of the latter method to the 3-particle problem in order to evaluate both the 3-particle term in the pair distribution function and the third virial coefficient.

2. THEORY OF THE PAIR DISTRIBUTION FUNCTION

2.1 Definition of the Pair Distribution Function in Terms of the Density Matrix

To clarify the mathematical model to be used for He^4 we assume that the system of interest is a gas of N identical particles in a volume V in the limit as $N, V \to \infty$ with $n = N/V$ held constant. The particles, the coordinates of which are denoted by $\underset{\sim}{i}$, $i=1,2,\ldots,N$, are assumed to interact by means of an additive, spherically symmetric pair potential $V(r_{ij})$, where $r_{ij} = |\underset{\sim}{i}-\underset{\sim}{j}|$, so that the interaction energy for the N-particle system is

$$U(\underset{\sim}{1},\underset{\sim}{2},\ldots,\underset{\sim}{N}) = \frac{1}{2} \sum_{i \neq j} V(r_{ij}). \tag{2.1.1}$$

In the numerical calculations the potential function will be taken to be the Lennard-Jones (12-6) potential

$$V(r) = 4\kappa\left[\left(\frac{\sigma}{r}\right)^{12} - \left(\frac{\sigma}{r}\right)^{6} \right], \tag{2.1.2}$$

where $\kappa = 14.04 \times 10^{-16}$ erg and $\sigma = 2.56 \times 10^{-8}$ cm. This potential is taken because it is computationally simple and gives almost as good a fit to second virial coefficient data, at least, as any of the other potentials proposed for He^4. The constants κ and σ are taken after de Boer and Michels [7] to give a good fit to high temperature second virial coefficients. The assumption of an additive pair potential is not essential to the theoretical development below. In order to

produce results for more realistic potentials one need only replace the 3-particle potential energy, $U_3(\underset{\sim}{1},\underset{\sim}{2},\underset{\sim}{3})$, in the final formulae by the appropriate 3-particle interaction.

The pair distribution function $n_2(\underset{\sim}{1},\underset{\sim}{2})d^3\underset{\sim}{1}\, d^3\underset{\sim}{2}$ is defined as the probability that one of the particles of the system is found in the volume element $d^3\underset{\sim}{1}$ at $\underset{\sim}{1}$ while some other particle is simultaneously in volume $d^3\underset{\sim}{2}$ at $\underset{\sim}{2}$. In the gaseous system under consideration, in fact in any homogeneous fluid, $n_2(\underset{\sim}{1},\underset{\sim}{2})$ must depend only on the separation r_{12} between the particles except in the region near the boundaries of the system which becomes negligible as $V \to \infty$. In a classical gas of non-interacting particles the probability of finding a particle in a given volume element becomes a constant independent of the positions of the other particles, so in this case

$$n_2(\underset{\sim}{1},\underset{\sim}{2}) = \frac{N(N-1)}{V^2} , \tag{2.1.3}$$

$$\lim_{\substack{N,V\to\infty \\ n = \text{const.}}} n_2(\underset{\sim}{1},\underset{\sim}{2}) = n^2 . \tag{2.1.4}$$

Quantum mechanically the situation is complicated by the exchange correlation between identical particles, but since this effect falls off as (see Section 3.2) $\exp[-\text{const.} \times (r_{12}/\lambda)^2]$, Eqs. (2.1.3) and (2.1.4) still hold in the limit $r_{12} \gg \lambda$, where

$$\lambda = \left(\frac{2\pi\hbar^2\beta}{m}\right)^{\frac{1}{2}}$$

is the thermal wavelength of a particle of mass m at inverse temperature $\beta = 1/kT$.

If $P_N(\underset{\sim}{1},\underset{\sim}{2},\ldots,\underset{\sim}{N})d^3\underset{\sim}{1}\, d^3\underset{\sim}{2} \ldots d^3\underset{\sim}{N}$ is the probability that particle i is in volume $d^3\underset{\sim}{i}$ at $\underset{\sim}{i}$ for i from 1 to N, then the pair distribution function is given by

$$n_2(\underset{\sim}{1},\underset{\sim}{2}) = N(N-1)\int \ldots \int_V P_N(\underset{\sim}{1},\underset{\sim}{2},\ldots,\underset{\sim}{N})d^3\underset{\sim}{3}\, d^3\underset{\sim}{4} \ldots d^3\underset{\sim}{N}. \qquad (2.1.5)$$

The configurational probability P_N can be simply expressed in terms of the diagonal elements of the density matrix for the quantum mechanical canonical ensemble

$$P_N(\underset{\sim}{1},\underset{\sim}{2},\ldots,\underset{\sim}{N}) = \frac{1}{N\lambda^{3N}Z_N} \langle \underset{\sim}{1},\underset{\sim}{2},\ldots,\underset{\sim}{N}|e^{-\beta H_N}|\underset{\sim}{1},\underset{\sim}{2},\ldots,\underset{\sim}{N}\rangle. \qquad (2.1.6)$$

Here H_N is the Hamiltonian operator of the N-particle system

$$H_N = -\sum_{i=1}^{N} \frac{\hbar^2}{2m} \nabla_{\underset{\sim}{i}}^2 + U_N(\underset{\sim}{1},\underset{\sim}{2},\ldots,\underset{\sim}{N}) , \qquad (2.1.7)$$

Z_N is the partition function

$$Z_N = \frac{1}{N\lambda^{3N}}\int \ldots \int_V \langle \underset{\sim}{1},\underset{\sim}{2},\ldots,\underset{\sim}{N}|e^{-\beta H_N}|\underset{\sim}{1},\underset{\sim}{2},\ldots,\underset{\sim}{N}\rangle\, d^3\underset{\sim}{1}\, d^3\underset{\sim}{2} \ldots d^3\underset{\sim}{N} , \qquad (2.1.8)$$

and the density matrix is given in terms of the energy eigenfunctions $\phi_j(\underset{\sim}{1},\underset{\sim}{2},\ldots,\underset{\sim}{N})$ of the system as

$$\langle \underset{\sim}{1}',\underset{\sim}{2}',\ldots,\underset{\sim}{N}'|e^{-\beta H_N}|\underset{\sim}{1},\underset{\sim}{2},\ldots,\underset{\sim}{N}\rangle$$

$$= N!\lambda^{3N}\Sigma_j \phi_j^*(\underset{\sim}{1}',\underset{\sim}{2}',\ldots,\underset{\sim}{N}')\phi_j(\underset{\sim}{1},\underset{\sim}{2},\ldots,\underset{\sim}{N})e^{-\beta E_j} \quad , \tag{2.1.9}$$

where $H_N\phi_j = E_j\phi_j$. The pair distribution function can then be written

$$n_2(\underset{\sim}{1},\underset{\sim}{2}) = \frac{1}{(N-2)!\lambda^{3N}Z_N}\int_V \cdots \int \langle \underset{\sim}{1},\underset{\sim}{2},\ldots,\underset{\sim}{N}|e^{-\beta H_N}|\underset{\sim}{1},\underset{\sim}{2},\ldots,\underset{\sim}{N}\rangle$$

$$\times\, d^3\underset{\sim}{3}\; d^3\underset{\sim}{4} \ldots d^3\underset{\sim}{N} \; . \tag{2.1.10}$$

2.2 The Effect of Spin and Statistics on the Density Matrix

It should be noted that for a system of identical particles the sum in Eq. (2.1.9) extends only over properly symmetrized eigenstates. It will be useful in the following to express density matrix elements for Bose and Fermi statistics in terms of matrix elements for Boltzmann statistics and thus to deal with unrestricted sums over eigenstates. If we let the subscripts + denote Bose statistics and - denote Fermi statistics, then the symmetrized N-particle states for both cases can be written

$$|\underset{\sim}{1},\underset{\sim}{2},\ldots,\underset{\sim}{N}\rangle_{\pm} = \Sigma_P \frac{\sigma_P^{\pm}}{\sqrt{N!}}\,|P(\underset{\sim}{1},\underset{\sim}{2},\ldots,\underset{\sim}{N})\rangle \; , \tag{2.2.1}$$

where P is one of the N! permutations of N elements and $\sigma_P^{\pm}$ is defined by

$$\sigma_P^+ = +1 ,$$

$$\sigma_P^- = \begin{cases} +1 , & \text{if P is an even permutation,} \\ -1 , & \text{if P is an odd permutation.} \end{cases} \qquad (2.2.2)$$

The Bose and Fermi matrix elements can thus be written in terms of the Boltzmann matrix elements as

$$\langle \underset{\sim}{1}', \underset{\sim}{2}', \ldots, \underset{\sim}{N}' | e^{-\beta H_N} | \underset{\sim}{1}, \underset{\sim}{2}, \ldots, \underset{\sim}{N} \rangle_{\pm}$$

$$= \Sigma_{P''} \Sigma_{P'} \sigma_{P''}^{\pm} \sigma_{P'}^{\pm} \langle P''(\underset{\sim}{1}', \underset{\sim}{2}', \ldots, \underset{\sim}{N}') | e^{-\beta H_N} | P'(\underset{\sim}{1}, \underset{\sim}{2}, \ldots, \underset{\sim}{N}) \rangle ,$$

$$= \Sigma_P \sigma_P^{\pm} \langle P(\underset{\sim}{1}', \underset{\sim}{2}', \ldots, \underset{\sim}{N}') | e^{-\beta H_N} | \underset{\sim}{1}, \underset{\sim}{2}, \ldots, \underset{\sim}{N} \rangle , \qquad (2.2.3)$$

since $\Sigma_{P''} \Sigma_{P'} = N! \Sigma_P$, where $P = P''P'$. When space averages are taken over the Boltzmann matrix elements on the right of Eq. (2.2.3) only $1/N!$ of phase space should be taken. To allow the integration to extend over all space, we define the Boltzmann matrix elements without the factor of N! appearing in the corresponding Bose and Fermi quantities,

$$\langle \underset{\sim}{1}', \underset{\sim}{2}', \ldots, \underset{\sim}{N}' | e^{-\beta H_N} | \underset{\sim}{1}, \underset{\sim}{2}, \ldots, \underset{\sim}{N} \rangle$$

$$= \lambda^{3N} \sum_{\text{all } j} \phi_j^*(\underset{\sim}{1}', \underset{\sim}{2}', \ldots, \underset{\sim}{N}') \phi_j(\underset{\sim}{1}, \underset{\sim}{2}, \ldots, \underset{\sim}{N}) e^{-\beta E_j} . \qquad (2.2.4)$$

Although the above expressions are correct for He^4, which has spin zero, modifications are needed for particles having nonzero spin. If the particles each have spin S, then an N-particle state, $|\underset{\sim}{1}, s_1, \underset{\sim}{2}, s_2, \ldots, \underset{\sim}{N}, s_N\rangle$, should specify a spin coordinate, s_i, as well as a space coordinate, $\underset{\sim}{i}$, for each particle. Since the Hamiltonian is spin independent, matrix elements between spin states yield Kronecker deltas,

$$\langle \underset{\sim}{1}', s_1', \underset{\sim}{2}', s_2', \ldots, \underset{\sim}{N}', s_N' | e^{-\beta H_N} | \underset{\sim}{1}, s_1, \underset{\sim}{2}, s_2, \ldots, \underset{\sim}{N}, s_N \rangle$$

$$= \delta(s_1', s_1) \ldots \delta(s_N', s_N) \langle \underset{\sim}{1}', \underset{\sim}{2}', \ldots, \underset{\sim}{N}' | e^{-\beta H_N} | \underset{\sim}{1}, \underset{\sim}{2}, \ldots, \underset{\sim}{N} \rangle . \qquad (2.2.5)$$

If one then averages over spin in Eq. (2.2.3), the spin averaged diagonal density matrix element becomes

$$\langle \underset{\sim}{1}, \underset{\sim}{2}, \ldots, \underset{\sim}{N} | e^{-\beta H_N} | \underset{\sim}{1}, \underset{\sim}{2}, \ldots, \underset{\sim}{N} \rangle_{\pm} = \frac{1}{(2S+1)^N} \sum_{s_1} \sum_{s_2} \cdots \sum_{s_N} \sum_P \sigma_P^{\pm} \delta(s_1, Ps_1) \ldots \delta(s_N, Ps_N)$$

$$\times \langle P(\underset{\sim}{1}, \underset{\sim}{2}, \ldots, \underset{\sim}{N}) | e^{-\beta H_N} | \underset{\sim}{1}, \underset{\sim}{2}, \ldots, \underset{\sim}{N} \rangle . \qquad (2.2.6)$$

Noting that

$$\sum_{s_i} \delta(s_i, Ps_i) = 2S+1, \quad \text{if } s_i = Ps_i ,$$

$$= 1, \text{ otherwise} ,$$

one finds that if the permutation P is decomposed into cycles, the term in $\langle P(\underset{\sim}{1},\underset{\sim}{2},\ldots,\underset{\sim}{N})|e^{-\beta H_N}|\underset{\sim}{1},\underset{\sim}{2},\ldots,\underset{\sim}{N}\rangle$ contains a factor of $(2S+1)^{-(i-1)}$ for each cycle of length i. As a specific example the diagonal element of the 3-particle density matrix is

$$\langle \underset{\sim}{1},\underset{\sim}{2},\underset{\sim}{3}|e^{-\beta H_3}|\underset{\sim}{1},\underset{\sim}{2},\underset{\sim}{3}\rangle_{\pm} = \langle \underset{\sim}{1},\underset{\sim}{2},\underset{\sim}{3}|e^{-\beta H_3}|\underset{\sim}{1},\underset{\sim}{2},\underset{\sim}{3}\rangle$$

$$\pm \frac{1}{2S+1} \langle \underset{\sim}{2},\underset{\sim}{1},\underset{\sim}{3}|e^{-\beta H_3}|\underset{\sim}{1},\underset{\sim}{2},\underset{\sim}{3}\rangle \pm \frac{1}{2S+1} \langle \underset{\sim}{1},\underset{\sim}{3},\underset{\sim}{2}|e^{-\beta H_3}|\underset{\sim}{1},\underset{\sim}{2},\underset{\sim}{3}\rangle$$

$$\pm \frac{1}{2S+1} \langle \underset{\sim}{3},\underset{\sim}{2},\underset{\sim}{1}|e^{-\beta H_3}|\underset{\sim}{1},\underset{\sim}{2},\underset{\sim}{3}\rangle + \frac{1}{(2S+1)^2} \langle \underset{\sim}{2},\underset{\sim}{3},\underset{\sim}{1}|e^{-\beta H_3}|\underset{\sim}{1},\underset{\sim}{2},\underset{\sim}{3}\rangle$$

$$+ \frac{1}{(2S+1)^2} \langle \underset{\sim}{3},\underset{\sim}{1},\underset{\sim}{2}|e^{-\beta H_3}|\underset{\sim}{1},\underset{\sim}{2},\underset{\sim}{3}\rangle . \qquad (2.2.7)$$

2.3 Cluster Expansion for the Pair Distribution Function

De Boer [8] has shown how the quantum mechanical cluster expansion of Kahn and Uhlenbeck [9] can be used to express the pair distribution function for a gas in terms of a power series in the

density. It turns out that the term in the j-th power of the density depends only on density matrix elements for systems of j+2 or fewer particles. The following brief summary of definitions and results draws from the treatment in de Boer's review article [8].

Denote the diagonal elements of the density matrix by

$$W_N(\underset{\sim}{1},\underset{\sim}{2},\ldots,\underset{\sim}{N}) = \langle \underset{\sim}{1},\underset{\sim}{2},\ldots,\underset{\sim}{N}|e^{-\beta H_N}|\underset{\sim}{1},\underset{\sim}{2},\ldots,\underset{\sim}{N}\rangle \ . \qquad (2.3.1)$$

Let $\underset{\sim}{r}^{(h)}$ stand for the set $(\underset{\sim}{1},\underset{\sim}{2},\ldots,\underset{\sim}{h})$ of coordinates of a group of h particles and define Ursell functions U_ℓ and modified Ursell functions $U_\ell^{(h)}$ by the relations

$$U_1(\underset{\sim}{i}) = W_1(\underset{\sim}{i}) \ ,$$

$$U_2(\underset{\sim}{i},\underset{\sim}{j}) = W_2(\underset{\sim}{i},\underset{\sim}{j}) - W_1(\underset{\sim}{i})W_1(\underset{\sim}{j}) \ ,$$

$$U_3(\underset{\sim}{i},\underset{\sim}{j},\underset{\sim}{k}) = W_3(\underset{\sim}{i},\underset{\sim}{j},\underset{\sim}{k}) - W_2(\underset{\sim}{i},\underset{\sim}{j})W_1(\underset{\sim}{k}) - W_2(\underset{\sim}{i},\underset{\sim}{k})W_1(\underset{\sim}{j})$$

$$- W_2(\underset{\sim}{j},\underset{\sim}{k})W_1(\underset{\sim}{i}) + 2W_1(\underset{\sim}{i})W_1(\underset{\sim}{j})W_1(\underset{\sim}{k}) \ , \text{ etc.} \qquad (2.3.2)$$

$$U_1^{(h)}(\underset{\sim}{r}^{(h)}) = W_h(\underset{\sim}{r}^{(h)}) \ ,$$

$$U_2^{(h)}(\underset{\sim}{r}^{(h)},\underset{\sim}{i}) = W_{h+1}(\underset{\sim}{r}^{(h)},\underset{\sim}{i}) - W_h(\underset{\sim}{r}^{(h)})W_1(\underset{\sim}{i}) \ ,$$

$$U_3^{(h)}(\underset{\sim}{r}^{(h)},\underset{\sim}{i},\underset{\sim}{j}) = W_{h+2}(\underset{\sim}{r}^{(h)},\underset{\sim}{i},\underset{\sim}{j}) - W_{h+1}(\underset{\sim}{r}^{(h)},\underset{\sim}{i})W_1(\underset{\sim}{j}) - W_{h+1}(\underset{\sim}{r}^{(h)},\underset{\sim}{j})W_1(\underset{\sim}{i})$$

$$- W_2(\underset{\sim}{i},\underset{\sim}{j})W_h(\underset{\sim}{r}^{(h)}) + 2W_h(\underset{\sim}{r}^{(h)})W_1(\underset{\sim}{i})W_1(\underset{\sim}{j}) \ , \text{ etc.} \qquad (2.3.3)$$

The Ursell functions have the property that if the particles of the system are separated into two groups such that the minimum distance between the groups is much greater than both the thermal wavelength and the range of the interparticle potential, then any Ursell function containing as arguments coordinates of particles in each group vanishes. The modified Ursell functions have the same property provided that the set of h particles specified by $\underset{\sim}{r}^{(h)}$ is considered as a single particle in the separation into groups. The Ursell functions are useful in treating a gas since in this case the average interparticle spacing is large enough that only those functions with a small number of arguments differ from zero.

The definition of the modified Ursell functions leads to an expression for W_N in terms of these functions

$$W_N(\underset{\sim}{1},\underset{\sim}{2},\cdots,\underset{\sim}{N}) = U_1^{(h)}(\underset{\sim}{r}^{(h)})W_{N-h}(\underset{\sim}{r}_{h+1},\cdots,\underset{\sim}{r}_N)$$

$$+ \sum_{i=h+1}^{N} U_2^{(h)}(\underset{\sim}{r}^{(h)},\underset{\sim}{r}_i)W_{N-h-1}(\underset{\sim}{r}_{h+1},\cdots,\underset{\sim}{r}_{i-1},\underset{\sim}{r}_{i+1},\cdots,\underset{\sim}{r}_N)$$

$$+ \sum_{i\neq j=h+1}^{N} U_3^{(h)}(\underset{\sim}{r}^{(h)},\underset{\sim}{r}_i,\underset{\sim}{r}_j)W_{N-h-2}(\underset{\sim}{r}_{h+1},\cdots,\underset{\sim}{r}_{i-1},\underset{\sim}{r}_{i+1},\cdots,\underset{\sim}{r}_{j-1},\underset{\sim}{r}_{j+1},\cdots,\underset{\sim}{r}_N)$$

$$+ \cdots \qquad (2.3.4)$$

where $\underset{\sim}{r}_i$ is used for the coordinate of the i-th particle. If we define cluster integrals $b_\ell^{(h)}$ by

$$b_\ell^{(h)}(\underset{\sim}{r}^{(h)}) = \frac{1}{\ell!}\int_V \cdots \int U_\ell^{(h)}(\underset{\sim}{r}^{(h)},\underset{\sim}{r}_{h+1},\cdots,\underset{\sim}{r}_{h+\ell-1})$$

$$\times d^3\underset{\sim}{r}_{h+1}d^3\underset{\sim}{r}_{h+2}\cdots d^3\underset{\sim}{r}_{h+\ell-1}\,, \qquad (2.3.5)$$

then using Eq. (2.3.4) with h = 2 the pair distribution function can be expressed as

$$n_2(\underset{\sim}{1},\underset{\sim}{2}) = \frac{N(N-1)}{N!\lambda^{3N}Z_N}\int_V \cdots \int_V W_N(\underset{\sim}{1},\underset{\sim}{2},\ldots,\underset{\sim}{N})d^3\underset{\sim}{3}\, d^3\underset{\sim}{4} \cdots d^3\underset{\sim}{N} ,$$

$$= \frac{1}{\lambda^6 Z_N} U_1^{(2)}(\underset{\sim}{r}^{(2)}) \int_V \cdots \int_V \frac{W_{N-2}(\underset{\sim}{3},\underset{\sim}{4},\ldots,\underset{\sim}{N})}{(N-2)!\lambda^{3(N-2)}} d^3\underset{\sim}{3}\, d^3\underset{\sim}{4} \cdots d^3\underset{\sim}{N}$$

$$+ \frac{2}{\lambda^9 Z_N}\int_V \frac{U_2^{(2)}(\underset{\sim}{r}^{(2)},\underset{\sim}{3})}{2!} d^3\underset{\sim}{3} \int_V \cdots \int_V \frac{W_{N-3}(\underset{\sim}{4},\underset{\sim}{5},\ldots,\underset{\sim}{N})}{(N-3)!\lambda^{3(N-3)}} d^3\underset{\sim}{4}\, d^3\underset{\sim}{5} \cdots d^3\underset{\sim}{N}$$

$$+ \frac{3}{\lambda^{12} Z_N} \int_V\int_V \frac{U_3^{(2)}(\underset{\sim}{r}^{(2)},\underset{\sim}{3},\underset{\sim}{4})}{3!} d^3\underset{\sim}{3}\, d^3\underset{\sim}{4}$$

$$\times \int_V \cdots \int_V \frac{W_{N-4}(\underset{\sim}{5},\underset{\sim}{6},\ldots,\underset{\sim}{N})}{(N-4)!\lambda^{3(N-4)}} d^3\underset{\sim}{5}\, d^3\underset{\sim}{6} \cdots d^3\underset{\sim}{N} + \cdots ,$$

$$= \sum_{\ell=1}^{N} \ell b_\ell^{(2)}(\underset{\sim}{1},\underset{\sim}{2})\lambda^{-3(\ell+1)} \frac{Z_{N-\ell-1}}{Z_N} . \qquad (2.3.6)$$

Defining the activity z by

$$\ell n(\lambda^3 z) = - \frac{d\ell n Z_N}{dN} , \qquad (2.3.7)$$

and assuming $N \gg \ell$ one obtains

$$\ell n(\lambda^3 z)^\ell = \ell n Z_{N-\ell} - \ell n Z_N ,$$

or

$$z^{\ell} = \lambda^{-3\ell} \frac{Z_{N-\ell}}{Z_N} \quad . \tag{2.3.8}$$

Thus, taking the limit as $N \to \infty$, the expansion of the pair distribution function in powers of the activity becomes

$$n_2(\underset{\sim}{1},\underset{\sim}{2}) = z \sum_{\ell=1}^{\infty} \ell b_{\ell}^{(2)}(\underset{\sim}{1},\underset{\sim}{2}) z^{\ell} \quad . \tag{2.3.9}$$

Using Eq. (2.3.4) with h=1 the density, n, can be found as a power series in z also

$$n = \sum_{\ell=1}^{\infty} \ell b_{\ell} z^{\ell} \quad , \tag{2.3.10}$$

where we drop the superscript on $b_{\ell}^{(1)}(\underset{\sim}{1})$ and omit the argument since we are dealing with a homogeneous fluid in which $b_{\ell}^{(1)}$ is independent of position. It should be noted that homogeneity also requires that the 2-particle cluster integrals depend only on r_{12}. From Eqs. (2.3.9) and (2.3.10) a series for $n_2(r_{12})$ in powers of n can be constructed

$$n_2(r_{12}) = \sum_{k=2}^{\infty} \gamma_k(r_{12}) n^k \quad . \tag{2.3.11}$$

The first two coefficients of the series are given by

$$\gamma_2(r_{12}) = b_1^{(2)}(r_{12}) ,$$

$$\gamma_3(r_{12}) = 2b_2^{(2)}(r_{12}) - 4b_2 b_1^{(2)}(r_{12}) . \qquad (2.3.12)$$

The function obtained experimentally, usually by x ray or neutron diffraction, is the Fourier transform of the pair correlation function

$$g(r_{12}) = \frac{n_2(r_{12})}{n^2} . \qquad (2.3.13)$$

From the comments following Eqs. (2.1.3) and (2.1.4) it is seen that the pair correlation function, $g(r_{12})$, is normalized so that

$$\lim_{r_{12}\to\infty} g(r_{12}) = 1 , \qquad (2.3.14)$$

provided that the interparticle potential has a finite range. If one defines $g_i(r_{12})$, i=1,2,3,..., by

$$g(r_{12}) = b_1^{(2)}(r_{12})\left[1 + \sum_{i=1}^{\infty} n^i g_i(r_{12})\right] , \qquad (2.3.15)$$

it is seen from Eq. (2.3.12) that the coefficient of the term linear in the density is

$$g_1(r_{12}) = \frac{1}{b_1^{(2)}(r_{12})}\left[2b_2^{(2)}(r_{12}) - 4b_2 b_1^{(2)}(r_{12})\right] , \qquad (2.3.16)$$

which can be written in terms of the diagonal density matrix elements, W, as

$$g_1(r_{12}) = \frac{1}{W_2(\underset{\sim}{1},\underset{\sim}{2})} \int \Big[W_3(\underset{\sim}{1},\underset{\sim}{2},\underset{\sim}{3}) - W_2(\underset{\sim}{1},\underset{\sim}{2}) W_2(\underset{\sim}{1},\underset{\sim}{3}) - W_2(\underset{\sim}{1},\underset{\sim}{2}) W_2(\underset{\sim}{2},\underset{\sim}{3}) + W_2(\underset{\sim}{1},\underset{\sim}{2}) \Big] d^3\underset{\sim}{3}. \quad (2.3.17)$$

The linear term in the density expansion of $g(r_{12})$ (or $n_2(r_{12})$) is thus expressed in terms of the density matrix elements of systems of three or fewer particles.

Similar manipulations with the cluster expansion of W_N yield the well known virial expansion for the pressure P (for example see Huang [10])

$$\frac{PV}{N_0 kT} = 1 + \frac{B(T)}{V} + \frac{C(T)}{V^2} + \cdots , \quad (2.3.18)$$

where the third virial coefficient, C(T), is given in terms of the cluster integrals by

$$C = -N_0^2 (2b_3 - 4b_2^2) , \quad (2.3.19)$$

and where N_0 is Avogadro's number and V is the molar volume. Using the definition of the cluster integrals and of $g_1(r_{12})$, C can be written as

$$C = -\frac{N_0^2}{3}\left[\int g_1(r_{12})W_2(r_{12})d^3\underset{\sim}{r}_2 - 4b_2^2\right] . \qquad (2.3.29)$$

Since $W_2(r_{12})$ and b_2 have already been evaluated for the Lennard-Jones (12-6) potential [6] it remains to calculate $g_1(r_{12})$ in order to obtain both the pair distribution function to first order in the density and the third virial coefficient.

3. PATH INTEGRAL FORMULATION FOR THE DENSITY MATRIX

3.1 Expression of Density Matrix Elements in Terms of Wiener Integrals

The expression of the quantum mechanical density matrix in terms of functional integrals has been treated by several authors [11,12,13,14,15]. The mathematically rigorous form of the functional integral in question is the Wiener integral or expectation value, $E\{F[x(\tau)]\}$, of a functional, $F[x(\tau)]$, over Wiener measure on the set of continuous functions, $x(\tau)$, over a finite interval in the independent variable τ. The following treatment will make use of the Wiener integral formulation [11,12,13,14], which exhibits normalization constants more explicitly, rather than the more intuitive notation of Feynman [15], which clarifies the transformation properties of the path integral.

The quantity directly related to the density matrix is the conditional Wiener integral, which involves Wiener measure on the subset of continuous paths which have fixed values at both endpoints of the τ interval. Let the 3N-dimensional vector (the number of dimensions is arbitrary, but 3N is specified for later application to the system of N particles in 3 dimensions), $\underset{\sim}{r}(\tau) = (\underset{\sim}{r}_1(\tau),\ldots,\underset{\sim}{r}_N(\tau))$, be a continuous vector function of the variable τ on the interval $0 \leq \tau \leq \beta$. Let the interval $[0,\beta]$ be divided into k equal intervals of length $\Delta\tau = \beta/k$, and take the division points to be $0 = \tau_0 < \tau_1 < \ldots < \tau_{k-1} < \tau_k = \beta$. Let $\underset{\sim}{r}(\tau;k)$ be a continuous vector function of τ consisting of linear segments over the intervals (τ_{i-1},τ_i), $i = 1,2,\ldots,k$, with $\underset{\sim}{r}_i = \underset{\sim}{r}(\tau_i;k)$, and satisfying the endpoint conditions $\underset{\sim}{r}_0 = 0$, $\underset{\sim}{r}_k = \underset{\sim}{R}$.

If the functional $F[\underset{\sim}{r}(\tau)]$ is defined on all continuous functions, $\underset{\sim}{r}(\tau)$, satisfying the above endpoint conditions, then the conditional Wiener integral can be defined by the limiting process

$$E\{F[\underset{\sim}{r}(\tau)]|\underset{\sim}{r}(\beta) = \underset{\sim}{R}\} = \lim_{k\to\infty} \int_{-\infty}^{\infty} \cdots \int_{-\infty}^{\infty} F[\underset{\sim}{r}(\tau;k)]d\mu_k, \tag{3.1.1}$$

where the measure $d\mu_k$ is given by

$$d\mu_k = (2\pi)^{\frac{3N}{2}} \exp(\frac{\underset{\sim}{R}^2}{2})(2\pi\Delta\tau)^{\frac{-3Nk}{2}} \exp\left[\sum_{i=1}^{k} \frac{(\underset{\sim}{r}_i - \underset{\sim}{r}_{i-1})^2}{2\Delta\tau} \right] \prod_{i=1}^{k-1} d^{3N}\underset{\sim}{r}_i \ . \tag{3.1.2}$$

Note that the measure $d\mu_k$ is normalized so that

$$\int_{-\infty}^{\infty} \cdots \int_{-\infty}^{\infty} d\mu_k = 1 \ , \tag{3.1.3}$$

and thus

$$E\{1|\underset{\sim}{r}(\beta) = \underset{\sim}{R}\} = 1 \ . \tag{3.1.4}$$

The relationship between the conditional Wiener integral and the density matrix is given by a theorem due to Kac [13,14]. It states that if the scalar field $U(\underset{\sim}{r})$ has a finite number of discontinuities and is bounded below, then

$$\Sigma_j \Psi_j^*(\underset{\sim}{R})\Psi_j(\underset{\sim}{R}')e^{-\beta E_j} = (2\pi\beta)^{\frac{-3N}{2}} \exp\left[-\frac{(\underset{\sim}{R}'-\underset{\sim}{R})^2}{2\beta}\right]$$

$$\times E\left\{\exp\left[-\int_0^\beta U(\underset{\sim}{r}(\tau) + \underset{\sim}{R})d\tau\right]\middle|\underset{\sim}{r}(\beta) = \underset{\sim}{R}'-\underset{\sim}{R}\right\}, \qquad (3.1.5)$$

where $\Psi_j(\underset{\sim}{R})$ are the normalized eigenfunctions of

$$\frac{1}{2}\Sigma_i \nabla_{\underset{\sim}{i}}^2 \Psi_j(\underset{\sim}{R}) + \left[E_j - U(\underset{\sim}{R})\right]\Psi_j(\underset{\sim}{R}) = 0 . \qquad (3.1.6)$$

If one transforms the variable, $\underset{\sim}{R}$, in order to make Eq. (3.1.6) into the time independent Schrödinger equation for a system with the Hamiltonian

$$H = -\Sigma_i \frac{\hbar^2}{2m} \nabla_{\underset{\sim}{i}}^2 + U(\underset{\sim}{R}), \qquad (3.1.7)$$

and makes the further transformation $\tau \to \tau/\beta$, $\underset{\sim}{r}(\tau) \to \underset{\sim}{r}(\tau)/\sqrt{\beta}$, which normalizes the τ interval to [0,1] while leaving the Wiener integral invariant, then the general density matrix element can be written

$$\langle \underset{\sim}{R}|e^{-\beta H_N}|\underset{\sim}{R}'\rangle = \exp\left[-\frac{\pi}{\lambda^2}(\underset{\sim}{R}'-\underset{\sim}{R})^2\right]$$

$$\times E\left\{\exp\left[-\beta\int_0^1 U\left(\frac{\lambda}{\sqrt{2\pi}}\,\underset{\sim}{r}(\tau) + \underset{\sim}{R}\right)d\tau\right]\middle|\underset{\sim}{r}(1) = \frac{\sqrt{2\pi}}{\lambda}(\underset{\sim}{R}'-\underset{\sim}{R})\right\} . \qquad (3.1.8)$$

This relationship holds only for the Boltzmann matrix elements since the sum in Kac' theorem is over all eigenstates, regardless of symmetry.

As stated in the references [13,14], Kac' theorem also requires that $U(\underset{\sim}{r})$ be such that the eigenvalue problem, Eq. (3.1.6), yields a discrete spectrum. If the system is enclosed on a box of volume V, then $U(\underset{\sim}{r})$ should have a component due to the walls of the box. This component certainly causes the spectrum to be discrete and gives a natural normalization for the eigenfunctions. However, if one restricts the temperature to values larger than those at which long range order phenomena, such as Bose condensation, become important, then the potential of the box contributes nothing to the problem in the limit $V \to \infty$. One may neglect this component of $U(\underset{\sim}{r})$ provided one considers the wave functions of the continuous spectrum to have delta function normalization and treats the sum over states Σ_j as representing a sum over the discrete states plus an integral over the continuous spectrum.

A slight reformulation of Eq. (3.1.8) will be useful in the following work. Wiener measure on $\underset{\sim}{r}(\tau)$ gives rise to the interpolation formula [16]

$$\underset{\sim}{r}(\tau) = \frac{\underset{\sim}{r}(\tau')(\tau''-\tau) + \underset{\sim}{r}(\tau'')(\tau-\tau')}{\tau''-\tau'} + \underset{\sim}{\xi} \left[\frac{(\tau-\tau')(\tau''-\tau)}{(\tau''-\tau')} \right]^{\frac{1}{2}}, \quad (3.1.9)$$

where $\tau' < \tau < \tau''$ and where $\underset{\sim}{\xi}$ is a 3N-dimensional random variable whose coordinate random variables are independent and normally distributed with mean 0 and variance 1. From this formula it can be seen that if $\underset{\sim}{r}'(\tau)$ obeys the endpoint conditions, $\underset{\sim}{r}'(0) = \underset{\sim}{r}'(1) = 0$ then both $\underset{\sim}{r}(\tau)$ and $\underset{\sim}{r}'(\tau) + \frac{\tau\sqrt{2\pi}}{\lambda}(\underset{\sim}{R}'-\underset{\sim}{R})$ are distributed as the random variable

$$\tau \frac{\sqrt{2\pi}}{\lambda} (\underset{\sim}{R}'-\underset{\sim}{R}) + \underset{\sim}{\xi}[\tau(1-\tau)]^{\frac{1}{2}} .$$

Equation (3.1.8) can then be written

$$\langle \underset{\sim}{R} | e^{-\beta H_N} | \underset{\sim}{R}' \rangle = \exp\left[-\frac{\pi}{\lambda^2} (\underset{\sim}{R}'-\underset{\sim}{R})^2 \right]$$

$$\times E\left\{ \exp\left[-\beta \int_0^1 U \left(\frac{\lambda}{\sqrt{2\pi}} \underset{\sim}{r}(\tau) + \underset{\sim}{R} + \tau(\underset{\sim}{R}'-\underset{\sim}{R}) \right) d\tau \right] \middle| \underset{\sim}{r}(1)=0 \right\} , \qquad (3.1.10)$$

where the prime on $\underset{\sim}{r}'(\tau)$ has been dropped.

A useful intuitive picture of the Wiener integral is obtained by thinking of an imaginary motion of a system of N particles over a unit "time" interval, $0 < \tau < 1$. At time $\tau = 0$ the coordinates of the particles are given by $\underset{\sim}{R}$ and at $\tau = 1$ by $\underset{\sim}{R}'$. The quantity $(\underset{\sim}{R}'-\underset{\sim}{R})^2$ is thus the sum of the squares of the distances between the initial and final positions of each particle, and the Wiener integral in Eq. (3.1.10) is the average, over all possible paths of the motion, of the Boltzmann factor, $e^{-\beta U}$, with the potential energy U replaced by the average of the potential over the path. The paths are weighted by Wiener measure which is related to the average over the path of the total kinetic energy of the system.

It should be noted that

$$\frac{\lambda}{\sqrt{2\pi}} \underset{\sim}{r}(\tau)$$

is a measure of the deviation of the motion from the shortest straight line path from $\underset{\sim}{R}$ to $\underset{\sim}{R}'$, and as the classical limit is obtained by letting $\lambda \to 0$, the deviation vanishes in this limit. The off-diagonal matrix elements vanish in the classical limit since

$$\lim_{\lambda \to 0} \exp\left[-\frac{\pi}{\lambda^2}(\underset{\sim}{R}'-\underset{\sim}{R})^2\right] \propto \delta(\underset{\sim}{R}'-\underset{\sim}{R}) \ , \qquad (3.1.11)$$

where δ is the Dirac delta function, and the diagonal matrix element approaches the Boltzmann factor

$$\lim_{\lambda \to 0} \langle \underset{\sim}{R} | e^{-\beta H_N} | \underset{\sim}{R} \rangle = e^{-\beta U(\underset{\sim}{R})} \ . \qquad (3.1.12)$$

3.2 Upper Bounds on Off-Diagonal Matrix Elements

Both diagonal and off-diagonal matrix elements for Boltzmann statistics are involved in the calculation of $g_1(r_{12})$ for a Bose or Fermi system. For example, in the evaluation of the 3-particle term,

$$\langle \underset{\sim}{1},\underset{\sim}{2},\underset{\sim}{3} | e^{-\beta H_3} | \underset{\sim}{1},\underset{\sim}{2},\underset{\sim}{3} \rangle_{\pm} ,$$

two types of off-diagonal Boltzmann matrix elements arise. One involves the exchange of coordinates of two of the three particles and is of the form

$$\langle \underset{\sim}{1},\underset{\sim}{2},\underset{\sim}{3}|e^{-\beta H_3}|\underset{\sim}{2},\underset{\sim}{1},\underset{\sim}{3}\rangle = \exp\left(-\frac{\pi}{\lambda^2}\left[(\underset{\sim}{2}-\underset{\sim}{1})^2 + (\underset{\sim}{1}-\underset{\sim}{2})^2\right]\right)$$

$$\times E\left\{\exp\left[-\beta\int_0^1 U_3\left(\frac{\lambda}{\sqrt{2\pi}}\,\underset{\sim}{r}(\tau) + (\underset{\sim}{2},\underset{\sim}{1},\underset{\sim}{3}) + \tau[(\underset{\sim}{1},\underset{\sim}{2},\underset{\sim}{3})-(\underset{\sim}{2},\underset{\sim}{1},\underset{\sim}{3})]\right)d\tau\right]\middle|\underset{\sim}{r}(1)=0\right\}. \tag{3.2.1}$$

The other type involves a cyclic exchange of the coordinates of all three particles and is typified by the matrix element

$$\langle \underset{\sim}{1},\underset{\sim}{2},\underset{\sim}{3}|e^{-\beta H_3}|\underset{\sim}{2},\underset{\sim}{3},\underset{\sim}{1}\rangle = \exp\left(-\frac{\pi}{\lambda^2}\left[(\underset{\sim}{2}-\underset{\sim}{1})^2 + (\underset{\sim}{3}-\underset{\sim}{2})^2 + (\underset{\sim}{1}-\underset{\sim}{3})^2\right]\right)$$

$$\times E\left\{\exp\left[-\beta\int_0^1 U_3\left(\frac{\lambda}{\sqrt{2\pi}}\,\underset{\sim}{r}(\tau) + (\underset{\sim}{2},\underset{\sim}{3},\underset{\sim}{1}) + \tau[(\underset{\sim}{1},\underset{\sim}{2},\underset{\sim}{3})-(\underset{\sim}{2},\underset{\sim}{3},\underset{\sim}{1})]\right)d\tau\right]\middle|\underset{\sim}{r}(1)=0\right\}. \tag{3.2.2}$$

The form of the factors multiplying the Wiener integrals in these expressions yields a significant estimate of the size and temperature dependence of these off-diagonal elements for intermolecular potentials for which the particles are characterized by strong repulsive cores. Suppose the 3-body potential satisfies

$$U_3(\underset{\sim}{r}_1,\underset{\sim}{r}_2,\underset{\sim}{r}_3) = \infty, \text{ if } r_{ij} < \sigma \text{ for any pair } i\neq j=1,2,3. \tag{3.2.3}$$

The Wiener integrals in Eqs. (3.2.1) and (3.2.2) must vanish if the initial distance between any pair of particles is less than σ. Hence

wherever the matrix element is nonzero the factor multiplying the Wiener integral is smaller than $\exp(-2\pi\sigma^2/\lambda^2)$ for the 2-particle exchange term and smaller than $\exp(-3\pi\sigma^2/\lambda^2)$ for the 3-particle exchange term.

For He^4, approximating the repulsive core diameter by the parameter $\sigma = 2.56 \times 10^{-8}$ cm of the Lennard-Jones (12-6) potential, one finds that the larger of the two multiplying factors, that for the 2-particle exchange, is approximately $e^{-.6T}$. Thus at $10^{\circ}K$ one expects the off-diagonal elements to be smaller by a factor of at least .0025 than the diagonal element, for which the multiplying factor is unity. The argument for the 2-particle exchange term in $\langle \underset{\sim}{1},\underset{\sim}{2}|e^{-\beta H_2}|\underset{\sim}{1},\underset{\sim}{2}\rangle_{\pm}$ is the same as the argument for the similar 3-particle term in Eq. (3.2.1) and yields the same result. Due to restrictions of computing time the numerical scheme to be developed below for the calculation of the diagonal matrix element is limited in accuracy at low temperatures. In all cases, the above bound on the exchange terms shows them to be negligible compared to the numerical uncertainty of the diagonal term. Therefore, in subsequent sections the exchange terms will be discarded and the diagonal Boltzmann matrix element will be used as if it were the same as the diagonal element for a Bose or Fermi system.

The above argument was first used in connection with the 2-particle exchange term in the second virial coefficient [17]. The suppression of this 2-particle exchange term with increasing temperature is actually somewhat stronger than is indicated above. This is verified

both by numerical calculations [5,6] and by upper and lower bounds obtained analytically by Lieb [18], who shows that at high temperatures the term is asymptotically proportional to

$$\exp\left\{-\frac{\pi}{3}\left(\frac{\sigma}{\lambda}\right)^2+\sigma\left[\left(\frac{\sigma}{\lambda}\right)^{\frac{2}{3}}\right]\right\}.$$

Qualitatively the increase in the constant multiplying $-\lambda^{-2}$ in the exponent comes about because the Wiener integral in Eq. (3.2.1), as well as the multiplying factor, decreases exponentially with increasing temperature. This is due to the fact that the set of paths for which the "motion" of the system from time $\tau = 0$ to time $\tau = 1$ brings the two exchanged particles no closer than σ from each other for any τ is assigned exponentially smaller Wiener measure as $T \to \infty$.

3.3 Approximation of the Diagonal Matrix Element by a Multiple Riemann Integral

The calculation of the diagonal matrix elements for Boltzmann statistics is now reduced to the evaluation of a Wiener integral. For the diagonal element of the 3-particle density matrix Eq. (3.1.8) becomes

$$\langle \underset{\sim}{1},\underset{\sim}{2},\underset{\sim}{3}|e^{-\beta H_3}|\underset{\sim}{1},\underset{\sim}{2},\underset{\sim}{3}\rangle$$

$$= E\left\{\exp\left[-\beta\int_0^1 U_3\left(\frac{\lambda}{\sqrt{2\pi}}\,\underset{\sim}{r}(\tau) + (\underset{\sim}{1},\underset{\sim}{2},\underset{\sim}{3})\right)d\tau\right]\Bigg|\underset{\sim}{r}(1)=0\right\} . \qquad (3.3.1)$$

Analytical evaluation of the above Wiener integral is possible, however, only in the cases

$$U_3(\underset{\sim}{r}_1,\underset{\sim}{r}_2,\underset{\sim}{r}_3) \equiv 0 ,$$

and

$$U_3(\underset{\sim}{r}_1,\underset{\sim}{r}_2,\underset{\sim}{r}_3) = \sum_{i=1}^{3} f_i(\underset{\sim}{r}_i) ,$$

where $f_i(\underset{\sim}{r}_i)$ is quadratic in each coordinate of $\underset{\sim}{r}_i$. Thus for a realistic interparticle potential it is necessary to rely on a numerical evaluation of the Wiener integral.

Numerical schemes for evaluating Wiener integrals have been proposed and applied by several authors [6,19,20,21,22,23]. The simplest of these methods involves taking a finite but large value of k in the limit definition for the conditional Wiener integral, Eqs. (3.1.1) and (3.1.2), and using the result of a numerical evaluation of the k-fold multiple integral as an approximation to the Wiener integral. Since k is large and the weight function $d\mu_k$ can be conveniently expressed in terms of Gaussian density functions the evaluation of the k-fold integral is usually done by the Monte Carlo method.

This simple scheme is adequate for one or two particles under the influence of a computationally simple potential and has been applied successfully to such problems [6,20,22]. As the evaluation of the integrand of the multiple integral becomes more complex, however, the computing time requirements become unreasonably large, and for this reason methods have been proposed for reducing the multiplicity k of the integral to be performed [19,21,23]. The present calculation makes use of a slight modification of the procedure developed by Fosdick [21].

The Wiener integral in Eq. (3.3.1) can be written as a Riemann integral of a product of Wiener integrals involving a smaller value of β (higher temperature). If the interval $0 \leq \tau \leq 1$ is divided into k equal subintervals, (τ_{i-1},τ_i), i=1,2,...,k, then the integrand in Eq. (3.3.1) can be written as a product of functionals depending on $\underset{\sim}{r}(\tau)$ over only one subinterval

$$F[\underset{\sim}{r}(\tau)] = \exp\left[-\beta \int_0^1 U_3\left(\frac{\lambda}{\sqrt{2\pi}}\,\underset{\sim}{r}(\tau) + (\underset{\sim}{1},\underset{\sim}{2},\underset{\sim}{3})\right) d\tau\right]$$

$$= \prod_{i=1}^{k} f_i[\underset{\sim}{r}(\tau)] , \qquad (3.3.2)$$

where

$$f_i[\underset{\sim}{r}(\tau)] = \exp\left[-\beta \int_{\tau_{i-1}}^{\tau_i} U_3\left(\frac{\lambda}{\sqrt{2\pi}}\,\underset{\sim}{r}(\tau) + (\underset{\sim}{1},\underset{\sim}{2},\underset{\sim}{3})\right) d\tau\right] . \qquad (3.3.3)$$

If each of the k subdivisions is now further subdivided into n equal parts, Eq. (3.1.1) may be written in the form

$$E\{F[\underset{\sim}{r}(\tau)]\,|\,\underset{\sim}{r}(1) = 0\} = \lim_{n\to\infty} \int_{-\infty}^{\infty} \cdots \int_{-\infty}^{\infty} d\mu_{nk} F[\underset{\sim}{r}(\tau;nk)] \ ,$$

$$= \int_{-\infty}^{\infty} \cdots \int_{-\infty}^{\infty} d\mu_k \prod_{i=1}^{k} \lim_{n\to\infty} \int_{-\infty}^{\infty} \cdots \int_{-\infty}^{\infty} d\mu_{i,n} f_i[\underset{\sim}{r}(\tau;nk)] \ , \qquad (3.3.4)$$

where $d\mu_k$ is defined as in Eq. (3.1.2) in terms of the coarse subdivision only and

$$d\mu_{i,n} = \left(2\pi\frac{\beta}{k}\right)^{\frac{3N}{2}} \exp\left[\frac{(\underset{\sim}{r}_{i;n} - \underset{\sim}{r}_{i;0})^2}{2(\beta/nk)}\right] \left(2\pi\frac{\beta}{nk}\right)^{-\frac{3Nn}{2}}$$

$$\times \exp\left[-\sum_{j=1}^{n} \frac{(\underset{\sim}{r}_{i;j} - \underset{\sim}{r}_{i;j-1})^2}{2(\beta/nk)}\right] \prod_{j=1}^{k-1} d^{3N}\underset{\sim}{r}_{i;j} \ , \qquad (3.3.5)$$

where $\underset{\sim}{r}_{i;j} = \underset{\sim}{r}(\tau_{ni+j};nk)$. The limit on the right hand side of Eq. (3.3.4) is just the definition of a conditional Wiener integral

$$\lim_{n\to\infty} \int_{-\infty}^{\infty} \cdots \int_{-\infty}^{\infty} d\mu_{i,n} f_i[\underset{\sim}{r}(\tau;nk)] = E\left\{\exp\left[-\beta \int_{\tau_{i-1}}^{\tau_i} U_3\left(\frac{\lambda}{\sqrt{2\pi}}\,\underset{\sim}{r}(\tau) + (\underset{\sim}{1},\underset{\sim}{2},\underset{\sim}{3})\right) d\tau\right] \right.$$

$$\left. \Big| \underset{\sim}{r}(\tau_{i-1}) = \underset{\sim}{r}_{i-1}, \underset{\sim}{r}(\tau_i) = \underset{\sim}{r}_i \right\} . \qquad (3.3.6)$$

The time interval in Eq. (3.3.6) may be renormalized and the endpoint conditions altered by the transformations

$$\tau' = k(\tau - \tau_{i-1}) ,$$

$$\underset{\sim}{r}'(\tau) = \sqrt{k}[\underset{\sim}{r}(\tau) - \underset{\sim}{r}_{i-1} - \tau(\underset{\sim}{r}_i - \underset{\sim}{r}_{i-1})] . \qquad (3.3.7)$$

Equation (3.3.4) then becomes

$$E\{F[\underset{\sim}{r}(\tau)]|\underset{\sim}{r}(1) = 0\} = \int_{-\infty}^{\infty} \cdots \int_{-\infty}^{\infty} d\mu_k$$

$$\times \prod_{i=1}^{k} E\left\{\exp\left[-\frac{\beta}{k}\int_0^1 U_3\left(\frac{\lambda}{\sqrt{2\pi}}\left[\frac{\underset{\sim}{r}(\tau)}{\sqrt{k}} + \underset{\sim}{r}_{i-1} + \tau(\underset{\sim}{r}_i - \underset{\sim}{r}_{i-1})\right] + (\underset{\sim}{1},\underset{\sim}{2},\underset{\sim}{3})\right)d\tau\right]\right| \underset{\sim}{r}(1)=0\Big\} , \qquad (3.3.8)$$

where the primes on $\underset{\sim}{r}(\tau)$ and τ have been dropped. Since

$$\lambda/\sqrt{k} = \left[2\pi\hbar^2(\beta/k)/m\right]^{\frac{1}{2}} ,$$

the Wiener integrals on the right of Eq. (3.3.8) involve a temperature k times that in the Wiener integral on the left. We proceed, then, by finding a high temperature approximation for the Wiener integral and using Eq. (3.3.8) to extend its range of validity to lower temperatures.

The high temperature approximation to be used is the well known Wigner-Kirkwood expansion in powers of β and λ^2[1,24]. The most useful form of this expansion for the following work will be the expansion for the quantity

$$G = \ell n E\left\{\exp\left[-\beta\int_0^1 U_3\left(\frac{\lambda}{\sqrt{2\pi}}\,\underset{\sim}{r}(\tau) + \underset{\sim}{r} + \tau(\underset{\sim}{s}-\underset{\sim}{r})\right)d\tau\right]\Big|\underset{\sim}{r}(1)=0\right\} . \qquad (3.3.9)$$

Introduce a parameter η multiplying the path, $\underset{\sim}{r}(\tau)$, in the Wiener integral, and define the following functions of η

$$f(\eta) = \exp\left[-\beta\int_0^1 U_3\left(\frac{\lambda\eta}{\sqrt{2\pi}}\,\underset{\sim}{r}(\tau) + \underset{\sim}{r} + \tau(\underset{\sim}{s}-\underset{\sim}{r})\right)d\tau\right] ,$$

$$F(\eta) = E\{f(\eta)\,|\,\underset{\sim}{r}(1) = 0\} ,$$

and

$$G(\eta) = \ell n F(\eta) . \qquad (3.3.10)$$

A formal series expansion for G may then be found by expanding $G(\eta)$ as a power series in η about $\eta = 0$ and taking the limit $\eta \to 1$ to obtain

$$G = \lim_{\eta\to 1} G(\eta) . \qquad (3.3.11)$$

Up to order η^2 one finds

$$G(\eta) = \ell n F(0) + \frac{\eta}{F(0)} \left.\frac{dF(\eta)}{d\eta}\right|_{\eta=0}$$

$$+ \frac{\eta^2}{2}\left\{-\left[\frac{1}{F(0)}\left.\frac{dF(\eta)}{d\eta}\right|_{\eta=0}\right]^2 + \frac{1}{F(0)}\left.\frac{d^2F(\eta)}{d\eta^2}\right|_{\eta=0}\right\} + \ldots . \qquad (3.3.12)$$

The integrand of the Wiener integral $F(0)$ is independent of the path so it is seen from the normalization condition, Eq. (3.1.4), that

$$F(0) = f(0) = \exp\left[-\beta \int_0^1 U_3(\underset{\sim}{r} + \tau(\underset{\sim}{s}-\underset{\sim}{r}))d\tau\right] . \qquad (3.3.13)$$

The first term in the expansion for G is then

$$G \simeq -\beta \int_0^1 U_3(\underset{\sim}{r}+\tau(\underset{\sim}{s}-\underset{\sim}{r}))d\tau , \qquad (3.3.14)$$

which is just the exponent of the classical Boltzmann factor with the potential replaced by its average over the straight line path from $\underset{\sim}{r}$ to $\underset{\sim}{s}$. If this approximation is used on the right hand side of Eq. (3.3.8), the result is precisely that of using Eq. (3.1.1) with a finite value of k as mentioned above.

The coefficient of η in the expansion for G is

$$\frac{1}{F(0)} \frac{dF(\eta)}{d\eta}\bigg|_{\eta=0}$$

$$= \frac{1}{F(0)} E\left\{-\beta f(0) \int_0^1 \frac{\lambda}{\sqrt{2\pi}} \underset{\sim}{r}(\tau) \cdot \underset{\sim}{\nabla} U_3(\underset{\sim}{r}+\tau(\underset{\sim}{s}-\underset{\sim}{r}))d\tau \,\middle|\, \underset{\sim}{r}(1)=0\right\} , \qquad (3.3.15)$$

where $\underset{\sim}{\nabla}$ is the 9-dimensional gradient operator. If one reverses the order of the Wiener integration and the integration over τ, the Wiener integral depends on $\underset{\sim}{r}(\tau)$ only for a fixed τ. This Wiener integral may be evaluated by using the interpolation formula, Eq. (3.1.9), for $\underset{\sim}{r}(\tau)$ with $\tau' = 0$, $\tau'' = 1$ and taking the expectation value over the normal distribution of the random variable $\underset{\sim}{\xi}$

$$E\{\underset{\sim}{r}(\tau) \,|\, \underset{\sim}{r}(1) = 0\} = \langle \underset{\sim}{\xi}[\tau(1-\tau)]^{\frac{1}{2}} \rangle_{av} = 0 , \qquad (3.3.16)$$

therefore

$$\frac{dF(\eta)}{d\eta}\bigg|_{\eta=0} = 0 . \qquad (3.3.17)$$

The coefficient of η thus vanishes and the coefficient of $\eta^2/2$ becomes

$$\frac{1}{F(0)}\frac{d^2F(\eta)}{d\eta^2}\bigg|_{\eta=0} = E\left\{\left[-\beta\int_0^1 \frac{\lambda}{\sqrt{2\pi}}\,\underset{\sim}{r}(\tau)\cdot\underset{\sim}{\nabla}U_3(\underset{\sim}{r}+\tau(\underset{\sim}{s}-\underset{\sim}{r}))d\tau\right]^2\bigg|\underset{\sim}{r}(1)=0\right\}$$

$$+ E\left\{-\beta\int_0^1 \frac{\lambda^2}{2\pi}\sum_{i=1}^{9}\sum_{j=1}^{9} r_i(\tau)r_j(\tau)\,\frac{\partial^2}{\partial i\partial j}\,U_3(\underset{\sim}{r}+\tau(\underset{\sim}{s}-\underset{\sim}{r}))d\tau\bigg|\underset{\sim}{r}(1)=0\right\}, \tag{3.3.18}$$

where $r_i(\tau)$ is the i-th coordinate function of $\underset{\sim}{r}(\tau)$ and $\frac{\partial U_3}{\partial i}$ denotes partial differentiation of U_3 with respect to its i-th argument. The first term on the right of Eq. (3.3.18) is of order $\beta^2\lambda^2\propto T^{-3}$ while the second term is of order $\beta\lambda^2\propto T^{-2}$. Thus to lowest order in $1/T$

$$\frac{1}{F(0)}\frac{d^2F(\eta)}{d\eta^2}\bigg|_{\eta=0}$$

$$\simeq -\frac{\beta\lambda^2}{2\pi}\int_0^1 \sum_{i=1}^{9}\sum_{j=1}^{9}\frac{\partial^2}{\partial i\partial j}\,U_3(\underset{\sim}{r}+\tau(\underset{\sim}{s}-\underset{\sim}{r}))E\{r_i(\tau)r_j(\tau)|\underset{\sim}{r}(1)=0\}d\tau\,. \tag{3.3.19}$$

Using the interpolation formula again one finds

$$E\{r_i(\tau)r_j(\tau)|\underset{\sim}{r}(1)=0\} = \begin{cases} 0\,, & (i\neq j) \\ \tau(1-\tau)\,, & (i=j)\,. \end{cases} \tag{3.3.20}$$

Therefore to order T^{-2}

$$G \simeq -\beta \int_0^1 U_3(\underset{\sim}{r}+\tau(\underset{\sim}{r}-\underset{\sim}{s}))d\tau - \frac{\beta\lambda^2}{4\pi}\int_0^1 \nabla^2 U_3(\underset{\sim}{r}+\tau(\underset{\sim}{s}-\underset{\sim}{r}))\tau(1-\tau)d\tau. \qquad (3.3.21)$$

If Eq. (3.3.21) is used for the Wiener integrals on the right of Eq. (3.3.8) one obtains the approximation

$$E\{F[\underset{\sim}{r}(\tau)]\,|\,\underset{\sim}{r}(1)=0\} = \int_{-\infty}^{\infty}\cdots\int_{-\infty}^{\infty} d\mu_k F[\underset{\sim}{r}(\tau;k)]C_k\ , \qquad (3.3.22)$$

where

$$C_k = \prod_{i=1}^{k} \exp\left[-\frac{\beta\lambda^2}{4\pi k^2}\int_0^1 \nabla^2 U_3\left(\frac{\lambda}{\sqrt{2\pi}}\left[\underset{\sim}{r}_{i-1}+\tau(\underset{\sim}{r}_i-\underset{\sim}{r}_{i-1})\right] + (\underset{\sim}{1},\underset{\sim}{2},\underset{\sim}{3})\right)\tau(1-\tau)d\tau\right]. \qquad (3.3.23)$$

If, for each i=1,2,...,k, the exponential in Eq. (3.3.23) is replaced by the first two terms in its power series expansion, it is seen that to order k^{-2}

$$C_k = \prod_{i=1}^{k}\left[1 - \frac{\beta\lambda^2}{4\pi k^2}\int_0^1 \nabla^2 U_3\left(\frac{\lambda}{\sqrt{2\pi}}\left[\underset{\sim}{r}_{i-1}+\tau(\underset{\sim}{r}_i-\underset{\sim}{r}_{i-1})\right] + (\underset{\sim}{1},\underset{\sim}{2},\underset{\sim}{3})\right)\tau(1-\tau)d\tau\right]. \qquad (3.3.24)$$

Equation (3.3.22) with Eq. (3.3.24) for C_k is precisely the formula obtained by Fosdick [21] who shows that if U_3 is sufficiently regular, the formula is correct to order k^{-2}. In the present application, where $U_3(\underset{\sim}{1},\underset{\sim}{2},\underset{\sim}{3}) = \sum_{i\neq j=1}^{3} V(r_{ij})$ with V(r) given by Eq. (2.1.2), the regularity conditions are not satisfied due to the singularity of

$V(r)$ at $r = 0$. It has been found from calculations of the 2-particle density matrix elements that the use of Eq. (3.3.23) for C_k gives better results for small k than are obtained using Eq. (3.3.24) due to the fact that at the singularities of U_3, Eq. (3.3.23) is bounded in absolute value while Eq. (3.3.24) is not. For this reason the exponential form for C_k will be used in the following calculations.

The Wigner-Kirkwood expansion can be carried out in the above manner by repeated use of the interpolation formula to obtain approximations which are correct to order k^{-m} for any m under the appropriate regularity conditions on U. However, the increasing complexity of the C_k obtained in this way causes an increase in computing time which must be balanced against the decrease obtained by using a smaller value of k in Eq. (3.3.22). The special case k = 1, which is equivalent to expanding the logarithm of the diagonal matrix element directly, is simplified by the fact that the τ integrals may be done immediately. The result of the expansion to order T^{-3} in this case is

$$\ell n\, E\left\{\exp\left[-\beta\int_0^1 U_3\left(\frac{\lambda}{\sqrt{2\pi}}[\underset{\sim}{r}(\tau)+(\underset{\sim}{1},\underset{\sim}{2},\underset{\sim}{3})]\right)d\tau\,\middle|\,\underset{\sim}{r}(1)=0\right\}\right.$$

$$\simeq -\beta U_3(\underset{\sim}{1},\underset{\sim}{2},\underset{\sim}{3}) - \frac{\beta\lambda^2}{24\pi}\nabla^2 U_3(\underset{\sim}{1},\underset{\sim}{2},\underset{\sim}{3}) + \frac{\beta^2\lambda^2}{48\pi}[\underset{\sim}{\nabla} U_3(\underset{\sim}{1},\underset{\sim}{2},\underset{\sim}{3})]^2$$

$$+ \frac{\beta\lambda^4}{960\pi^2}\nabla^4 U_3(\underset{\sim}{1},\underset{\sim}{2},\underset{\sim}{3}) \,. \qquad (3.3.25)$$

4. EVALUATION OF $g_1(r_{12})$

4.1 The Multiple Integral Approximation for $g_1(r_{12})$

The complexity of the 3-particle functions entering into the calculation of $g_1(r_{12})$ can be reduced somewhat by consideration of the symmetries of the problem. Since there is no fixed external field, the density matrix must depend only on the relative positions of the particles, and hence the first simplification should be to separate out the center of mass motion. Define the usual center of mass and relative coordinates for a system of three particles, Figure 1, by

$$\underset{\sim}{r}_{CM} = \frac{1}{3}(\underset{\sim}{1}+\underset{\sim}{2}+\underset{\sim}{3}) ,$$

$$\underset{\sim}{r}_{12} = \underset{\sim}{2}-\underset{\sim}{1} ,$$

$$\underset{\sim}{Q} = \underset{\sim}{3}-\frac{1}{2}(\underset{\sim}{2}+\underset{\sim}{1}) . \qquad (4.1.1)$$

The Jacobian of this transformation is unity, and furthermore

$$\frac{\hbar^2}{2m}\sum_{i=1}^{3}\nabla_i^2 = \frac{\hbar^2}{2m}\left(\frac{1}{3}\nabla_{CM}^2 + 2\nabla_{12}^2 + \frac{3}{2}\nabla_Q^2\right) \qquad (4.1.2)$$

so that the coordinates $\underset{\sim}{r}_{CM}$, $\underset{\sim}{r}_{12}$, and $\underset{\sim}{Q}$ behave as independent particles of masses 3m, m/2, and 2m/3 respectively.

Taking U_3 to be the sum of pair interactions as in Eq. (2.1.1) and noting that $\underset{\sim}{r}_{13} = \underset{\sim}{3}-\underset{\sim}{1} = \underset{\sim}{Q}+\frac{1}{2}\underset{\sim}{r}_{12}$ and $\underset{\sim}{r}_{23} = \underset{\sim}{3}-\underset{\sim}{2} = \underset{\sim}{Q}-\frac{1}{2}\underset{\sim}{r}_{12}$ it is seen

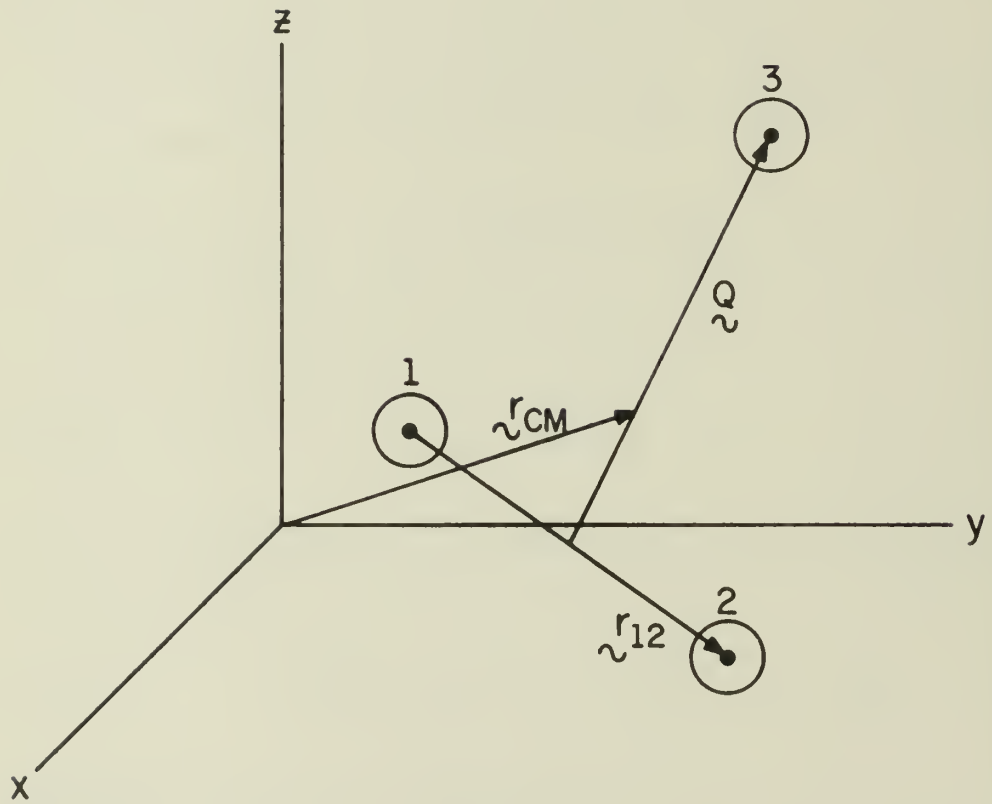

FIGURE 1. CENTER-OF-MASS AND RELATIVE COORDINATES FOR 3 PARTICLES.

that $W_3(\underset{\sim}{1},\underset{\sim}{2},\underset{\sim}{3})$ can be separated into the product of a center of mass factor which is independent of U_3 and a factor containing only the relative coordinates, $\underset{\sim}{r}_{12}$ and $\underset{\sim}{Q}$,

$$W_3(\underset{\sim}{1},\underset{\sim}{2},\underset{\sim}{3}) = \langle \underset{\sim}{1},\underset{\sim}{2},\underset{\sim}{3}|e^{-\beta H_3}|\underset{\sim}{1},\underset{\sim}{2},\underset{\sim}{3}\rangle ,$$

$$= \langle \underset{\sim}{r}_{CM}|e^{-\beta K_{CM}}|\underset{\sim}{r}_{CM}\rangle \langle \underset{\sim}{r}_{12},\underset{\sim}{Q}|e^{-\beta H_{rel}}|\underset{\sim}{r}_{12},\underset{\sim}{Q}\rangle , \qquad (4.1.3)$$

where

$$K_{CM} = -\frac{\hbar^2\nabla^2_{CM}}{2(3m)}$$

is the kinetic energy of the center of mass motion and

$$H_{rel} = -\frac{\hbar^2\nabla^2_{12}}{2(m/2)} - \frac{\hbar^2\nabla^2_{Q}}{2(2m/3)} + U_3(\underset{\sim}{r}_{12},\underset{\sim}{Q}) \qquad (4.1.4)$$

is the Hamiltonian operator for the relative coordinates. It is to be understood that the normalization factor of λ for each particle coordinate appearing in the definition, Eq. (2.2.4), of the Boltzmann matrix elements is to be replaced by the thermal wave length for a particle of mass corresponding to that associated with the appropriate transformed coordinate

$$\lambda_{CM} = \frac{\lambda}{\sqrt{3}} , \quad \lambda_{12} = \sqrt{2}\,\lambda , \text{ or } \lambda_{Q} = \left(\frac{3}{2}\right)^{\frac{1}{2}}\lambda . \qquad (4.1.5)$$

The normalization of the density matrix elements yields

$$\langle \underset{\sim}{r}_{CM} | e^{-\beta K_{CM}} | \underset{\sim}{r}_{CM} \rangle = 1 \tag{4.1.6}$$

so that, using Eq. (3.1.8), the diagonal density matrix element can be expressed in terms of a Wiener integral over paths in the 6-dimensional relative coordinate space of $\underset{\sim}{r}_{12}$ and $\underset{\sim}{Q}$:

$$W_3(\underset{\sim}{1},\underset{\sim}{2},\underset{\sim}{3})$$

$$= E\left\{ \exp\left[-\beta \int_0^1 U_3(\underset{\sim}{r}(\tau),\underset{\sim}{q}(\tau);\underset{\sim}{r}_{12},\underset{\sim}{Q}) d\tau \right] \middle| \underset{\sim}{r}(1)=\underset{\sim}{q}(1)=0 \right\} \tag{4.1.7}$$

where

$$U_3(\underset{\sim}{r}(\tau),\underset{\sim}{q}(\tau);\underset{\sim}{r}_{12},\underset{\sim}{Q}) = V\left(\frac{\lambda}{\sqrt{\pi}} \underset{\sim}{r}(\tau) + \underset{\sim}{r}_{12} \right)$$

$$+ V\left(\frac{\lambda}{2\sqrt{\pi}} (\sqrt{3}\, \underset{\sim}{q}(\tau) + \underset{\sim}{r}(\tau)) + \underset{\sim}{Q} + \frac{\underset{\sim}{r}_{12}}{2} \right) + V\left(\frac{\lambda}{2\sqrt{\pi}} (\sqrt{3}\, \underset{\sim}{q}(\tau) - \underset{\sim}{r}(\tau)) + \underset{\sim}{Q} - \frac{\underset{\sim}{r}_{12}}{2} \right) \tag{4.1.8}$$

and V(r) is given by Eq. (2.1.2).

The center of mass motion can also be eliminated from the 2-particle density matrix elements occurring in the expression for $g_1(r_{12})$, Eq. (2.3.17). A typical 2-particle diagonal matrix element is

$$W_2(\underset{\sim}{1},\underset{\sim}{2}) = E\left\{\exp\left[-\beta\int_0^1 V\left(\frac{\lambda}{\sqrt{\pi}}\,\underset{\sim}{q}'(\tau) + \underset{\sim}{Q} + \frac{\underset{\sim}{r}_{12}}{2}\right)d\tau\right]\middle|\underset{\sim}{q}'(1)=0\right\}. \tag{4.1.9}$$

One can thus write

$$g_1(r_{12}) = \frac{1}{W_2(\underset{\sim}{1},\underset{\sim}{2})}\int d^3\underset{\sim}{Q}\left[E\left\{F_{123}(\underset{\sim}{r}(\tau),\underset{\sim}{q}(\tau))\middle|\underset{\sim}{r}(1)=\underset{\sim}{q}(1)=0\right\}\right.$$

$$-E\left\{F_{12}(\underset{\sim}{r}'(\tau))F_{13}(\underset{\sim}{q}'(\tau))\middle|\underset{\sim}{r}'(1)=\underset{\sim}{q}'(1)=0\right\}$$

$$\left.-E\left\{F_{12}(\underset{\sim}{r}''(\tau))F_{23}(\underset{\sim}{q}''(\tau))\middle|\underset{\sim}{r}''(1)=\underset{\sim}{q}''(1)=0\right\} + E\left\{F_{12}(\underset{\sim}{r}'''(\tau))\middle|\underset{\sim}{r}'''(1)=0\right\}\right], \tag{4.1.10}$$

where

$$F_{123}(\underset{\sim}{r}(\tau),\underset{\sim}{q}(\tau)) = \exp\left[-\beta\int_0^1 U_3(\underset{\sim}{r}(\tau),\underset{\sim}{q}(\tau);\underset{\sim}{r}_{12},\underset{\sim}{Q})d\tau\right],$$

$$F_{12}(\underset{\sim}{r}'(\tau)) = \exp\left[-\beta\int_0^1 V\left(\frac{\lambda}{\sqrt{\pi}}\,\underset{\sim}{r}'(\tau)+\underset{\sim}{r}_{12}\right)d\tau\right],$$

$$F_{13}(\underset{\sim}{q}'(\tau)) = \exp\left[-\beta\int_0^1 V\left(\frac{\lambda}{\sqrt{\pi}}\,\underset{\sim}{q}'(\tau) + \underset{\sim}{Q} + \frac{\underset{\sim}{r}_{12}}{2}\right)d\tau\right],$$

and

$$F_{23}(\underset{\sim}{q}''(\tau)) = \exp\left[-\beta\int_0^1 V\left(\frac{\lambda}{\sqrt{\pi}}\,\underset{\sim}{q}''(\tau) + \underset{\sim}{Q} - \frac{\underset{\sim}{r}_{12}}{2}\right)d\tau\right]. \tag{4.1.11}$$

Since the expectation value is a linear operator, one may identify $\underset{\sim}{r}'(\tau)$, $\underset{\sim}{r}''(\tau)$, and $\underset{\sim}{r}'''(\tau)$ with $\underset{\sim}{r}(\tau)$ and $\underset{\sim}{q}'(\tau)$ and $\underset{\sim}{q}''(\tau)$ with $\underset{\sim}{q}(\tau)$. The quantity $g_1(r_{12})$ can then be written in terms of a single Wiener integral

$$g_1(r_{12}) = \frac{1}{W_2(\underset{\sim}{1},\underset{\sim}{2})} \int d^3\underset{\sim}{Q}\, E\Big\{F_{123}(\underset{\sim}{r}(\tau),\underset{\sim}{q}(\tau))-F_{12}(\underset{\sim}{r}(\tau))F_{13}(\underset{\sim}{q}(\tau))$$

$$-F_{12}(\underset{\sim}{r}(\tau))F_{23}(\underset{\sim}{q}(\tau))+F_{12}(\underset{\sim}{r}(\tau))\Big|\underset{\sim}{r}(1)=\underset{\sim}{q}(1)=0\Big\} . \qquad (4.1.12)$$

Now let

$$G(\underset{\sim}{r}_{12},\underset{\sim}{Q}) = \frac{1}{W_2(\underset{\sim}{1},\underset{\sim}{2})}\left[W_3(\underset{\sim}{1},\underset{\sim}{2},\underset{\sim}{3})-W_2(\underset{\sim}{1},\underset{\sim}{2})W_2(\underset{\sim}{1},\underset{\sim}{3})-W_2(\underset{\sim}{1},\underset{\sim}{2})W_2(\underset{\sim}{2},\underset{\sim}{3})+W_2(\underset{\sim}{1},\underset{\sim}{2})\right] \qquad (4.1.13)$$

be the $\underset{\sim}{Q}$-integrand of $g_1(r_{12})$. Noting that the interaction potentials depend only upon the magnitude of the separations, r_{12}, r_{13}, and r_{23} between the particles it can be seen that if r_{12} is taken to lie along the axis of polar coordinates, $(\rho_Q, \theta_Q, \varphi_Q)$, for $\underset{\sim}{Q}$, then $G(r_{12},\underset{\sim}{Q})$ is independent of the direction of the polar axis and of φ_Q. Thus one can write

$$g_1(r_{12}) = 2\pi \int_0^{\pi} \sin\theta_Q d\theta_Q \int_0^{\infty} \rho_Q^2 d\rho_Q\, G(r_{12},\rho_Q,\theta_Q) . \qquad (4.1.14)$$

The integral over the position of the third particle which appears in $g_1(r_{12})$ can thus be reduced to a twofold integral.

Equations (4.1.8) and (4.1.11) show that F_{123} can be written as a product

$$F_{123}(\underset{\sim}{r}(\tau),\underset{\sim}{q}(\tau)) = F_{12}(\underset{\sim}{r}(\tau))F_{13}\left(\frac{\sqrt{3}}{2}\,\underset{\sim}{q}(\tau)+\frac{1}{2}\underset{\sim}{r}(\tau)\right)F_{23}\left(\frac{\sqrt{3}}{2}\,\underset{\sim}{q}(\tau)-\frac{1}{2}\underset{\sim}{r}(\tau)\right) . \qquad (4.1.15)$$

It should be noted that if $\underset{\sim}{r}(\tau)$ and $\underset{\sim}{q}(\tau)$ are conditional Wiener paths with $\underset{\sim}{r}(0)=\underset{\sim}{q}(0)=\underset{\sim}{r}(1)=\underset{\sim}{q}(1)=0$ and variance $[\tau(1-\tau)]^{\frac{1}{2}}$, then the linear combinations

$$\frac{\sqrt{3}}{2}\,\underset{\sim}{q}(\tau) \pm \frac{1}{2}\underset{\sim}{r}(\tau)$$

are conditional Wiener paths with the same distributions as $\underset{\sim}{r}(\tau)$ and $\underset{\sim}{q}(\tau)$. This can be seen from the interpolation formula, Eq. (3.1.9). If we consider just one component of the 3-dimensional paths, the interpolation formula gives

$$q_x(\tau) = \xi_q[\tau(1-\tau)]^{\frac{1}{2}}, \quad r_x'(\tau) = \xi_r[\tau(1-\tau)]^{\frac{1}{2}}$$

and

$$\frac{\sqrt{3}}{2}\,q_x(\tau) \pm \frac{1}{2}r_x(\tau) = \left(\frac{\sqrt{3}}{2}\,\xi_q \pm \frac{1}{2}\,\xi_r\right)[\tau(1-\tau)]^{\frac{1}{2}}, \qquad (4.1.16)$$

where ξ_q and ξ_r are normally distributed independent random variables with mean 0 and variance 1. The linear combinations

$$\frac{\sqrt{3}}{2}\,\xi_q \pm \frac{1}{2}\,\xi_r$$

are thus normally distributed also and have mean 0 and variance $\frac{3}{4} + \frac{1}{4} = 1$. The distributions for the coordinates of $\underset{\sim}{q}(\tau)$, $\underset{\sim}{r}(\tau)$, and

$$\frac{\sqrt{3}}{2}\,\underset{\sim}{q}(\tau) \pm \frac{1}{2}\,\underset{\sim}{r}(\tau)$$

are thus equivalent.

Define now the quantity

$$g_c(r_{12}) = \int d^3\underset{\sim}{Q}\; G_c(r_{12},\underset{\sim}{Q}) \;, \tag{4.1.17}$$

where

$$G_c(r_{12},\underset{\sim}{Q}) = \frac{1}{W_2(\underset{\sim}{1},\underset{\sim}{2})}\, E\Big\{F_{123}(\underset{\sim}{r}(\tau),\underset{\sim}{q}(\tau)) - F_{12}(\underset{\sim}{r}(\tau))F_{13}\left(\frac{\sqrt{3}}{2}\,\underset{\sim}{q}(\tau) + \frac{1}{2}\,\underset{\sim}{r}(\tau)\right)$$

$$- F_{12}(\underset{\sim}{r}(\tau))F_{23}\left(\frac{\sqrt{3}}{2}\,\underset{\sim}{q}(\tau) - \frac{1}{2}\,\underset{\sim}{r}(\tau)\right) + F_{12}(\underset{\sim}{r}(\tau))\,\Big|\,\underset{\sim}{r}(1)=\underset{\sim}{q}(1)=0\Big\} \;. \tag{4.1.18}$$

Due to an oversight the quantity $g_c(r_{12})$ rather than $g(r_{12})$ was originally calculated. The difference between these two quantities arises because, although the distributions of the arguments of F_{13} and F_{23} in Eq. (4.1.18) are the same as the distributions of the arguments of these functions in Eq. (4.1.12), the use of a linear combination of $\underset{\sim}{q}(\tau)$ and $\underset{\sim}{r}(\tau)$ as the argument of F_{13} in Eq. (4.1.18) introduces a spurious correlation between

$$F_{13}\left(\frac{\sqrt{3}}{2}\,\underset{\sim}{q}(\tau) + \frac{1}{2}\,\underset{\sim}{r}(\tau)\right)$$

and the functional $F_{12}(\underset{\sim}{r}(\tau))$ multiplying it and similarly for the product $F_{12}\,F_{23}$. The two factors in these products should be

uncorrelated since they arise from the product of two independent Wiener integrals. The function $g_1(r_{12})$ can be written as the sum of $g_c(r_{12})$ and a term which corrects for the unwanted correlation:

$$g_1(r_{12}) = g_c(r_{12}) + g_e(r_{12}) \ , \tag{4.1.19}$$

where

$$g_e(r_{12}) = \int d^3\underset{\sim}{Q}\ G_e(r_{12},\underset{\sim}{Q}) \ ,$$

and

$$G_e(r_{12},\underset{\sim}{Q}) = \frac{1}{W_2(\underset{\sim}{1},\underset{\sim}{2})} E\Big\{F_{12}(\underset{\sim}{r}(\tau))\Big[F_{13}\Big(\frac{\sqrt{3}}{2}\,\underset{\sim}{q}(\tau) + \frac{1}{2}\,\underset{\sim}{r}(\tau)\Big) - F_{13}(\underset{\sim}{q}(\tau))$$
$$+ F_{23}\Big(\frac{\sqrt{3}}{2}\,\underset{\sim}{q}(\tau) - \frac{1}{2}\,\underset{\sim}{r}(\tau)\Big) - F_{23}(\underset{\sim}{q}(\tau))\Big]\Big|\ \underset{\sim}{r}(1)=\underset{\sim}{q}(1)=0\Big\} \ . \tag{4.1.20}$$

The numerical calculation will thus involve separate evaluations of the terms $g_c(r_{12})$ and $g_e(r_{12})$.

Using Eq. (4.1.15) the quantity $G_c(r_{12},\underset{\sim}{Q})$ can be written in the form

$$G_c(r_{12},\underset{\sim}{Q}) = \frac{1}{W_2(\underset{\sim}{1},\underset{\sim}{2})} E\Big\{F_{12}(\underset{\sim}{r}(\tau))\Big[F_{13}\Big(\frac{\sqrt{3}}{2}\,\underset{\sim}{q}(\tau) + \frac{1}{2}\,\underset{\sim}{r}(\tau)\Big) - 1\Big]$$
$$\times\Big[F_{23}\Big(\frac{\sqrt{3}}{2}\,\underset{\sim}{q}(\tau) - \frac{1}{2}\,\underset{\sim}{r}(\tau)\Big) - 1\Big]\Big|\underset{\sim}{r}(1)=\underset{\sim}{q}(1)=0\Big\} \ . \tag{4.1.21}$$

The results of Section 3.3 may now be used in order to express $G_c(r_{12},\underset{\sim}{Q})$ and $G_e(r_{12},\underset{\sim}{Q})$ in terms of multiple Riemann integrals over a 6k-dimensional space. Let $\underset{\sim}{r}(\tau;k)$ be the broken straight line path defined in Section 3.1 with breakpoints at $\underset{\sim}{r}_i$, i=0,1,...,k, and similarly for $\underset{\sim}{q}(\tau;k)$. Define the functions

$$D_{12}(\underset{\sim}{r}(\tau;k)) = F_{12}(\underset{\sim}{r}(\tau;k))$$

$$\times \exp\left[- \sum_{i=1}^{k} \frac{\beta\lambda^2}{2\pi k^2} \int_0^1 V''\left(\frac{\lambda}{\sqrt{\pi}} [\underset{\sim}{r}_{i-1} + \tau(\underset{\sim}{r}_i - \underset{\sim}{r}_{i-1})] + \underset{\sim}{r}_{12} \right) \tau(1-\tau) d\tau \right] ,$$

$$D_{13}(\underset{\sim}{q}(\tau;k)) = F_{13}(\underset{\sim}{q}(\tau;k))$$

$$\times \exp\left[- \sum_{i=1}^{k} \frac{\beta\lambda^2}{2\pi k^2} \int_0^1 V''\left(\frac{\lambda}{\sqrt{\pi}} [\underset{\sim}{q}_{i-1} + \tau(\underset{\sim}{q}_i - \underset{\sim}{q}_{i-1})] + \underset{\sim}{Q} + \frac{\underset{\sim}{r}_{12}}{2} \right) \tau(1-\tau) d\tau \right] ,$$

$$D_{23}(\underset{\sim}{q}(\tau;k)) = F_{23}(\underset{\sim}{q}(\tau;k))$$

$$\times \exp\left[- \sum_{i=1}^{k} \frac{\beta\lambda^2}{2\pi k^2} \int_0^1 V''\left(\frac{\lambda}{\sqrt{\pi}} [\underset{\sim}{q}_{i-1} + \tau(\underset{\sim}{q}_i - \underset{\sim}{q}_{i-1})] + \underset{\sim}{Q} - \frac{\underset{\sim}{r}_{12}}{2} \right) \tau(1-\tau) d\tau \right] ,$$

where (4.1.22)

$$V''(\underset{\sim}{r}) = \nabla^2 V(\underset{\sim}{r}) . \tag{4.1.23}$$

The approximations for G_c and G_e are then

$$G_c(r_{12}, \underset{\sim}{Q}) \simeq \frac{1}{W_2(\underset{\sim}{1}, \underset{\sim}{2})} \int_{-\infty}^{\infty} \cdots \int_{-\infty}^{\infty} D_{12}(\underset{\sim}{r}(\tau;k)) \left[D_{13}\left(\frac{\sqrt{3}}{2} \underset{\sim}{q}(\tau;k) + \frac{1}{2} \underset{\sim}{r}(\tau;k) \right) - 1 \right]$$

$$\times \left[D_{23}\left(\frac{\sqrt{3}}{2} \underset{\sim}{q}(\tau;k) - \frac{1}{2} \underset{\sim}{r}(\tau;k) \right) - 1 \right] d\mu_{rk} d\mu_{qk} , \tag{4.1.24}$$

and

$$G_e(r_{12},\underset{\sim}{Q}) \simeq \frac{1}{W_2(\underset{\sim}{1},\underset{\sim}{2})} \int_{-\infty}^{\infty}\cdots\int_{-\infty}^{\infty} D_{12}(\underset{\sim}{r}(\tau;k)) \left[D_{13}\left(\frac{\sqrt{3}}{2}\,\underset{\sim}{q}(\tau;k) + \frac{1}{2}\,\underset{\sim}{r}(\tau;k)\right)\right.$$

$$\left. - D_{13}(\underset{\sim}{q}(\tau;k)) + D_{23}\left(\frac{\sqrt{3}}{2}\,\underset{\sim}{q}(\tau;k) - \frac{1}{2}\,\underset{\sim}{r}(\tau;k)\right) - D_{23}(\underset{\sim}{q}(\tau;k))\right] d\mu_{rk}d\mu_{qk} \,, \tag{4.1.25}$$

where

$$d\mu_{sk} = (2\pi)^{\frac{3}{2}}(2\pi/k)^{-\frac{3k}{2}} \exp\left[- \sum_{i=1}^{k} \frac{(\underset{\sim}{s}_i - \underset{\sim}{s}_{i-1})^2}{2(1/k)} \right] \prod_{i=1}^{k-1} d^3\underset{\sim}{s}_i \,, \tag{4.1.26}$$

with s = r or q.

From the discussion in Section 3.3 of the order of accuracy of Eq. (3.3.22) as an approximation for the Wiener integral it is seen that the above approximations for G_c and G_e cannot be expected to be correct to more than order k^{-2}. The order of accuracy may be less due to the singularity of V(r). In view of this fact the integrals over τ in Eq. (4.1.22) may be replaced by their Simpson's rule approximations without decreasing the order of accuracy of these formulae. If we let $\underset{\sim}{r}^{(k)}$ and $\underset{\sim}{q}^{(k)}$ be the 3k-dimensional vectors $(\underset{\sim}{r}_1, \underset{\sim}{r}_2,\ldots,\underset{\sim}{r}_k)$ and $(\underset{\sim}{q}_1, \underset{\sim}{q}_2,\ldots,\underset{\sim}{q}_k)$ respectively and recall that $\underset{\sim}{r}_0 = \underset{\sim}{q}_0 = \underset{\sim}{r}_k = \underset{\sim}{q}_k = 0$, then

$$G_c(r_{12},\underset{\sim}{Q}) = \frac{1}{W_2(\underset{\sim}{1},\underset{\sim}{2})}\int_{-\infty}^{\infty}\cdots\int_{-\infty}^{\infty} D_{12}(\underset{\sim}{r}^{(k)})\left[D_{13}\left(\frac{\sqrt{3}}{2}\,\underset{\sim}{g}^{(k)}+\frac{1}{2}\,\underset{\sim}{r}^{(k)}\right)-1\right]$$

$$\times\left[D_{23}\left(\frac{\sqrt{3}}{2}\,\underset{\sim}{g}^{(k)}-\frac{1}{2}\,\underset{\sim}{r}^{(k)}\right)-1\right]d\mu_{rk}d\mu_{qk}\,, \qquad (4.1.27)$$

and

$$G_e(r_{12},\underset{\sim}{Q}) = \frac{1}{W_2(\underset{\sim}{1},\underset{\sim}{2})}\int_{-\infty}^{\infty}\cdots\int_{-\infty}^{\infty} D_{12}(\underset{\sim}{r}^{(k)})\left[D_{13}\left(\frac{\sqrt{3}}{2}\,\underset{\sim}{g}^{(k)}+\frac{1}{2}\,\underset{\sim}{r}^{(k)}\right)-D_{13}(\underset{\sim}{g}^{(k)})\right.$$

$$\left.+D_{23}\left(\frac{\sqrt{3}}{2}\,\underset{\sim}{g}^{(k)}-\frac{1}{2}\,\underset{\sim}{r}^{(k)}\right)-D_{23}(\underset{\sim}{g}^{(k)})\right]d\mu_{rk}d\mu_{qk}\,, \qquad (4.1.28)$$

where

$$D_{12}(\underset{\sim}{r}^{(k)}) = \exp\left\{\frac{-\beta}{6k}\sum_{i=1}^{k}\left[V\left(\frac{\lambda}{\sqrt{\pi}}\,\underset{\sim}{r}_{i-1}+\underset{\sim}{r}_{12}\right)+4V\left(\frac{\lambda}{\sqrt{\pi}}\,\left(\frac{\underset{\sim}{r}_i+\underset{\sim}{r}_{i-1}}{2}\right)+\underset{\sim}{r}_{12}\right)\right.\right.$$

$$\left.\left.+V\left(\frac{\lambda}{\sqrt{\pi}}\,\underset{\sim}{r}_i+\underset{\sim}{r}_{12}\right)+\frac{\lambda^2}{2\pi k}V''\left(\frac{\lambda}{\sqrt{\pi}}\,\left(\frac{\underset{\sim}{r}_i+\underset{\sim}{r}_{i-1}}{2}\right)+\underset{\sim}{r}_{12}\right)\right]\right\}\,,$$

$$D\left\{\begin{matrix}13\\23\end{matrix}\right\}(\underset{\sim}{q}^{(k)}) = \exp\left\{\frac{-\beta}{6k}\sum_{i=1}^{k}\left[V\left(\frac{\lambda}{\sqrt{\pi}}\,\underset{\sim}{q}_{i-1}+\underset{\sim}{Q}\pm\frac{\underset{\sim}{r}_{12}}{2}\right)+4V\left(\frac{\lambda}{\sqrt{\pi}}\,\left(\frac{\underset{\sim}{q}_i+\underset{\sim}{q}_{i-1}}{2}\right)+\underset{\sim}{Q}\pm\frac{\underset{\sim}{r}_{12}}{2}\right)\right.\right.$$

$$\left.\left.+V\left(\frac{\lambda}{\sqrt{\pi}}\,\underset{\sim}{q}_i+\underset{\sim}{Q}\pm\frac{\underset{\sim}{r}_{12}}{2}\right)+\frac{\lambda^2}{2\pi k}V''\left(\frac{\lambda}{\sqrt{\pi}}\left(\frac{\underset{\sim}{q}_i+\underset{\sim}{q}_{i-1}}{2}\right)+\underset{\sim}{Q}\pm\frac{\underset{\sim}{r}_{12}}{2}\right)\right]\right\}\,, \qquad (4.1.29)$$

where the + sign in the last equation corresponds to D_{13} and the - sign to D_{23}.

4.2 Monte Carlo Evaluation of the Multiple Integrals

It has been indicated above that the 6(k-1)-fold integrals appearing in Eqs. (4.1.27) and (4.1.28) can be evaluated by a Monte Carlo procedure. The quantities $d\mu_{rk}$ and $d\mu_{qk}$ have the properties of probability densities on 3(k-1)-dimensional spaces since the integral of either of these quantities over any 3(k-1)-dimensional Borel set is non-negative and the integral over the whole space is unity (see Eq. (3.1.2)). The simplest Monte Carlo scheme for evaluating the multiple integrals is to choose a sequence of independent 6k-dimensional vectors $(\underset{\sim}{r}_{\ell}^{(k)}, \underset{\sim}{q}_{\ell}^{(k)})$, $\underset{\sim}{r}_{k,\ell} = \underset{\sim}{q}_{k,\ell} = 0$, $\ell = 1, 2, \ldots, M$ with probability density $d\mu_{rk}\, d\mu_{qk}$, evaluate the integrands of G_c and G_e for each vector, and average over the set of M vectors. If one lets $I_c(\underset{\sim}{r}^{(k)}, \underset{\sim}{q}^{(k)})$ and $I_e(\underset{\sim}{r}^{(k)}, \underset{\sim}{q}^{(k)})$ represent the integrands of G_c and G_e respectively, then by the law of large numbers

$$\lim_{M\to\infty} \frac{1}{M} \sum_{\ell=1}^{M} I_c(\underset{\sim}{r}_{\ell}^{(k)}, \underset{\sim}{q}_{\ell}^{(k)}) = \int_{-\infty}^{\infty} \cdots \int_{-\infty}^{\infty} I_c(\underset{\sim}{r}^{(k)}, \underset{\sim}{q}^{(k)})\, d\mu_{rk}\, d\mu_{qk} = G_c, \tag{4.2.1}$$

with probability one and similarly for G_e.

Vectors $\underset{\sim}{r}^{(k)}$ with distribution $d\mu_{rk}$ can be generated from 3(k-1) independent, normally distributed random variables by means of the interpolation formula, Eq. (3.1.9). The endpoint conditions require that $\underset{\sim}{r}_o = \underset{\sim}{r}_k = 0$, and the other 3(k-1) coordinates can be generated by the equation

$$\underset{\sim}{r}_i = \frac{\underset{\sim}{r}_{i-1}\left(1 - \frac{i}{k}\right)}{1 - \frac{i-1}{k}} + \underset{\sim}{\xi}_i \left[\frac{\frac{1}{k}\left(1 - \frac{i}{k}\right)}{1 - \frac{i-1}{k}}\right]^{\frac{1}{2}}, \qquad (4.2.2)$$

for i = 1, 2, ..., k - 1, where $\underset{\sim}{\xi}_i$ is a 3-dimensional random variable, the coordinate variables of which are normally distributed with mean 0 and variance 1. The vectors $\underset{\sim}{q}_{\ell}^{(k)}$ are generated by the same procedure. This straightforward Monte Carlo scheme has been used [6] to compute the 2-particle density matrix element, $W_2(\underset{\sim}{1},\underset{\sim}{2})$.

The 3-particle functions G_c and G_e are well adapted to a more sophisticated Monte Carlo procedure which should have a smaller variance than the straightforward scheme, thereby reducing the number of samples necessary for a given accuracy. This procedure is the importance sampling technique first introduced by Metropolis and collaborators [25] for evaluating averages over the Boltzmann distribution. The following discussion is, to some extent, an

extension to a continuous sample space of the description of this technique given by Hammersly and Handscomb [26].

Let G_c and G_e both be typified by

$$G_d(r_{12}, \underset{\sim}{Q}) = \int_{-\infty}^{\infty} \cdots \int_{-\infty}^{\infty} I(\underset{\sim}{r}^{(k)}, \underset{\sim}{q}^{(k)})\, d\mu_{rk}\, d\mu_{qk}\,, \tag{4.2.3}$$

where

$$I(\underset{\sim}{r}^{(k)}, \underset{\sim}{q}^{(k)}) = \frac{D_{12}(\underset{\sim}{r}^{(k)})}{W_2(\underset{\sim}{1},\underset{\sim}{2})} L(\underset{\sim}{r}^{(k)}, \underset{\sim}{q}^{(k)}), \tag{4.2.4}$$

and let

$$P(\underset{\sim}{r}^{(k)}) = \frac{D_{12}(\underset{\sim}{r}^{(k)})}{W_2(\underset{\sim}{1},\underset{\sim}{2})}\,. \tag{4.2.5}$$

This factor, which appears in the integrands of both G_c and G_e, is the basis for the importance sampling procedure. It is seen from the definition, Eqs. (4.1.29), of $D_{12}(\underset{\sim}{r}^{(k)})$ that this quantity is non-negative. Furthermore, to the order of the approximation used in Eqs. (4.1.24) and (4.1.25), one can write

$$W_2(\underset{\sim}{1},\underset{\sim}{2}) = \int_{-\infty}^{\infty} \cdots \int_{-\infty}^{\infty} D_{12}(\underset{\sim}{r}^{(k)})\, d\mu_{rk}\,, \tag{4.2.6}$$

and hence

$$\int_{-\infty}^{\infty} \cdots \int_{-\infty}^{\infty} P(\underset{\sim}{r}^{(k)})\, d\mu_{rk} = 1 \,. \tag{4.2.7}$$

Thus $P(\underset{\sim}{r}^{(k)})\, d\mu_{rk}$ has the properties of a probability density on the $3(k-1)$-dimensional space of $\underset{\sim}{r}^{(k)}$. If vectors $\underset{\sim}{r}^{(k)}$ and $\underset{\sim}{q}^{(k)}$ are generated with probability density $P(\underset{\sim}{r}^{(k)})\, d\mu_{rk}\, d\mu_{qk}$ and $L(\underset{\sim}{r}^{(k)}, \underset{\sim}{q}^{(k)})$ is averaged over the vectors so generated, the average will approach G_d with probability one as the number of samples becomes infinite. Qualitatively, the advantage of this scheme over straightforward sampling is that some of the variation in the integrand $I(\underset{\sim}{r}^{(k)}, \underset{\sim}{q}^{(k)})$ has been absorbed into the probability density. The variance reduction is indicated intuitively by the fact that vectors $\underset{\sim}{r}^{(k)}$ for which $D_{12}(\underset{\sim}{r}^{(k)})$ and hence $I(\underset{\sim}{r}^{(k)}, \underset{\sim}{q}^{(k)})$ are small will be generated with low probability by the importance sampling procedure.

It remains to show how vectors $\underset{\sim}{r}^{(k)}$ can be generated with probability $P(\underset{\sim}{r}^{(k)})\, d\mu_{rk}$. This is accomplished by producing a Markov chain, $\{\underset{\sim}{r}_t^{(k)},\ t = 1, 2, 3, \ldots\}$, with a stationary transition probability function $p(\underset{\sim}{r}_{t+1}^{(k)} | \underset{\sim}{r}_t^{(k)})$, satisfying

$$\int_J \cdots \int P(\underset{\sim}{r}'^{(k)})\, d\mu_{r'k}$$

$$= \int_J \cdots \int_{-\infty}^{\infty} \int_{-\infty}^{\infty} \cdots \int_{-\infty}^{\infty} p(\underset{\sim}{r}'^{(k)} | \underset{\sim}{r}^{(k)})\, P(\underset{\sim}{r}^{(k)})\, d\mu_{rk}\, d^{3(k-1)}\underset{\sim}{r}' \,, \qquad (4.2.8)$$

where

$$d^{3(k-1)}\underset{\sim}{r}' = d^3\underset{\sim}{r}'_1 d^3\underset{\sim}{r}'_2 \cdots d^3\underset{\sim}{r}'_{k-1} \,, \qquad (4.2.9)$$

and where J is any set in the 3(k-1)-dimensional space of $\underset{\sim}{r}'^{(k)}$ which is measurable with respect to $P(\underset{\sim}{r}'^{(k)})\, d\mu_{r'k}$. The law of large numbers for Markov chains [27] states that if the Markov chain, $\{\underset{\sim}{r}_t^{(k)}\}$, is such that Eq. (4.2.8) is satisfied and if there is only one ergodic set then

$$\lim_{M\to\infty} \frac{1}{M} \sum_{t=1}^{M} L(\underset{\sim}{r}_t^{(k)}, \underset{\sim}{q}^{(k)}) = \int_{-\infty}^{\infty} \cdots \int_{-\infty}^{\infty} L(\underset{\sim}{r}^{(k)}, \underset{\sim}{q}^{(k)})\, P(\underset{\sim}{r}^{(k)})\, d\mu_{rk}, \qquad (4.2.10)$$

for almost all realizations of the Markov chain. Thus if $L(\underset{\sim}{r}^{(k)}, \underset{\sim}{q}^{(k)})$ is averaged over $\underset{\sim}{r}^{(k)}$ produced by the Markov chain and $\underset{\sim}{q}^{(k)}$ generated by the straightforward Monte Carlo scheme, the result will be an approximation for G_d.

We must now demonstrate a procedure which will generate a Markov chain which satisfies the above conditions. It will be convenient for the rest of this section to deal with only the

x-components, x_i, of each 3-dimensional vector, $\underset{\sim}{r}_i$. All quantities defined above in terms of the 3k-dimensional vector, $\underset{\sim}{r}^{(k)} = (\underset{\sim}{r}_1, \underset{\sim}{r}_2, \ldots, \underset{\sim}{r}_k)$, $\underset{\sim}{r}_0 = \underset{\sim}{r}_k = 0$, are assumed to have analogous definitions in terms of the k-dimensional vector $\underset{\sim}{x} = (x_1, x_2, \ldots, x_k)$, $x_0 = x_k = 0$. The generalization to three space components will be obvious, and the notation will be much simplified if we assume all vectors to be k-dimensional and drop the use of k as a superscript or subscript to indicate dimensionality for the rest of this section.

Let $w(\underset{\sim}{x})$ be defined by

$$d\mu_x = w(\underset{\sim}{x}) d^{k-1}\underset{\sim}{x}, \quad d^{k-1}\underset{\sim}{x} = dx_1\, dx_2 \ldots dx_{k-1}, \tag{4.2.11}$$

so that

$$w(\underset{\sim}{x}) = (2\pi)^{\frac{1}{2}} \left(\frac{k}{2\pi}\right)^{\frac{k}{2}} \exp\left[-\frac{k}{2}\sum_{i=1}^{k}(x_i - x_{i-1})^2\right]. \tag{4.2.12}$$

A transition probability function, $p(\underset{\sim}{x}'|\underset{\sim}{x})$, is then needed to satisfy Eq. (4.2.8), which now becomes

$$\int_J \cdots \int P(\underset{\sim}{x}')\, w(\underset{\sim}{x}') d^{k-1}\underset{\sim}{x}'$$

$$= \int_J \cdots \int_{-\infty}^{\infty} \cdots \int_{-\infty}^{\infty} p(\underset{\sim}{x}'|\underset{\sim}{x})\, P(\underset{\sim}{x}) w(\underset{\sim}{x})\, d^{k-1}\underset{\sim}{x}\, d^{k-1}\underset{\sim}{x}' \,. \tag{4.2.13}$$

First define the function

$$p^*(\underset{\sim}{x}'|\underset{\sim}{x}) = \left(\frac{k}{\pi}\right)^{\frac{k-1}{2}} \exp\left[-k \sum_{i=1}^{k-1} \left(x_i' - \frac{x_{i-1}' + x_{i+1}}{2}\right)^2\right] . \tag{4.2.14}$$

This function satisfies the criteria for a transition probability function since

$$p^*(\underset{\sim}{x}'|\underset{\sim}{x}) \geq 0 \tag{4.2.15}$$

and

$$\int_{-\infty}^{\infty} \cdots \int_{-\infty}^{\infty} p^*(\underset{\sim}{x}'|\underset{\sim}{x}) d^{k-1}\underset{\sim}{x}' = 1. \tag{4.2.16}$$

The function $p(\underset{\sim}{x}'|\underset{\sim}{x})$ is now defined by

$$p(\underset{\sim}{x}'|\underset{\sim}{x}) = \begin{cases} p^*(\underset{\sim}{x}'|\underset{\sim}{x}) \ \dfrac{P(\underset{\sim}{x}')}{P(\underset{\sim}{x})} , \text{ if } P(\underset{\sim}{x}') < P(\underset{\sim}{x}) , \\ p^*(\underset{\sim}{x}'|\underset{\sim}{x}) + \underset{\sim}{\delta}(\underset{\sim}{x}',\underset{\sim}{x}) \int \cdots \int_{\{\underset{\sim}{x}''|P(\underset{\sim}{x}'') < P(\underset{\sim}{x})\}} p^*(\underset{\sim}{x}''|\underset{\sim}{x}) \left[1 - \dfrac{P(\underset{\sim}{x}'')}{P(\underset{\sim}{x})}\right] d^{k-1}\underset{\sim}{x}'', \\ \text{if } P(\underset{\sim}{x}') \geq P(\underset{\sim}{x}) , \end{cases} \tag{4.2.17}$$

where $\{\underset{\sim}{x}''|P(\underset{\sim}{x}'') < P(\underset{\sim}{x})\}$ is the set of all $\underset{\sim}{x}''$ such that $P(\underset{\sim}{x}'') < P(\underset{\sim}{x})$ and

δ is the Dirac delta function. The function $p(\underset{\sim}{x}'|\underset{\sim}{x})$ is a valid transition function since it is non-negative and satisfies

$$\int_{-\infty}^{\infty} \cdots \int_{-\infty}^{\infty} p(\underset{\sim}{x}'|\underset{\sim}{x}) d^{k-1}\underset{\sim}{x}'$$

$$= \int_{\{\underset{\sim}{x}'|P(\underset{\sim}{x}') \geq P(\underset{\sim}{x})\}} \cdots \int \left[p^*(\underset{\sim}{x}'|\underset{\sim}{x}) \right.$$

$$\left. + \delta(\underset{\sim}{x}', \underset{\sim}{x}) \int_{\{\underset{\sim}{x}''|P(\underset{\sim}{x}'') < P(\underset{\sim}{x})\}} \cdots \int p^*(\underset{\sim}{x}''|\underset{\sim}{x}) \left(1 - \frac{P(\underset{\sim}{x}'')}{P(\underset{\sim}{x})} \right) d^{k-1}\underset{\sim}{x}'' \right] d^{k-1}\underset{\sim}{x}'$$

$$+ \int_{\{\underset{\sim}{x}'|P(\underset{\sim}{x}') < P(\underset{\sim}{x})\}} \cdots \int p^*(\underset{\sim}{x}'|\underset{\sim}{x}) \frac{P(\underset{\sim}{x}')}{P(\underset{\sim}{x})} d^{k-1}\underset{\sim}{x}' ,$$

$$= \int_{\{\underset{\sim}{x}'|P(\underset{\sim}{x}') \geq P(\underset{\sim}{x})\}} \cdots \int p^*(\underset{\sim}{x}'|\underset{\sim}{x}) d^{k-1}\underset{\sim}{x}'$$

$$+ \int_{\{\underset{\sim}{x}''|P(\underset{\sim}{x}'') < P(\underset{\sim}{x})\}} \cdots \int p^*(\underset{\sim}{x}''|\underset{\sim}{x}) d^{k-1}\underset{\sim}{x}'' ,$$

$$= 1. \qquad (4.2.18)$$

In order to show that $p(\underset{\sim}{x}'|\underset{\sim}{x})$ satisfies Eq. (4.2.13) it will be useful to define the "transpose", $\underset{\sim}{x}^T$, of a vector, $\underset{\sim}{x} = (x_1, x_2, \ldots, x_k)$, $x_0 = x_k = 0$, by $x_i^T = x_{k-i}$, $i = 0, 1, \ldots, k$. From Eqs. (4.1.29), (4.2.5), and (4.2.12) it can be seen that

$$w(\underset{\sim}{x}) = w(\underset{\sim}{x}^T) \ , \tag{4.2.19}$$

and

$$P(\underset{\sim}{x}) = P(\underset{\sim}{x}^T) \ . \tag{4.2.20}$$

Since $P(\underset{\sim}{x})w(\underset{\sim}{x})d^{k-1}\underset{\sim}{x} = P(\underset{\sim}{x}^T)w(\underset{\sim}{x}^T)d^{k-1}\underset{\sim}{x}^T$, and since the integration with respect to $\underset{\sim}{x}$ in Eq. (4.2.13) is carried out over all space, it is clear that Eq. (4.2.13) is equivalent to

$$\int_J \cdots \int P(\underset{\sim}{x}')w(\underset{\sim}{x}')d^{k-1}\underset{\sim}{x}'$$

$$= \int_J \cdots \int \frac{P(\underset{\sim}{x}')w(\underset{\sim}{x}') + P(\underset{\sim}{x}'^T)w(\underset{\sim}{x}'^T)}{2} d^{k-1}\underset{\sim}{x}' \ ,$$

$$= \int_J \cdots \int_{-\infty}^{\infty} \cdots \int_{-\infty}^{\infty} \left[\frac{p(\underset{\sim}{x}'|\underset{\sim}{x}) + p(\underset{\sim}{x}'^T|\underset{\sim}{x}^T)}{2}\right] P(\underset{\sim}{x})w(\underset{\sim}{x})\, d^{k-1}\underset{\sim}{x}\, d^{k-1}\underset{\sim}{x}' \ . \tag{4.2.21}$$

As a lemma for the proof of Eq. (4.2.21) it is shown in Appendix A that

$$p^*(\underset{\sim}{x}'|\underset{\sim}{x})w(\underset{\sim}{x}) = p^*(\underset{\sim}{x}^T|\underset{\sim}{x}'^T)w(\underset{\sim}{x}'^T) \ . \tag{4.2.22}$$

To prove that $p(\underset{\sim}{x}'|\underset{\sim}{x})$ satisfies Eq. (4.2.21) it is sufficient to show that

$$\begin{aligned} \nu(\underset{\sim}{x}') &= \int_{-\infty}^{\infty} \cdots \int_{-\infty}^{\infty} \left[p(\underset{\sim}{x}'|\underset{\sim}{x}) + p(\underset{\sim}{x}'^T|\underset{\sim}{x}^T) \right] P(\underset{\sim}{x})w(\underset{\sim}{x})d^{k-1}\underset{\sim}{x} \ , \\ &= 2P(\underset{\sim}{x}')w(\underset{\sim}{x}') \ , \end{aligned} \tag{4.2.23}$$

where $\nu(\underset{\sim}{x}')$ is defined by the above equation. Using the definition, Eq. (4.2.17), of $p(\underset{\sim}{x}'|\underset{\sim}{x})$ and keeping in mind that $P(\underset{\sim}{x})$ and $w(\underset{\sim}{x})$ are invariant under transposition of the coordinates of $\underset{\sim}{x}$ it follows that

$$\begin{aligned} \nu(\underset{\sim}{x}') = &\int_{\{\underset{\sim}{x}|P(\underset{\sim}{x}) > P(\underset{\sim}{x}')\}} \cdots \int \left[p^*(\underset{\sim}{x}'|\underset{\sim}{x}) + p^*(\underset{\sim}{x}'^T|\underset{\sim}{x}^T) \right] P(\underset{\sim}{x}')w(\underset{\sim}{x})d^{k-1}\underset{\sim}{x} \\ &+ \int_{\{\underset{\sim}{x}|P(\underset{\sim}{x}) < P(\underset{\sim}{x}')\}} \cdots \int \left\{ \left[p^*(\underset{\sim}{x}'|\underset{\sim}{x}) + p^*(\underset{\sim}{x}'^T|\underset{\sim}{x}^T) \right] \right. \\ &+ \delta(\underset{\sim}{x}',\underset{\sim}{x}) \int_{\{\underset{\sim}{x}''|P(\underset{\sim}{x}'') < P(\underset{\sim}{x})\}} \cdots \int \left[p^*(\underset{\sim}{x}''|\underset{\sim}{x}) + p^*(\underset{\sim}{x}''^T|\underset{\sim}{x}^T) \right] \\ &\left. \times \left(1 - \frac{P(\underset{\sim}{x}'')}{P(\underset{\sim}{x})} \right) d^{k-1}\underset{\sim}{x}'' \right\} P(\underset{\sim}{x})w(\underset{\sim}{x})d^{k-1}\underset{\sim}{x} \ , \end{aligned} \tag{4.2.24}$$

where the integral multiplying the delta function can be extended over the set $\{\underset{\sim}{x}''|P(\underset{\sim}{x}'') \leq P(\underset{\sim}{x})\}$ since the integrand vanishes for $P(\underset{\sim}{x}'') = P(\underset{\sim}{x})$. Performing the integral over the delta function $\nu(\underset{\sim}{x}')$ becomes

$$\nu(\underset{\sim}{x}') = P(\underset{\sim}{x}') \int_{\{\underset{\sim}{x}|P(\underset{\sim}{x}) > P(\underset{\sim}{x}')\}} \cdots \int \left[p^*(\underset{\sim}{x}'|\underset{\sim}{x}) + p^*(\underset{\sim}{x}'^T|\underset{\sim}{x}^T) \right] w(\underset{\sim}{x}) d^{k-1}\underset{\sim}{x}$$

$$+ \int_{\{\underset{\sim}{x}|P(\underset{\sim}{x}) \leq P(\underset{\sim}{x}')\}} \cdots \int \left[p^*(\underset{\sim}{x}'|\underset{\sim}{x}) + p^*(\underset{\sim}{x}'^T|\underset{\sim}{x}^T) \right] P(\underset{\sim}{x}) w(\underset{\sim}{x}) d^{k-1}\underset{\sim}{x}$$

$$+ \int_{\{\underset{\sim}{x}''|P(\underset{\sim}{x}'') \leq P(\underset{\sim}{x}')\}} \cdots \int \left[p^*(\underset{\sim}{x}''|\underset{\sim}{x}') + p^*(\underset{\sim}{x}''^T|\underset{\sim}{x}'^T) \right] P(\underset{\sim}{x}') w(\underset{\sim}{x}') d^{k-1}\underset{\sim}{x}''$$

$$- \int_{\{\underset{\sim}{x}''|P(\underset{\sim}{x}'') \leq P(\underset{\sim}{x}')\}} \cdots \int \left[p^*(\underset{\sim}{x}''|\underset{\sim}{x}') + p^*(\underset{\sim}{x}''^T|\underset{\sim}{x}'^T) \right] P(\underset{\sim}{x}'') w(\underset{\sim}{x}') d^{k-1}\underset{\sim}{x}'' \,. \tag{4.2.25}$$

Applying Eq. (4.2.22) to the first and second terms in the last equation one finds that the second and fourth terms cancel and there remains

$$\nu(\underset{\sim}{x}') = P(\underset{\sim}{x}') w(\underset{\sim}{x}') \int_{\{\underset{\sim}{x}|P(\underset{\sim}{x}) > P(\underset{\sim}{x}')\}} \cdots \int \left[p^*(\underset{\sim}{x}^T|\underset{\sim}{x}'^T) + p^*(\underset{\sim}{x}|\underset{\sim}{x}') \right] d^{k-1}\underset{\sim}{x}$$

$$+ P(\underset{\sim}{x}') w(\underset{\sim}{x}') \int_{\{\underset{\sim}{x}''|P(\underset{\sim}{x}'') \leq P(\underset{\sim}{x}')\}} \cdots \int \left[p^*(\underset{\sim}{x}''|\underset{\sim}{x}') + p^*(\underset{\sim}{x}''^T|\underset{\sim}{x}'^T) \right] d^{k-1}\underset{\sim}{x}'' \,. \tag{4.2.26}$$

Since the sets over which the two integrations are carried out are complements, the integrals may be combined into an integral over the whole space. Bearing in mind that the variable of integration, $\underset{\sim}{x}$, may just as well be replaced by $\underset{\sim}{x}^T$ one obtains the result

$$v(\underset{\sim}{x}') = P(\underset{\sim}{x}')w(\underset{\sim}{x}')\left[\int_{-\infty}^{\infty}\cdots\int_{-\infty}^{\infty} p^*(\underset{\sim}{x}|\underset{\sim}{x}')d^{k-1}\underset{\sim}{x} + \int_{-\infty}^{\infty}\cdots\int_{-\infty}^{\infty} p^*(\underset{\sim}{x}^T|\underset{\sim}{x}'^T)d^{k-1}\underset{\sim}{x}^T\right],$$

$$= 2P(\underset{\sim}{x}')w(\underset{\sim}{x}') \ , \qquad (4.2.27)$$

where the final step makes use of the normalization condition on $p^*(\underset{\sim}{x}|\underset{\sim}{x}')$, Eq. (4.2.16).

It can be seen from the definitions of $p(\underset{\sim}{x}'|\underset{\sim}{x})$ and $p^*(\underset{\sim}{x}'|\underset{\sim}{x})$ that there can be only one ergodic class since the probability of the one step transition from any vector, $\underset{\sim}{x}$, to a vector in the volume $d^{k-1}\underset{\sim}{x}'$ about $\underset{\sim}{x}'$ is strictly greater than zero for all vectors, $\underset{\sim}{x}'$, satisfying $P(\underset{\sim}{x}') > 0$. Equation (4.2.10) is thus satisfied for the $p(\underset{\sim}{x}'|\underset{\sim}{x})$ defined above, and a procedure which generates a Markov chain with this transition function is a valid importance sampling scheme for the present problem. The transition from a vector, $\underset{\sim}{x}$, of the chain to the next vector, $\underset{\sim}{x}'$, can be made using k-1 normally distributed random variables and one uniformly distributed random variable. Let

$$x''_0 = x''_k = 0 ,$$

$$x''_i = \sqrt{\frac{1}{2k}}\ \xi_i + \frac{x''_{i-1} + x_{i+1}}{2} , \quad i = 1,2,\ldots,k-1 , \tag{4.2.28}$$

where ξ_i, i=1,2,...,k-1, are normally distributed random variables with mean 0 and variance 1. If $P(\underset{\sim}{x}'') < P(\underset{\sim}{x})$, generate a random variable, ζ, which is uniformly distributed on the interval (0,1) and set

$$\underset{\sim}{x}' = \begin{cases} \underset{\sim}{x}'' , & \text{if } \zeta < \dfrac{P(\underset{\sim}{x}'')}{P(\underset{\sim}{x})} , \\ \underset{\sim}{x} , & \text{otherwise.} \end{cases} \tag{4.2.29}$$

If $P(\underset{\sim}{x}'') \geq P(\underset{\sim}{x})$ set

$$\underset{\sim}{x}' = \underset{\sim}{x}''. \tag{4.2.30}$$

It can be seen that the probability of $\underset{\sim}{x}''$ given $\underset{\sim}{x}$ is $p^*(\underset{\sim}{x}''|\underset{\sim}{x})$ while the probability of $\underset{\sim}{x}'$ given $\underset{\sim}{x}$ is $p(\underset{\sim}{x}'|\underset{\sim}{x})$.

4.3 Integration over the Position of the Third Particle

Besides the $6(k-1)$-fold integration arising from the approximation to the Wiener integral, it is also necessary to perform the twofold integration over the position of the third particle. This is the integration over (ρ_Q, θ_Q) in Eq. (4.1.14). Since a large number of Monte Carlo samples are necessary for reasonable accuracy in the Wiener integral approximation, it is impractical to compute $G_c(r_{12}, \underset{\sim}{Q})$ and $G_e(r_{12}, \underset{\sim}{Q})$ at each point of a 2-dimensional grid in $\underset{\sim}{Q}$ and apply a standard numerical integration technique. If we perform this last twofold integration by a Monte Carlo technique, however, the sampling may be combined with that for the $6(k-1)$-fold integrals. The procedure then is to generate M samples $\{(\underset{\sim}{r}_t^{(k)}, \underset{\sim}{q}_t^{(k)}, \underset{\sim}{Q}_t), t = 1,2,\ldots,M\}$ and to form

$$g_d(r_{12};M) = \frac{1}{M} \sum_{t=1}^{M} L(\underset{\sim}{r}_t^{(k)}, \underset{\sim}{q}_t^{(k)}, \underset{\sim}{Q}_t)\, \Gamma^{-1}(\underset{\sim}{Q}_t), \tag{4.3.1}$$

where L is defined by Eq. (4.2.4), $\underset{\sim}{r}_t^{(k)}$ is generated from the Markov chain, $\underset{\sim}{q}_t^{(k)}$ is produced by the straightforward sampling scheme for Wiener paths, and $\underset{\sim}{Q}_t = (\rho_Q, \theta_Q, 0)_t$ is picked according to a 2-dimensional distribution

$$\Gamma(\underset{\sim}{Q})d^2\underset{\sim}{Q} = \Gamma_\rho(\rho_Q)\Gamma_\theta(\theta_Q)d\rho_Q d\theta_Q, \tag{4.3.2}$$

or

$$\Gamma(\underset{\sim}{Q})d^2\underset{\sim}{Q} = \Gamma_x(Q_x)\Gamma_y(Q_y)dQ_x dQ_y, \tag{4.3.3}$$

in Cartesian coordinates. If Eq. (4.3.3) is used a factor of $\frac{1}{2}$ must be included in L if the range of Q_y is $-\infty < Q_y < \infty$. One will then have by the law of large numbers that

$$\lim_{M\to\infty} g_d(r_{12};M) = g_d(r_{12}) \tag{4.3.4}$$

with probability one, where $g_d(r_{12})$ represents either $g_c(r_{12})$ or $g_e(r_{12})$ depending on the form of the integrand $L(\underset{\sim}{r}^{(k)}, \underset{\sim}{q}^{(k)}, \underset{\sim}{Q})$.

Including the integration over $\underset{\sim}{Q}$ in the Monte Carlo scheme will increase the number of samples necessary for a given accuracy since $L(\underset{\sim}{r}^{(k)}, \underset{\sim}{q}^{(k)}, \underset{\sim}{Q})$ will have an increased variation on being taken as a function of $\underset{\sim}{Q}$ as well as of $\underset{\sim}{r}^{(k)}$ and $\underset{\sim}{q}^{(k)}$. The variation with respect to $\underset{\sim}{Q}$ turns out to be the dominant part of the variance of the Monte Carlo scheme at moderate temperatures with the distributions of $\underset{\sim}{r}^{(k)}$ and $\underset{\sim}{q}^{(k)}$ being fairly sharply peaked about $\underset{\sim}{r}^{(k)} = \underset{\sim}{q}^{(k)} \equiv 0$. This variance in $\underset{\sim}{Q}$ can be reduced somewhat by making use of the latitude that exists in the choice of the distribution $\Gamma(\underset{\sim}{Q})$. Qualitatively the variance with respect to $\underset{\sim}{Q}$ will be reduced if the global behavior of $\Gamma(\underset{\sim}{Q})$ is similar to that of $L(\underset{\sim}{r}^{(k)}, \underset{\sim}{q}^{(k)}, \underset{\sim}{Q})$

as a function of $\underset{\sim}{Q}$. Since L is also a function of $\underset{\sim}{r}^{(k)}$ and $\underset{\sim}{q}^{(k)}$ computing time restrictions indicate that it would probably not be worthwhile to develop an elaborate importance sampling scheme in the variable $\underset{\sim}{Q}$. The choice of $\Gamma(\underset{\sim}{Q})$ will therefore be restricted to distributions which can be generated easily from uniform or normally distributed pseudo random numbers.

In order to get an idea of the form of $L(\underset{\sim}{r}^{(k)}, \underset{\sim}{q}^{(k)}, \underset{\sim}{Q})$ as a function of $\underset{\sim}{Q}$ one must consider $g_c(r_{12})$ and $g_e(r_{12})$ separately. For the function $g_c(r_{12})$ the integrand is

$$L_c(\underset{\sim}{r}^{(k)}, \underset{\sim}{q}^{(k)}, \underset{\sim}{Q}) = \left[D_{13}\left(\frac{\sqrt{3}}{2}\,\underset{\sim}{q}^{(k)} + \frac{1}{2}\,\underset{\sim}{r}^{(k)}\right) - 1\right] \times \left[D_{23}\left(\frac{\sqrt{3}}{2}\,\underset{\sim}{q}^{(k)} - \frac{1}{2}\,\underset{\sim}{r}^{(k)}\right) - 1\right], \tag{4.3.5}$$

while for $g_e(r_{12})$ the integrand is

$$L_e(\underset{\sim}{r}^{(k)}, \underset{\sim}{q}^{(k)}, \underset{\sim}{Q}) = \left[D_{13}\left(\frac{\sqrt{3}}{2}\,\underset{\sim}{q}^{(k)} + \frac{1}{2}\,\underset{\sim}{r}^{(k)}\right) - D_{13}\,(\underset{\sim}{q}^{(k)}) + D_{23}\left(\frac{\sqrt{3}}{2}\,\underset{\sim}{q}^{(k)} - \frac{1}{2}\,\underset{\sim}{r}^{(k)}\right) - D_{23}\,(\underset{\sim}{q}^{(k)})\right]. \tag{4.3.6}$$

Since the distributions of $\underset{\sim}{r}^{(k)}$ and $\underset{\sim}{q}^{(k)}$ are peaked near $\underset{\sim}{r}^{(k)} = \underset{\sim}{q}^{(k)} \equiv 0$, the function

$$L_c(0,0,\underset{\sim}{Q}) = \left[\exp\{-\beta V(\underset{\sim}{Q} + \frac{\underset{\sim}{r}_{12}}{2}) - \frac{\beta\lambda^2}{2\pi k} V''(\underset{\sim}{Q} + \frac{\underset{\sim}{r}_{12}}{2})\} - 1\right] \times \left[\exp\{-\beta V(\underset{\sim}{Q} - \frac{\underset{\sim}{r}_{12}}{2}) - \frac{\beta\lambda^2}{2\pi k} V''(\underset{\sim}{Q} - \frac{\underset{\sim}{r}_{12}}{2})\} - 1\right], \qquad (4.3.7)$$

gives some idea of the variation of L_c with respect to $\underset{\sim}{Q}$. Equation (4.3.7) is just the second order Wigner-Kirkwood approximation to the classical cluster function

$$f_{13}f_{23} = (e^{-V(\underset{\sim}{r}_{13})} - 1)(e^{-V(\underset{\sim}{r}_{23})} - 1) \quad , \qquad (4.3.8)$$

so that the behavior of this classical function with respect to $\underset{\sim}{Q}$ will give some idea of the global structure of L_c as a function of $\underset{\sim}{Q}$.

Figure 2 shows a rough contour map of $f_{13}f_{23}$ for $T = 20^{\circ}K$ and $r_{12} = 1.1\sigma$, where σ is defined by Eq. (2.1.2). The structure of this cluster function is too complex to attempt to fit it in detail with a simple probability distribution. It can be seen, however, that the structure of the function is centered about $\underset{\sim}{Q} = 0$ and that the function becomes negligible at a distance of 2 or 3 times σ in the Q_y direction and at a slightly larger distance in the Q_x direction. A reasonable sampling distribution for such a function

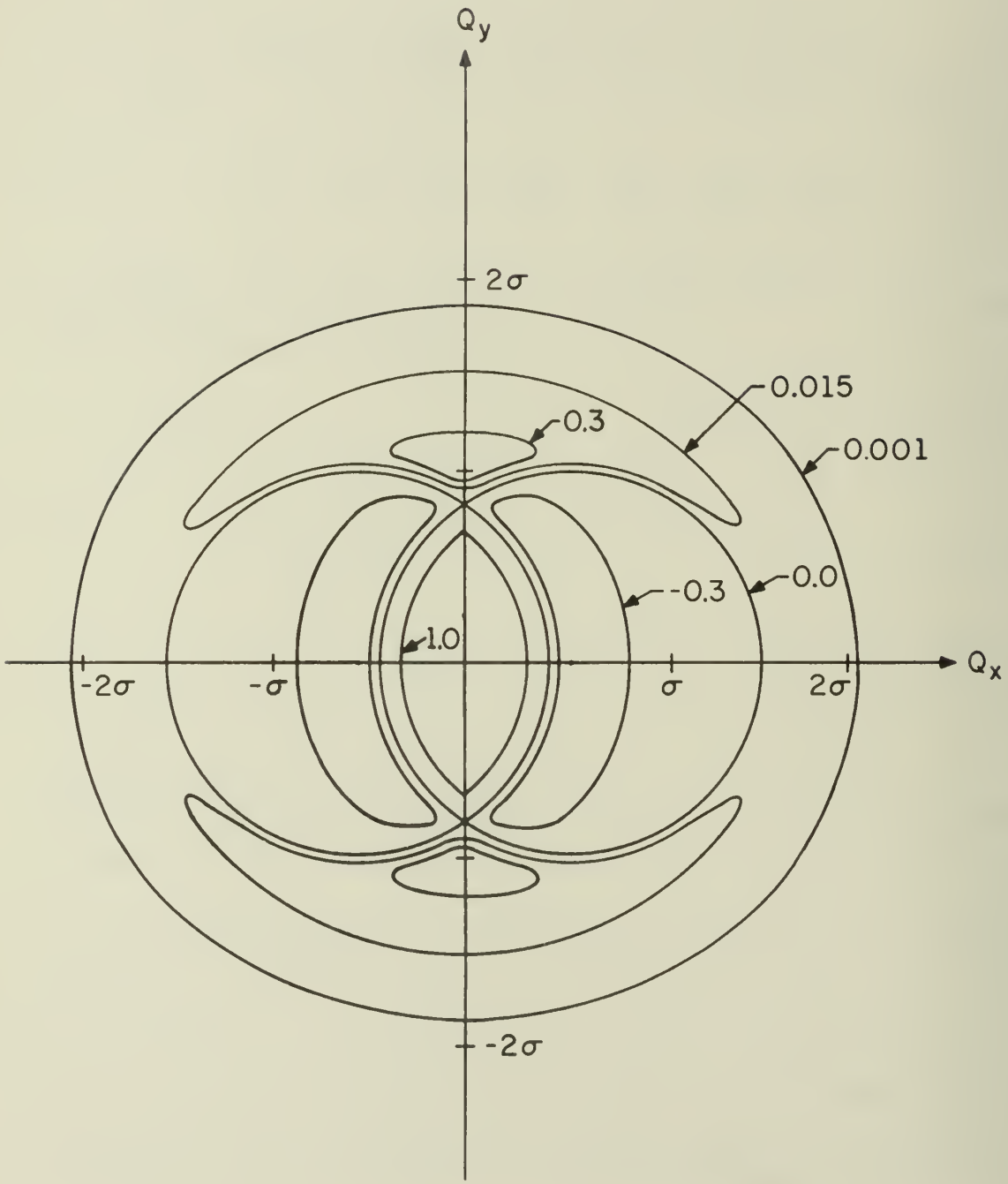

FIGURE 2. $f_{13}(r_{12},\underset{\sim}{Q})Xf_{23}(r_{12},\underset{\sim}{Q})$ AS A FUNCTION OF $\underset{\sim}{Q}$ FOR $r_{12}=1.1\sigma$ AND T=20°K.

might be a 2-dimensional normal distribution with a standard deviation on the order of σ in the Q_y direction and a standard deviation in the Q_x direction on the order of σ + const. $\times r_{12}$. The distribution used for the integration over $\underset{\sim}{Q}$ in the numerical computations to follow was

$$\Gamma_c(\underset{\sim}{Q})d^2\underset{\sim}{Q} = \frac{1}{\sqrt{2\pi}\gamma_x} \exp\left(-\frac{Q_x^2}{2\gamma_x^2}\right) \frac{1}{\sqrt{2\pi}\gamma_y} \exp\left(-\frac{Q_y^2}{2\gamma_y^2}\right) dQ_x dQ_y \quad , \qquad (4.3.9)$$

where the standard deviations γ_x and γ_y were chosen empirically to minimize the variance of $g_c(r_{12};M)$ for a small value of M.

If one tries to take $\underset{\sim}{r}^{(k)} = \underset{\sim}{q}^{(k)} \equiv 0$ in $L_e(\underset{\sim}{r}^{(k)}, \underset{\sim}{q}^{(k)}, \underset{\sim}{Q})$ the function vanishes. In fact this function vanishes to order T^{-3} in the Wigner-Kirkwood expansion, Eq. (3.2.25), and it is thus to be expected that the correction term $g_e(r_{12})$ will be negligible except at low temperatures and for small r_{12}. In order to find an efficient sampling scheme for $g_e(r_{12})$ advantage can be taken of several symmetries of the integrand. The function g_e can be written as the sum of two integrals

$$g_e(r_{12}) = g_e^{(1)}(r_{12}) + g_e^{(2)}(r_{12}) \quad , \qquad (4.3.10)$$

where

$$g_e^{(1)}(r_{12}) = \frac{1}{W_2(\underset{\sim}{1},\underset{\sim}{2})} \int d^3\underset{\sim}{Q}$$

$$\times \; E\left\{F_{12}(\underset{\sim}{r}(\tau)) \left[F_{13}\left(\frac{\sqrt{3}}{2}\,\underset{\sim}{q}(\tau) + \frac{\underset{\sim}{r}(\tau)}{2}\right) - F_{13}(\underset{\sim}{q}(\tau))\right] \,\middle|\, \underset{\sim}{r}(1) = \underset{\sim}{q}(1) = 0\right\},$$

$$g_e^{(2)}(r_{12}) = \frac{1}{W_2(\underset{\sim}{1},\underset{\sim}{2})} \int d^3\underset{\sim}{Q}$$

$$\times \; E\left\{F_{12}(\underset{\sim}{r}(\tau)) \left[F_{23}\left(\frac{\sqrt{3}}{2}\,\underset{\sim}{q}(\tau) - \frac{\underset{\sim}{r}(\tau)}{2}\right) - F_{23}(\underset{\sim}{q}(\tau))\right] \,\middle|\, \underset{\sim}{r}(1) = \underset{\sim}{q}(1) = 0\right\}, \tag{4.3.11}$$

and where F_{12}, F_{13}, and F_{23} are defined by Eq. (4.1.11). Both $g_e^{(1)}$ and $g_e^{(2)}$ are functions of the magnitude r_{12} only, so $\underset{\sim}{r}_{12}$ may be replaced by $-\underset{\sim}{r}_{12}$ wherever it appears in $g_e^{(2)}(r_{12})$. Furthermore, Wiener measure on $\underset{\sim}{r}(\tau)$ is invariant to the replacement of $\underset{\sim}{r}(\tau)$ by $-\underset{\sim}{r}(\tau)$. If one makes the two changes of variables $\underset{\sim}{r}_{12} \to -\underset{\sim}{r}_{12}$ and $\underset{\sim}{r}(\tau) \to -\underset{\sim}{r}(\tau)$ in $g_e^{(2)}$, then $F_{12}(\underset{\sim}{r}(\tau))$ is unchanged due to the spherical symmetry of $V(r)$ while

$$F_{23}\left(\frac{\sqrt{3}}{2}\,\underset{\sim}{q}(\tau) - \frac{\underset{\sim}{r}(\tau)}{2}\right) \to F_{13}\left(\frac{\sqrt{3}}{2}\,\underset{\sim}{q}(\tau) + \frac{\underset{\sim}{r}(\tau)}{2}\right)$$

and

$$F_{23}(\underset{\sim}{q}(\tau)) \to F_{13}(\underset{\sim}{q}(\tau)) \; .$$

Thus

$$g_e^{(1)}(r_{12}) = g_e^{(2)}(r_{12}) \tag{4.3.12}$$

and $g_e(r_{12})$ may be written as

$$g_e(r_{12}) = \frac{2}{W_2(\underset{\sim}{1},\underset{\sim}{2})} \int d^3\underset{\sim}{Q}$$

$$\times \; E\left\{F_{12}(\underset{\sim}{r}(\tau)) \left[F_{13}\left(\frac{\sqrt{3}}{2}\,\underset{\sim}{q}(\tau) + \frac{\underset{\sim}{r}(\tau)}{2}\right) - F_{13}(\underset{\sim}{q}(\tau))\right] \;\middle|\; \underset{\sim}{r}(1) = \underset{\sim}{q}(1) = 0\right\}. \tag{4.3.13}$$

In this last form a more natural origin for the integration over $\underset{\sim}{Q}$ is $\underset{\sim}{Q} = -\frac{\underset{\sim}{r}_{12}}{2}$, so let the variable of integration be changed to

$$\underset{\sim}{Q}' = \underset{\sim}{Q} + \frac{\underset{\sim}{r}_{12}}{2} \; . \tag{4.3.14}$$

Then

$$g_e(r_{12}) = \int d^3\underset{\sim}{Q}' \; G_e(r_{12},\underset{\sim}{Q}') \quad , \tag{4.3.15}$$

where

$$G_e(r_{12},\underset{\sim}{Q}') = 2E\left\{\frac{F_{12}(\underset{\sim}{r}(\tau))}{W_2(\underset{\sim}{1},\underset{\sim}{2})}\left[F_{13}\left(\underset{\sim}{Q}', \frac{\sqrt{3}}{2}\underset{\sim}{q}(\tau) + \frac{\underset{\sim}{r}(\tau)}{2}\right) - F_{13}(\underset{\sim}{Q}',\underset{\sim}{q}(\tau))\right]\right| \underset{\sim}{r}(1) = \underset{\sim}{q}(1) = 0\Big\}, \tag{4.3.16}$$

and where

$$F_{13}(\underset{\sim}{Q}',\underset{\sim}{q}(\tau)) = \exp\left[-\beta\int_0^1 V\left(\frac{\lambda}{\sqrt{\pi}}\ \underset{\sim}{q}(\tau) + \underset{\sim}{Q}'\right)d\tau\right]. \tag{4.3.17}$$

The prime on $\underset{\sim}{Q}'$ will be dropped for the remainder of the discussion of $g_e(r_{12})$. In spherical coordinates the cylindrical symmetry in Φ_Q is not altered by the change in origin provided the polar axis remains in the Q_x direction.

The integrand of $g_e(r_{12})$ is the difference of two terms depending on $\underset{\sim}{Q}$. This difference will be small if both terms are small or nearly equal so we consider the behavior of

$$F_{13}(\underset{\sim}{Q},0) = e^{-\beta V(\underset{\sim}{Q})} \tag{4.3.18}$$

with respect to $\underset{\sim}{Q}$. This function is the limit of both of the terms in the square brackets in Eq. (4.3.16) for $\underset{\sim}{r}(\tau) = \underset{\sim}{q}(\tau) \equiv 0$. For $\rho_Q < \sigma$,

$F_{13}(\underset{\sim}{Q},0)$ goes to zero rapidly. The function has a maximum at $\rho_Q \simeq 1.12\sigma$ and approaches one asymptotically as $\left(1 + \frac{\sigma^6}{\rho_Q^6}\right)$ for $\rho_Q \gg \sigma$. The integrand in Eq. (4.3.15) should thus be zero for $\rho_Q \ll \sigma$ and approach zero again for $\rho_Q \gg \sigma$ as both terms in the difference approach unity. A simple probability distribution with this same qualitative behavior is the χ^2 distribution with n degrees of freedom for $n \geq 4$. For the $\underset{\sim}{Q}$ integration in $g_e(r_{12})$ then a χ^2 distribution with 12 degrees of freedom was used for ρ_Q and $\xi_Q = \cos\theta_Q$ was chosen from a uniform distribution, $-1 \leq \xi_Q \leq 1$. Thus we define

$$\Gamma_e(\underset{\sim}{Q})d^2\underset{\sim}{Q} = \frac{\rho_Q^5}{6!\gamma_\rho^2} \exp\left(-\frac{\rho_Q}{\gamma_\rho}\right) d\rho_Q d\xi_Q. \qquad (4.3.19)$$

The number of degrees of freedom and the value of γ_ρ were chosen empirically during preliminary computations to minimize the variance of $g_e(r_{12};M)$ for small M.

In initial calculations of $g_e(r_{12};M)$ it was found that $g_e(r_{12})$ was indeed small compared to $g_c(r_{12})$ but that the variance of $g_e(r_{12};M)$ was quite large. It was thus necessary to apply a further variance reducing technique to the Monte Carlo sampling in the calculation of g_e. The technique used was the method of antithetic variates described by Hammersly and Handscomb [26], and although it applies to the Monte Carlo sampling as a whole, it is best described in connection with the sampling in the $\underset{\sim}{Q}$ integration. The principle of

the antithetic variates method is to generate several correlated samples simultaneously in such a way that their sum has a considerably smaller variance than the samples taken independently. In the present case it is recognized that $g_e(r_{12})$ is small so that one tries to correlate the samples in such a way that their sum is near zero.

From Eq. (4.3.16) it can be seen that the cylindrical symmetry of $G_e(r_{12},\underset{\sim}{Q})$ about the Q_x axis requires that

$$G_e(r_{12},-\underset{\sim}{Q}) = G_e(r_{12},\rho_Q,\theta_Q + \frac{\pi}{2},\Phi_Q). \tag{4.3.20}$$

Thus the range of θ_Q can be restricted to $0 \leq \theta_Q \leq \pi$, $(0 \leq \xi_Q \leq 1)$ and the integrand taken as the sum of $G_e(r_{12},\underset{\sim}{Q})$ and $G_e(r_{12},-\underset{\sim}{Q})$. Another pairing of samples can be made due to the fact that the probability of a Wiener path $\underset{\sim}{q}(\tau)$ is the same as the probability of $-\underset{\sim}{q}(\tau)$. Since successive path approximations $\underset{\sim}{q}^{(k)}$ are chosen independently the samples for $\underset{\sim}{q}^{(k)}$ and $-\underset{\sim}{q}^{(k)}$ may be combined.

From Eqs. (4.1.28), (4.1.29), and (4.2.4) it is seen that the integrand of the multiple integral approximation for $G_e(r_{12},\underset{\sim}{Q})$ as given in Eq. (4.3.16) is

$$L_e(\underset{\sim}{r}^{(k)}, \underset{\sim}{q}^{(k)}, \underset{\sim}{Q}) = 2\left[D_{13}\left(\underset{\sim}{Q}, \frac{\sqrt{3}}{2}\underset{\sim}{q}^{(k)} + \frac{\underset{\sim}{r}^{(k)}}{2}\right) - D_{13}(\underset{\sim}{Q}, \underset{\sim}{q}^{(k)})\right], \tag{4.3.21}$$

where

$$D_{13}(\underset{\sim}{Q},\underset{\sim}{q}^{(k)}) = \exp\left\{\frac{-\beta}{6k}\sum_{i=1}^{k}\left[V\left(\frac{\lambda}{\sqrt{\pi}}\,\underset{\sim}{q}_{i-1}+\underset{\sim}{Q}\right)+4V\left(\frac{\lambda}{\sqrt{\pi}}\left(\frac{\underset{\sim}{q}_i+\underset{\sim}{q}_{i-1}}{2}\right)+\underset{\sim}{Q}\right)\right.\right.$$

$$\left.\left.+V\left(\frac{\lambda}{\sqrt{\pi}}\,\underset{\sim}{q}_i+\underset{\sim}{Q}\right)+\frac{\lambda^2}{2\pi k}\,V''\left(\frac{\lambda}{\sqrt{\pi}}\left(\frac{\underset{\sim}{q}_i+\underset{\sim}{q}_{i-1}}{2}\right)+\underset{\sim}{Q}\right)\right]\right\}. \tag{4.3.22}$$

Then if $\underset{\sim}{r}_t^{(k)}$ is generated from the Markov chain, $\underset{\sim}{q}_t^{(k)}$ is generated by the straightforward scheme for Wiener paths, and $\underset{\sim}{Q}_t$ is chosen from the distribution $\Gamma_e(\underset{\sim}{Q})$ defined by Eq. (4.3.19) but with ξ_Q restricted to the range $0 \le \xi_Q \le 1$, then with probability one

$$g_e(r_{12}) = \lim_{M\to\infty}\frac{1}{M}\sum_{t=1}^{M} A(\underset{\sim}{r}_t^{(k)}, \underset{\sim}{q}_t^{(k)}, \underset{\sim}{Q}_t)\,\Gamma^{-1}(\underset{\sim}{Q}_t)\,, \tag{4.3.23}$$

where the antithetic variates sample

$$A(\underset{\sim}{r}^{(k)}, \underset{\sim}{q}^{(k)}, \underset{\sim}{Q})$$

is defined by

$$A(\underset{\sim}{r}^{(k)}, \underset{\sim}{q}^{(k)}, \underset{\sim}{Q}) = \frac{1}{2}\left[L_e(\underset{\sim}{r}^{(k)}, \underset{\sim}{q}^{(k)}, \underset{\sim}{Q}) + L_e(\underset{\sim}{r}^{(k)}, \underset{\sim}{q}^{(k)}, -\underset{\sim}{Q})\right.$$

$$\left. + L_e(\underset{\sim}{r}^{(k)}, -\underset{\sim}{q}^{(k)}, \underset{\sim}{Q}) + L_e(\underset{\sim}{r}^{(k)}, -\underset{\sim}{q}^{(k)}, -\underset{\sim}{Q})\right]. \tag{4.3.24}$$

This sum should be more nearly zero than its component terms since the portion of L_e which is antisymmetric in $\underset{\sim}{Q}$ will cancel between terms 1 and 2 and between terms 3 and 4 on the right side of Eq. (4.3.24) while similar cancellation will take place for the component of L_e which is antisymmetric in the variable $\underset{\sim}{q}^{(k)}$ between terms 1 and 3 and between terms 2 and 4.

5. NUMERICAL RESULTS

5.1 Results and Accuracy Considerations

Using the methods developed in the preceding sections $g_c(r_{12}; 20{,}000)$ and $g_e(r_{12}; 20{,}000)$ were calculated for temperatures $T = 5^\circ K$, $10^\circ K$, $20^\circ K$, $30^\circ K$, $40^\circ K$, $50^\circ K$, $75^\circ K$, $100^\circ K$, and $273.18^\circ K$ and for values of r_{12} in the range $0.6 \leq r_{12}/\sigma \leq 4.0$. The third virial coefficient $C(T)$ was computed for all but the lowest temperature, $5^\circ K$, using Eq. (2.3.20). A straightforward numerical integration was performed over r_{12} with $g_1(r_{12})$ approximated by $g_c(r_{12}; 20{,}000) + g_e(r_{12}; 20{,}000)$ and with the values of $W_2(r_{12})$ and b_2 given in [6]. The computations were performed on the ILLIAC II computer located at the University of Illinois. The details of the computation and a comprehensive table of results are presented in Appendix B. A summary of the results for $g_1(r_{12}; 20{,}000) = g_c(r_{12}; 20{,}000) + g_e(r_{12}; 20{,}000)$ over the range of temperature is shown in Figure 3, and the computed third virial coefficient $C(T)$ is plotted versus temperature in Figure 4.

There are two sources of computational error which cause $g_1(r_{12}; 20{,}000)$ and $C(T)$ to differ from the correct theoretical values of $g_1(r_{12})$ and the third virial coefficient for the interaction potential of Eqs. (2.1.1) and (2.1.2). These are the error introduced by the k-fold integral approximation to the Wiener integrals and the Monte Carlo sampling error. The order k of the approximations $\underset{\sim}{r}^{(k)}$ and $\underset{\sim}{q}^{(k)}$ to the Wiener paths $\underset{\sim}{r}(\tau)$ and $\underset{\sim}{q}(\tau)$ was chosen for each temperature T so that $Tk \geq 260^\circ K$. Thus the accuracy of the multiple

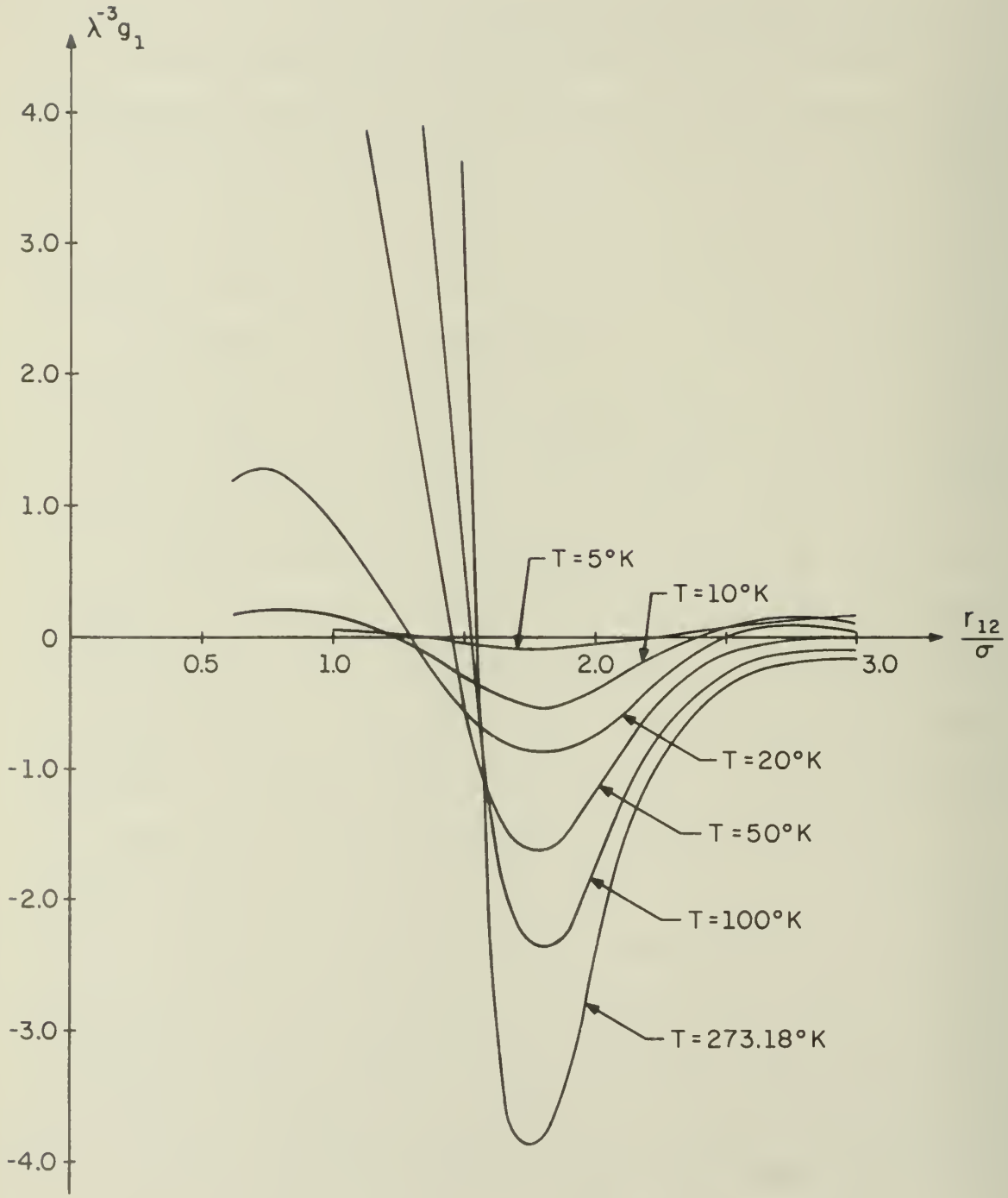

FIGURE 3. $\lambda^{-3}g_1(r_{12}\,;20{,}000)$ AS A FUNCTION OF r_{12}/σ AND T.

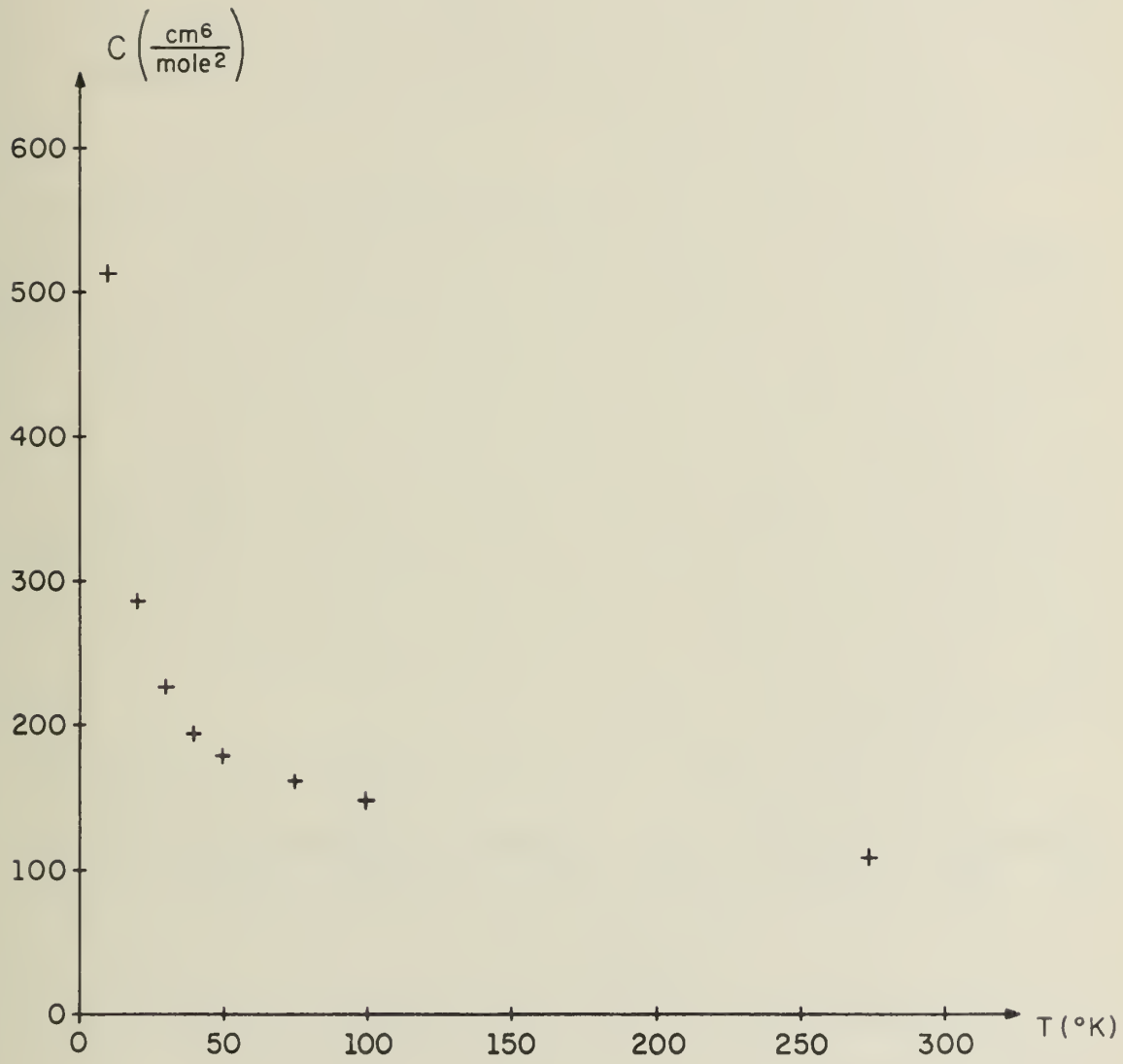

FIGURE 4. COMPUTED THIRD VIRIAL COEFFICIENT AS A FUNCTION OF TEMPERATURE.

integral approximations at any temperature is at least equal to the accuracy of the two term Wigner-Kirkwood approximation (first two terms in Eq. (3.3.25)) at 260°K. As an estimate of this accuracy the third term in the Wigner-Kirkwood approximation to the second virial coefficient of He^4 at 260°K amounts to only 0.7% of the total. It will be seen that an error of this magnitude is negligible compared to the Monte Carlo sampling error.

As an estimate of the Monte Carlo sampling error the sample standard deviations of the sample means, $g_c(r_{12}; 20{,}000)$ and $g_e(r_{12}; 20{,}000)$, were computed. The numerical results for $g_1(r_{12}; 20{,}000)$ and the associated error estimates are shown plotted against r_{12}/σ for T = 5°K, 20°K, 75°K, and 273.18°K in Figures 5, 6, 7, and 8, respectively. The complete set of graphs can be found in Appendix B. The length of the error bar associated with $\lambda^{-3} g_1(r_{12}; 20{,}000)$ is equal to twice the sum of the sample standard deviations of $\lambda^{-3} g_c(r_{12}; 20{,}000)$ and $\lambda^{-3} g_e(r_{12}; 20{,}000)$.

Although the Monte Carlo sampling connected with the Wiener integration and with the Riemann integration of $G(r_{12}, \underset{\sim}{Q})$ over the position $\underset{\sim}{Q}$ of the third particle is done as a single process, it is convenient to consider the sampling error to be a sum of separate contributions from these two sources. The sampling error in the integration with respect to $\underset{\sim}{Q}$ depends on the variation of $G(r_{12}, \underset{\sim}{Q})\, \Gamma^{-1}(\underset{\sim}{Q})$ as a function of $\underset{\sim}{Q}$. Since $G(r_{12}, \underset{\sim}{Q})$ contains functions of the form $e^{-\beta V(\underset{\sim}{Q} \pm \underset{\sim}{r}_{12}/2)}$ which have an increasing variation in $\underset{\sim}{Q}$ as β increases, it is to be expected that the sampling error due to the $\underset{\sim}{Q}$

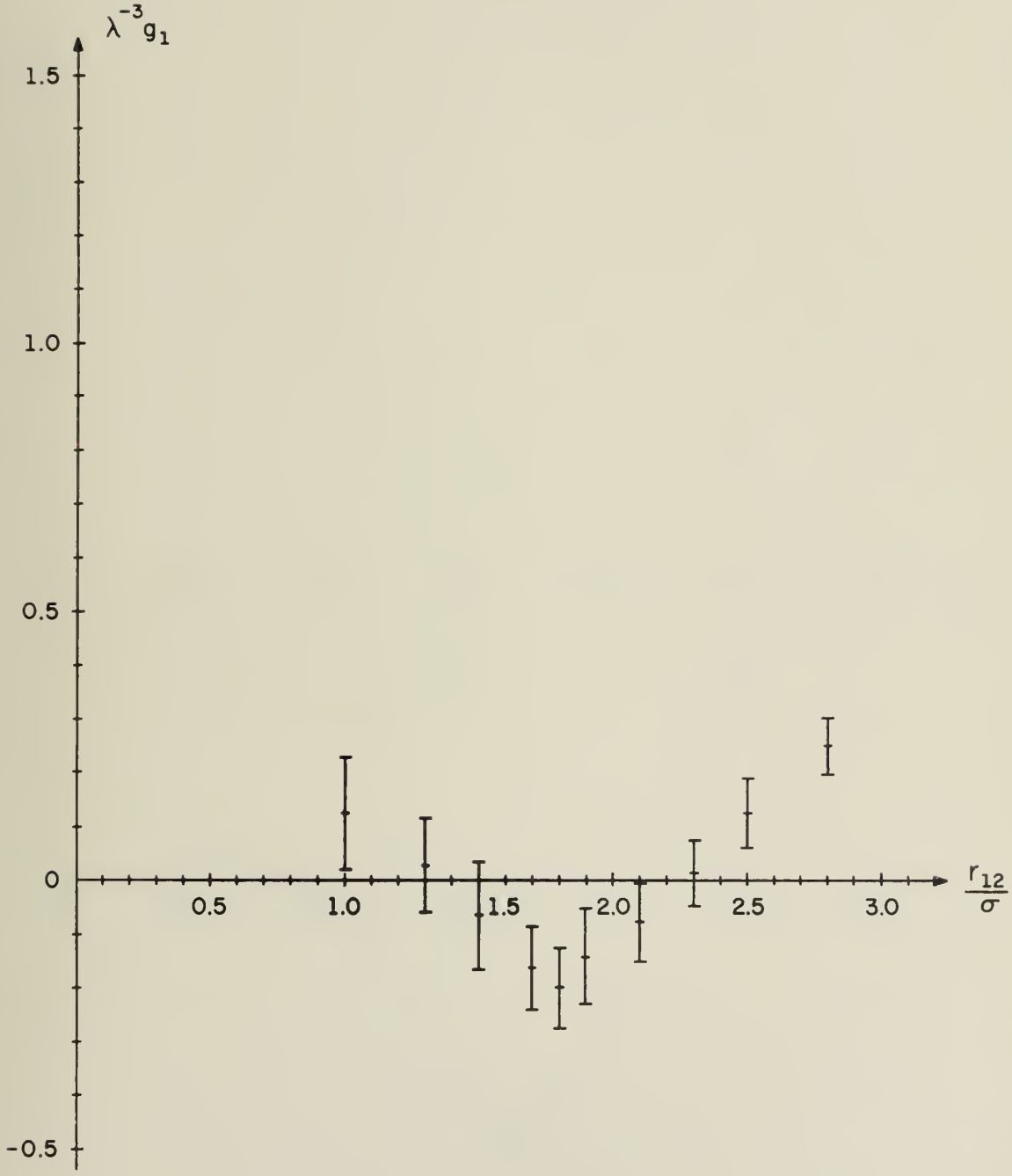

FIGURE 5. $\lambda^{-3} g_1$ AND SAMPLING ERROR FOR T=5°K.

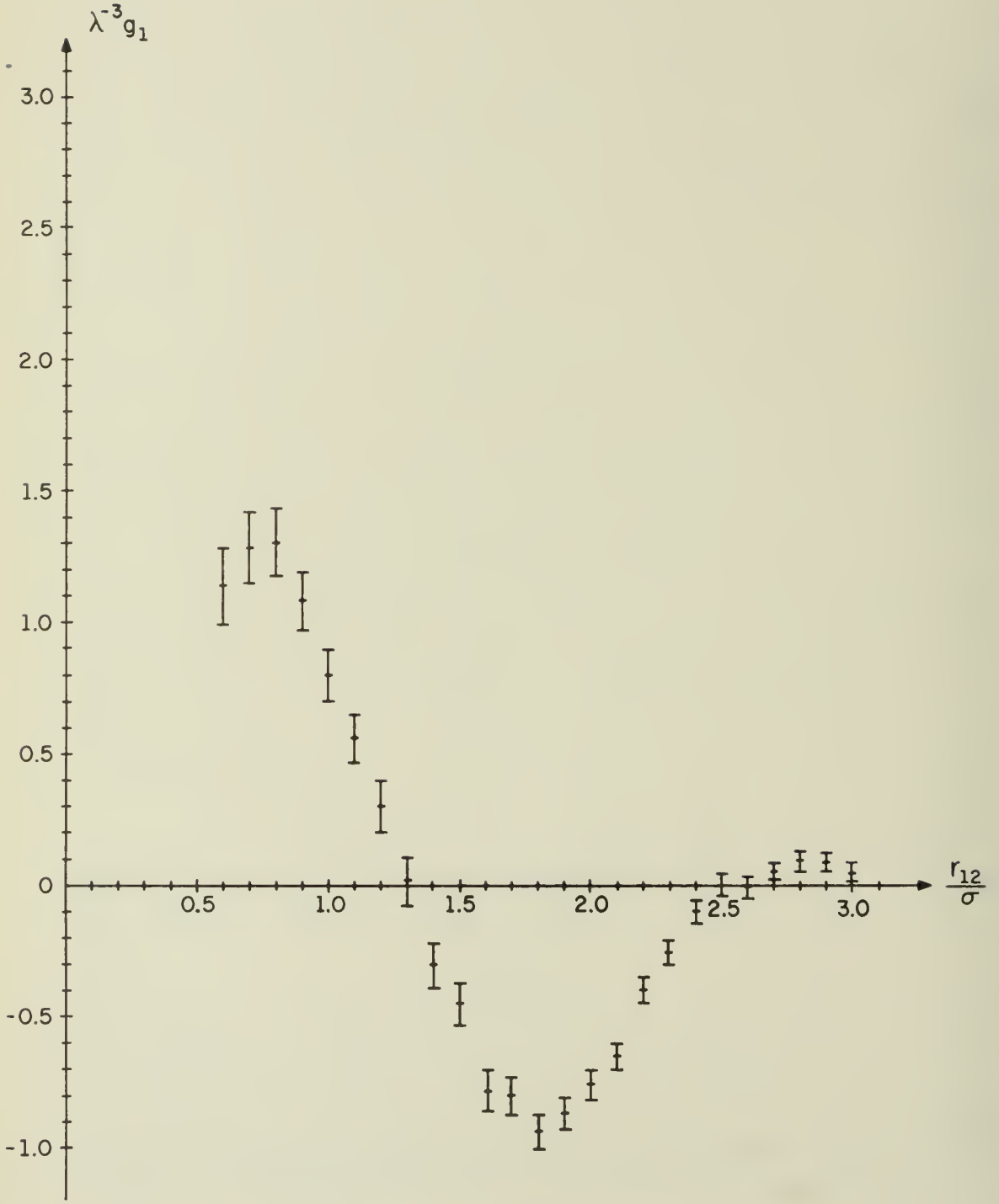

FIGURE 6. $\lambda^{-3}g_1$ AND SAMPLING ERROR FOR T=20°K.

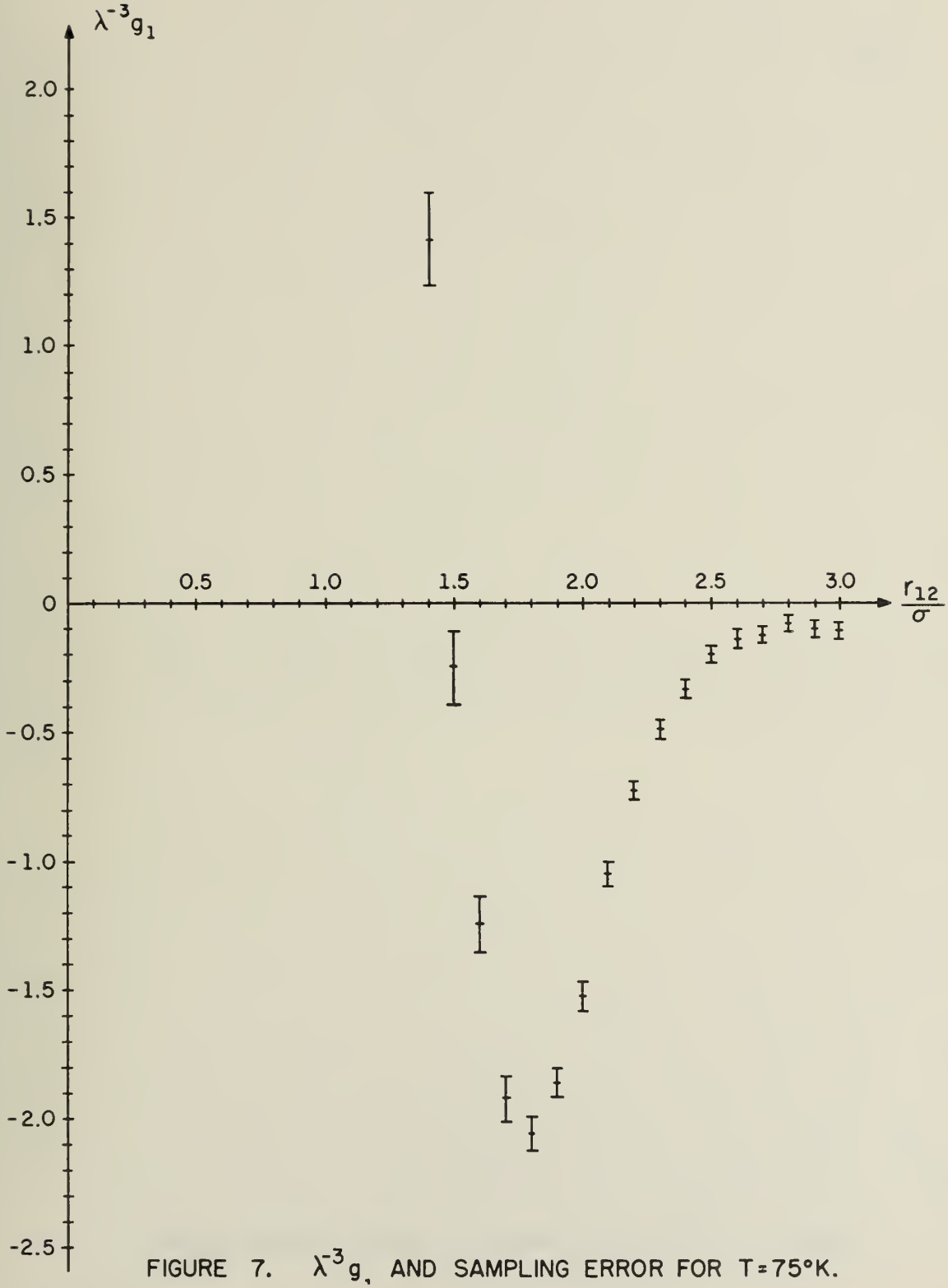

FIGURE 7. $\lambda^{-3}g_1$ AND SAMPLING ERROR FOR T=75°K.

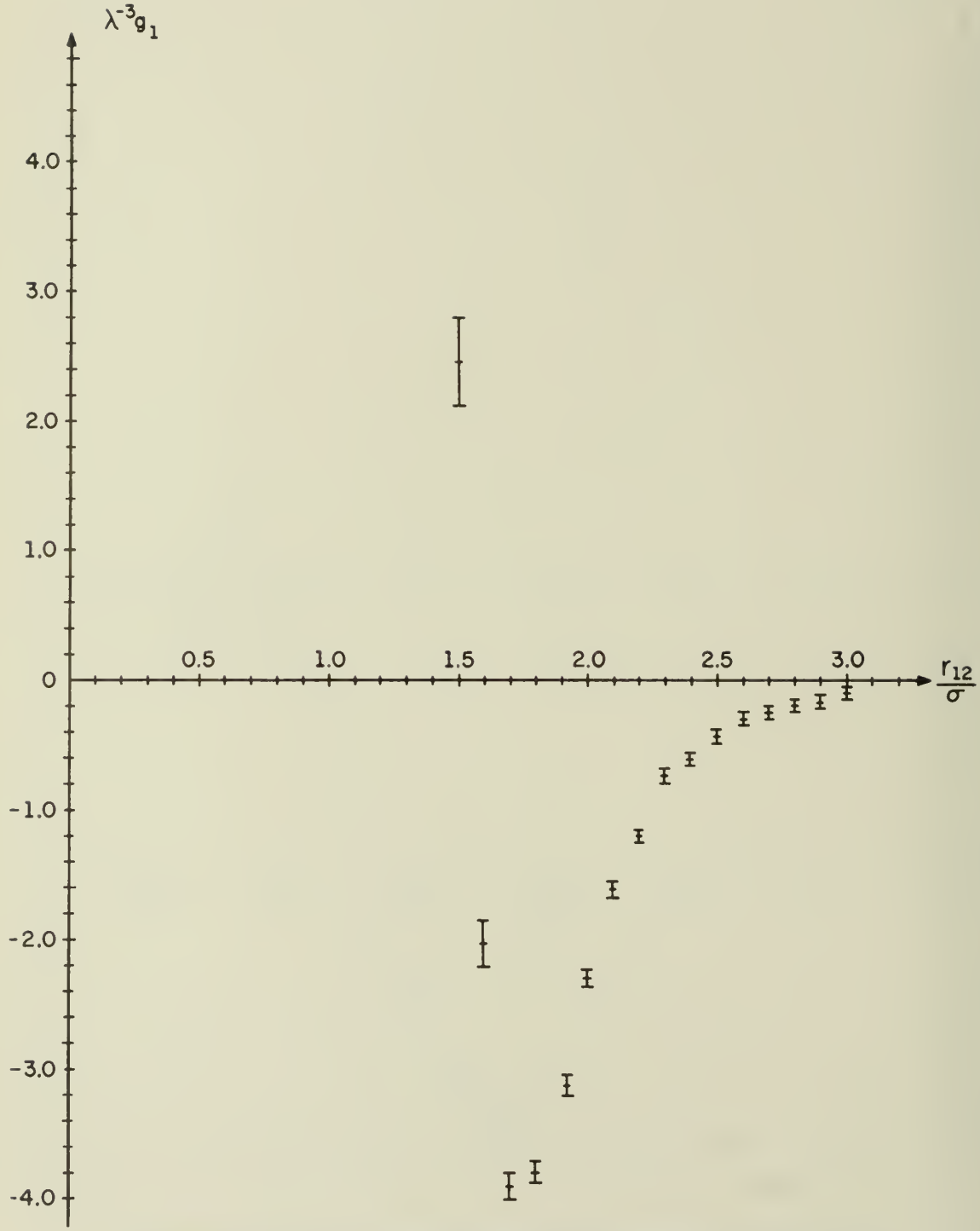

FIGURE 8. $\lambda^{-3}g_1$ AND SAMPLING ERROR FOR T=273.18°K.

integration will increase with decreasing temperature.

A factor of β also multiplies the exponent of the functional integrand of the Wiener integration so that the variance of the Monte Carlo procedure for computing the multiple integral approximation to the Wiener integral will also increase as T decreases as a result of the increase in β. The variance of the multiple integral approximation is further influenced by the fact that the Wiener random functions $\underset{\sim}{r}(\tau)$ and $\underset{\sim}{q}(\tau)$ in Eqs. (4.1.8) and (4.1.11) are multiplied by the thermal wavelength λ. Since λ increases with decreasing temperature the variance again increases as T decreases. A final contribution to the same behavior of increasing variance with decreasing T results from the fact noted above that k was increased with decreasing T in order to maintain the accuracy of the multiple integral approximation to the Wiener integrals. The multiplicity, $6(k-1)$, of the integral thus increases with decreasing T resulting in an increasing variance for the Monte Carlo procedure.

The standard deviation of the multiple integral results also depends upon the choice of the initial vector $\underset{\sim}{r}_o^{(k)}$ of the Markov chain $\{\underset{\sim}{r}_t^{(k)}\}$. Due to the one step memory inherent in the chain the choice of an initial vector $\underset{\sim}{r}_o^{(k)}$ which is improbable with respect to the probability density $P(\underset{\sim}{r}^{(k)})d\mu_{rk}$ (Eqs. (4.1.26) and (4.2.5)) can cause a large variation in the integrand as the vectors $\underset{\sim}{r}_t^{(k)}$ move from $\underset{\sim}{r}_o^{(k)}$ toward the region of maximum $P(\underset{\sim}{r}^{(k)})d\mu_{rk}$. An attempt was made to reduce the error caused by a bad choice of $\underset{\sim}{r}_o^{(k)}$ for each pair of values of r_{12} and T. At high temperatures $P(\underset{\sim}{r}^{(k)})d\mu_{rk}$ assigns the

highest probability to vectors in the neighborhood of $\underset{\sim}{r}^{(k)} \equiv 0$ provided that $P(\underset{\sim}{r}^{(k)})$ is slowly varying over the range of $\underset{\sim}{r}_{12} + \underset{\sim}{r}^{(k)}$. Thus for the highest temperature and largest r_{12} the initial vector was taken to be $\underset{\sim}{r}_o^{(k)} \equiv 0$. At lower temperatures the initial vector for the largest value of r_{12} was taken to be the last vector $\underset{\sim}{r}_M^{(k)}$ generated by the Markov chain for the same value of r_{12} at the next higher temperature. For successively smaller values of r_{12} the initial vector was taken to be the last vector generated at the same temperature and the next higher value of r_{12}.

It can be seen from the tables in Appendix B that $g_e(r_{12};\ 20{,}000)$ is small with respect to $g_c(r_{12};\ 20{,}000)$ as was to be expected from the fact that $g_e(r_{12})$ vanishes to order T^{-3} in the Wigner-Kirkwood expansion. $\lambda^{-3}g_e(r_{12};\ 20{,}000)$ is, on the average, an order of magnitude smaller than $\lambda^{-3}g_c(r_{12};\ 20{,}000)$. The standard deviations of these quantities, however, are of approximately the same size so that the effect of adding g_e to g_c in the approximation for g_1 is primarily an increase in the expected error in g_1.

The quantities $g_c(r_{12};\ M)$ and $g_e(r_{12};\ M)$ were also computed with $M < 20{,}000$ at several pairs of values for r_{12} and T. The standard deviations in these quantities were observed to decrease as $M^{-\frac{1}{2}}$ as would be expected of a well-formulated Monte Carlo procedure.

5.2 Numerical Comparisons with Theory and Experiment

It can be seen from Figure 3 that the position of the minimum in $g_1(r_{12})$ remains fairly constant at $r_{12} \simeq 1.8\sigma$ over the entire temperature range. The position of the minimum in $g_1(r_{12})$ can be interpreted in terms of a crude argument about the spatial arrangement of three particles. If one takes the most probable arrangement of particles as a linear arrangement with each particle falling at the minimum of the potentials due to its two nearest neighbors, then for the Lennard-Jones (12-6) potential there should be maximum probability of finding a particle at distances of 1.12σ and 2.24σ from a reference particle. Correspondingly there should be a minimum probability of finding a particle midway between these two positions or at 1.69σ. If $W_2(r_{12})$ is slowly varying near this minimum of the pair distribution function, then the corresponding minimum in $g_1(r_{12})$ should fall at approximately the same value of r_{12}. The calculated position of the minimum, 1.8σ, agrees well enough with this result to indicate that the minimum can be interpreted physically as the gap between the first and second shells of atoms about the reference atom.

Classical and two term Wigner-Kirkwood approximations for $g_1(r_{12})$ have also been claculated using respectively the first and first two terms of Eq. (3.3.25) for $\langle \underset{\sim}{1},\underset{\sim}{2},\underset{\sim}{3} | e^{-\beta H_3} | \underset{\sim}{1},\underset{\sim}{2},\underset{\sim}{3} \rangle$.

The integration over the position of the third particle was carried out by a straightforward iterated Simpson's rule approximation. Comparisons between the classical, Wigner-Kirkwood, and quantum calculations are shown in Figures 9, 10, 11, and 12. The classical values of $g_1(r_{12})$ have previously been calculated by Henderson [28], and the results presented agree with his calculations wherever there is overlap. In observing these comparisons it should be noted that when $g_1(r_{12})$ is used to calculate a physically measurable quantity it is multiplied by $W_2(r_{12})$ which goes to zero rapidly with decreasing r_{12} for $r_{12}/\sigma < 1$. Thus values of $g_1(r_{12})$ for $r_{12} \lesssim 0.8\sigma$ are not significant.

The two term Wigner-Kirkwood approximation is fairly accurate down to about $T = 10^{\circ}K$. The position of the minimum in $g_1(r_{12})$ corresponding to the intershell gap remains approximately constant for the Wigner-Kirkwood data while a significant shift toward smaller values of r_{12} with decreasing temperature occurs in the classical position of this minimum. At $5^{\circ}K$ the Wiener integral method gives results which differ markedly from the two term Wigner-Kirkwood approximation. Results were obtained for only a few values of r_{12} at $T = 5^{\circ}K$ due to the amount of computation time involved in the Monte Carlo procedure for large values of the order, k, of the Wiener integral approximation ($k = 52$ at $T = 5^{\circ}K$). Considering the a posteriori information on the accuracy of the two term Wigner-Kirkwood approximation it would seem that reasonably

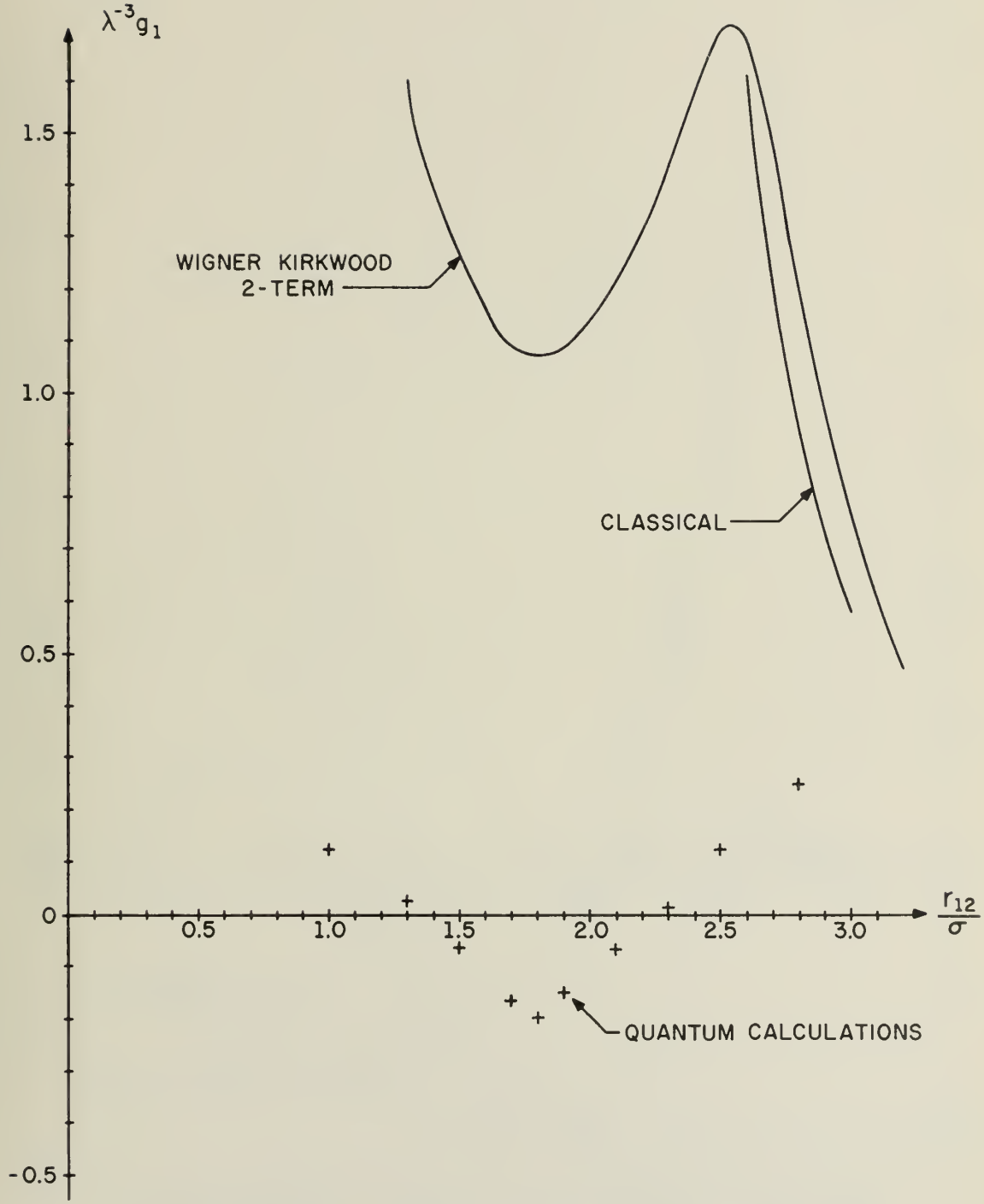

FIGURE 9. COMPARISON OF $\lambda^{-3}g_1$ WITH CLASSICAL AND SEMI-CLASSICAL VALUES FOR T=5°K.

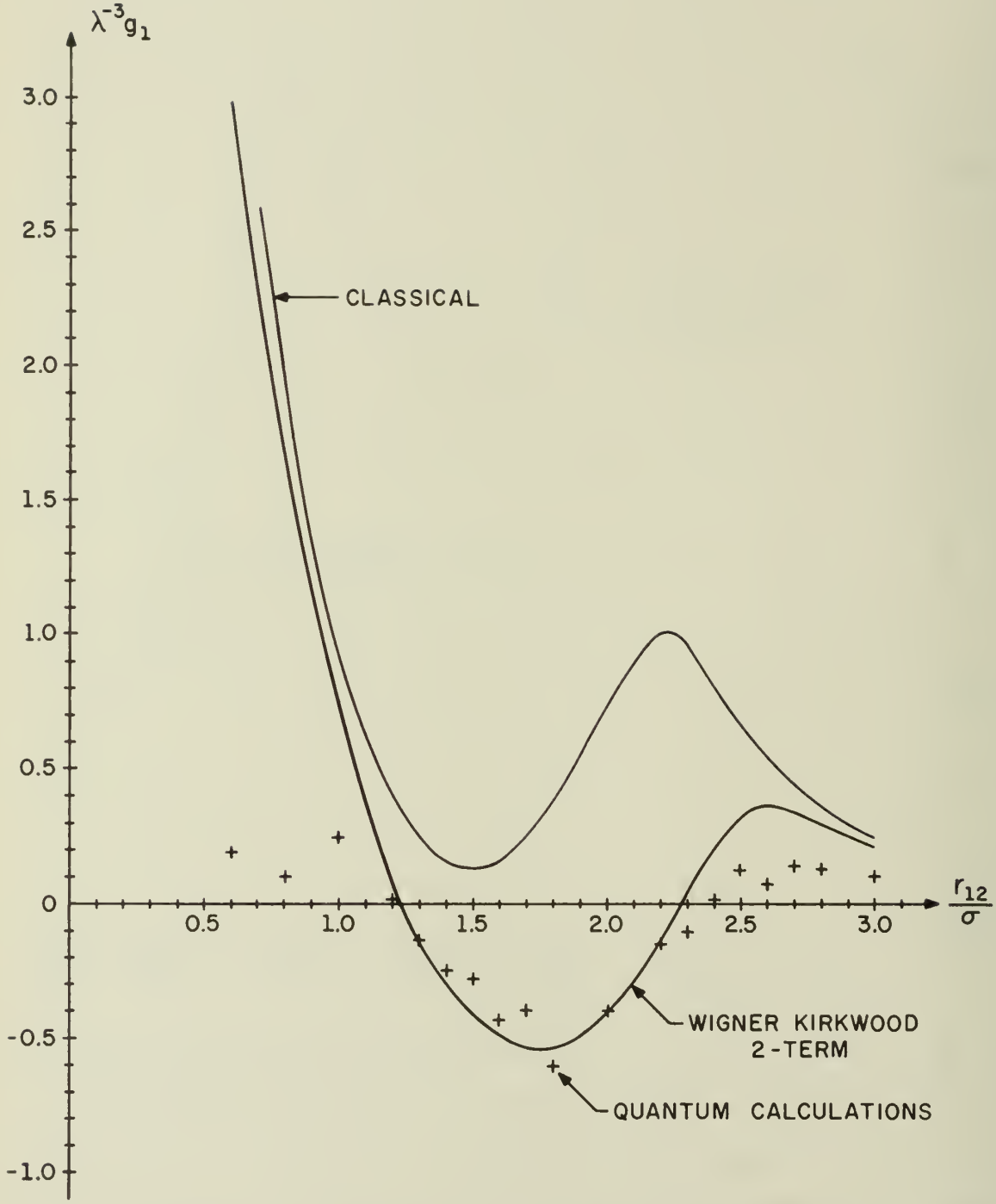

FIGURE 10. COMPARISON OF $\lambda^{-3}g_1$ WITH CLASSICAL AND SEMI-CLASSICAL VALUES FOR T=10°K.

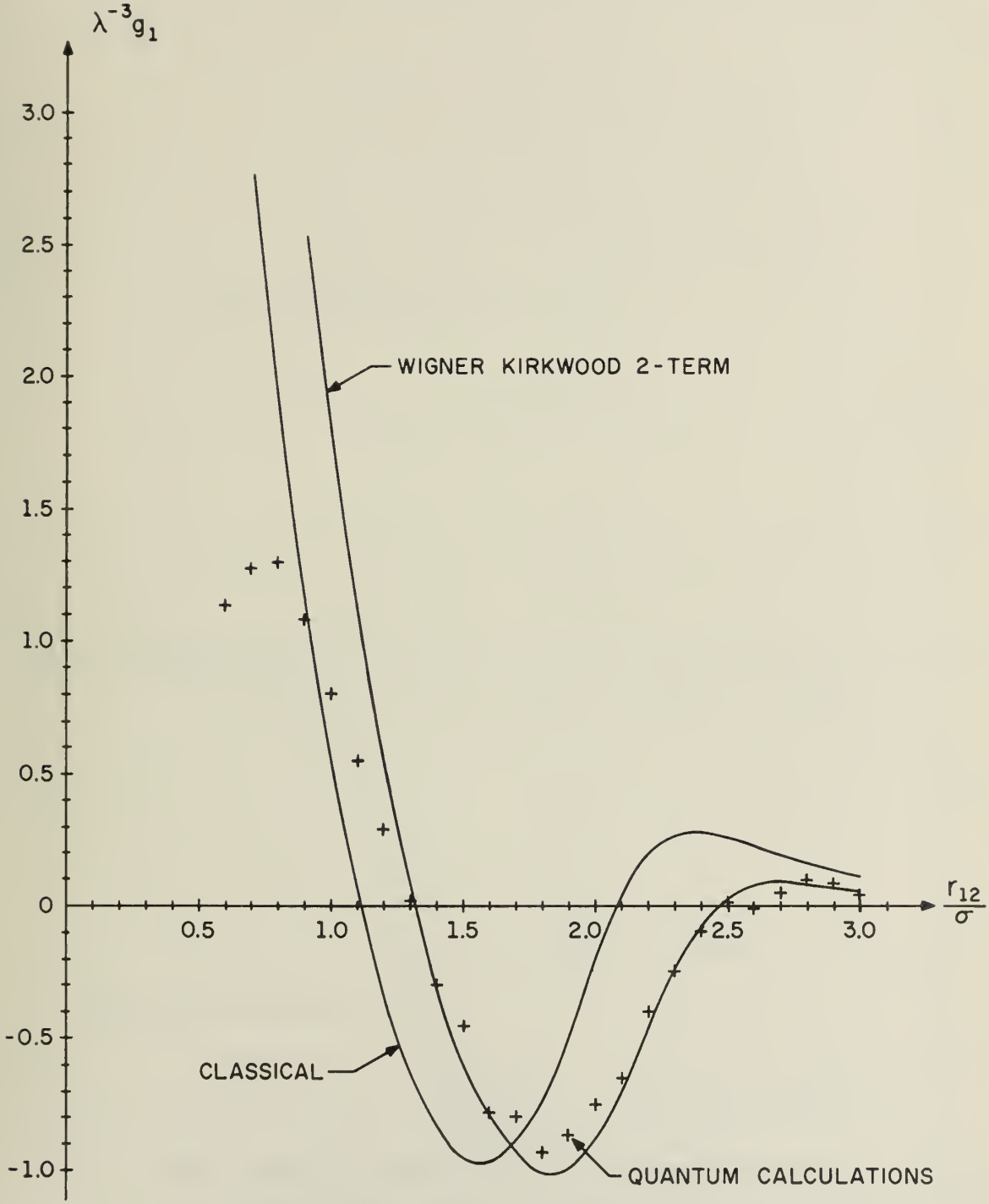

FIGURE 11. COMPARISON OF $\lambda^{-3}g_1$ WITH CLASSICAL AND SEMI-CLASSICAL VALUES FOR T=20°K.

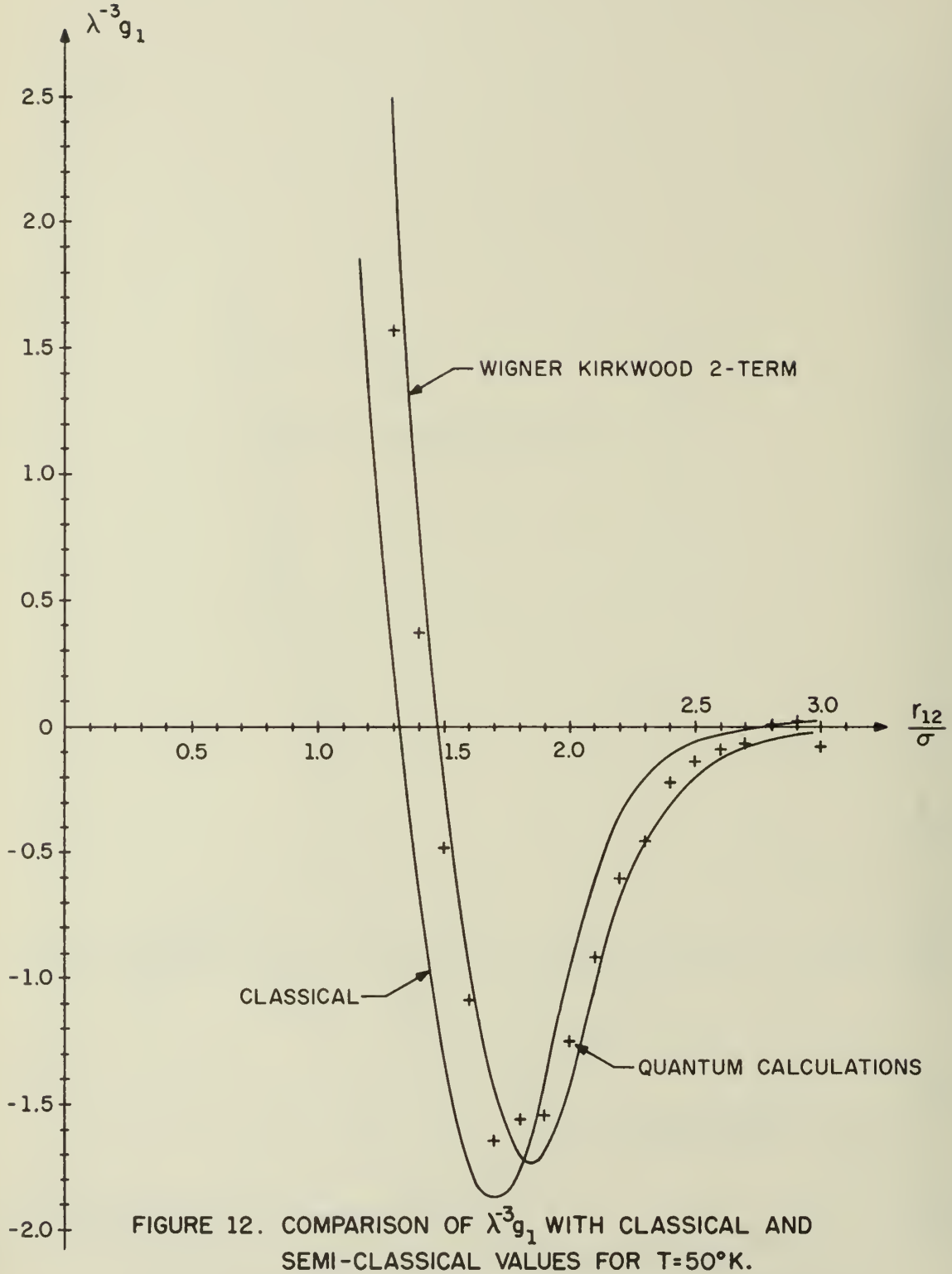

FIGURE 12. COMPARISON OF $\lambda^{-3}g_1$ WITH CLASSICAL AND SEMI-CLASSICAL VALUES FOR T=50°K.

accurate results could be obtained with $Tk \gtrsim 30^{\circ}K$ rather than $Tk \gtrsim 260^{\circ}K$ so that it would be possible to repeat the $5^{\circ}K$ computation in one tenth the time.

There seems to be no experimental data on the pair distribution function in He^4 gas at low temperatures. The pair distribution function for liquid helium, however, has been measured by neutron diffraction (Henshaw [29]) for several values of the density. Figures 13 and 14 show

$$W_2(r_{12}) \left[1 + n\, g_1(r_{12})\right] \simeq \frac{n_2(r_{12})}{n^2} = \frac{\rho(r_{12})}{\rho_o} \tag{5.2.1}$$

for $T = 5^{\circ}K$ and number densities n corresponding to mass densities $\rho_o = 0.095$ gm/cc and $\rho_o = 0.184$ gm/cc respectively compared with Henshaw's data for these same densities. Since only 3-particle effects have been taken into account in the computation, agreement cannot be expected beyond the second peak in the distribution function. To indicate the variation of $\rho(r_{12})/\rho_o$ with temperature, smooth curves have been fitted to the numerical results for

$$W_2(r_{12}) \left[1 + n\, g_1(r_{12})\right] \simeq \frac{\rho(r_{12})}{\rho_o} \tag{5.2.2}$$

for temperatures $10^{\circ}K$, $20^{\circ}K$, and $40^{\circ}K$ at a density of $\rho_o = 0.184$ gm/cc. The resulting curves are shown in Figure 15.

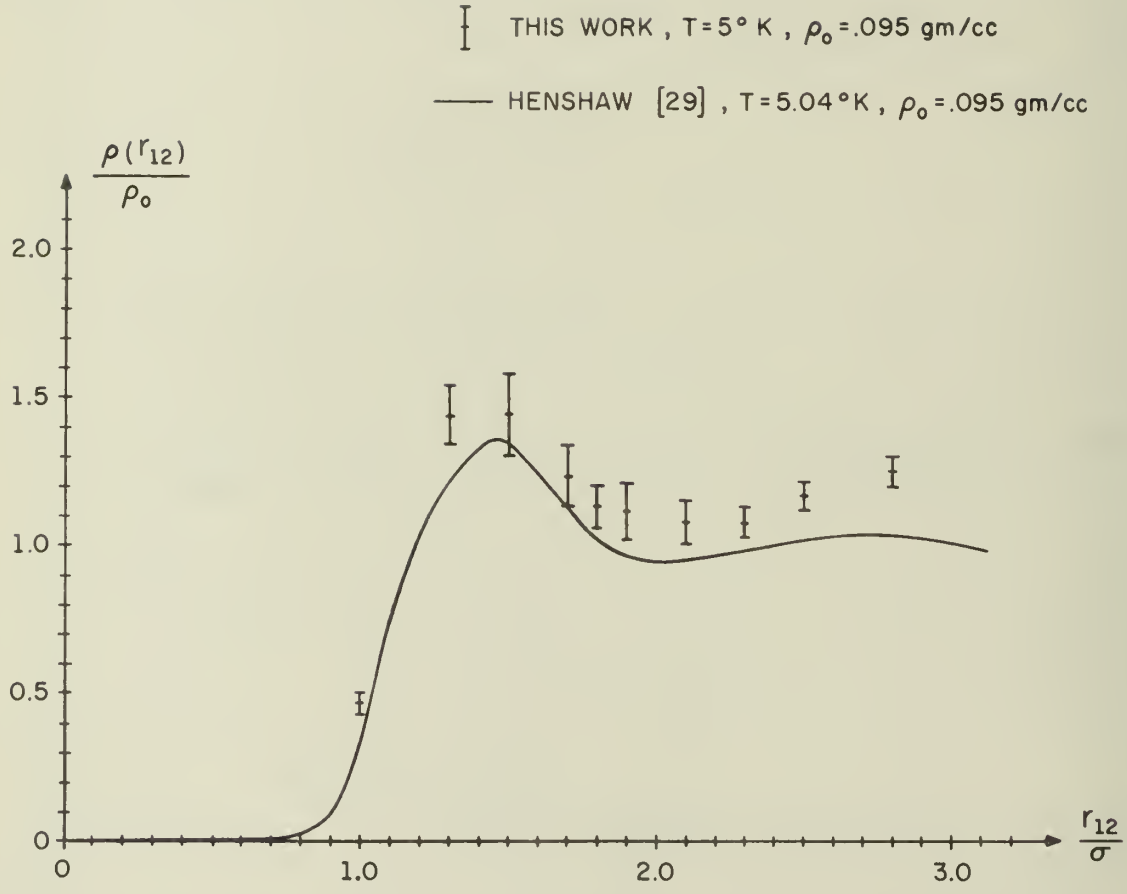

FIGURE 13. THE PAIR DISTRIBUTION FUNCTION FOR AVERAGE DENSITY ρ_0 =.095 gm/cc.

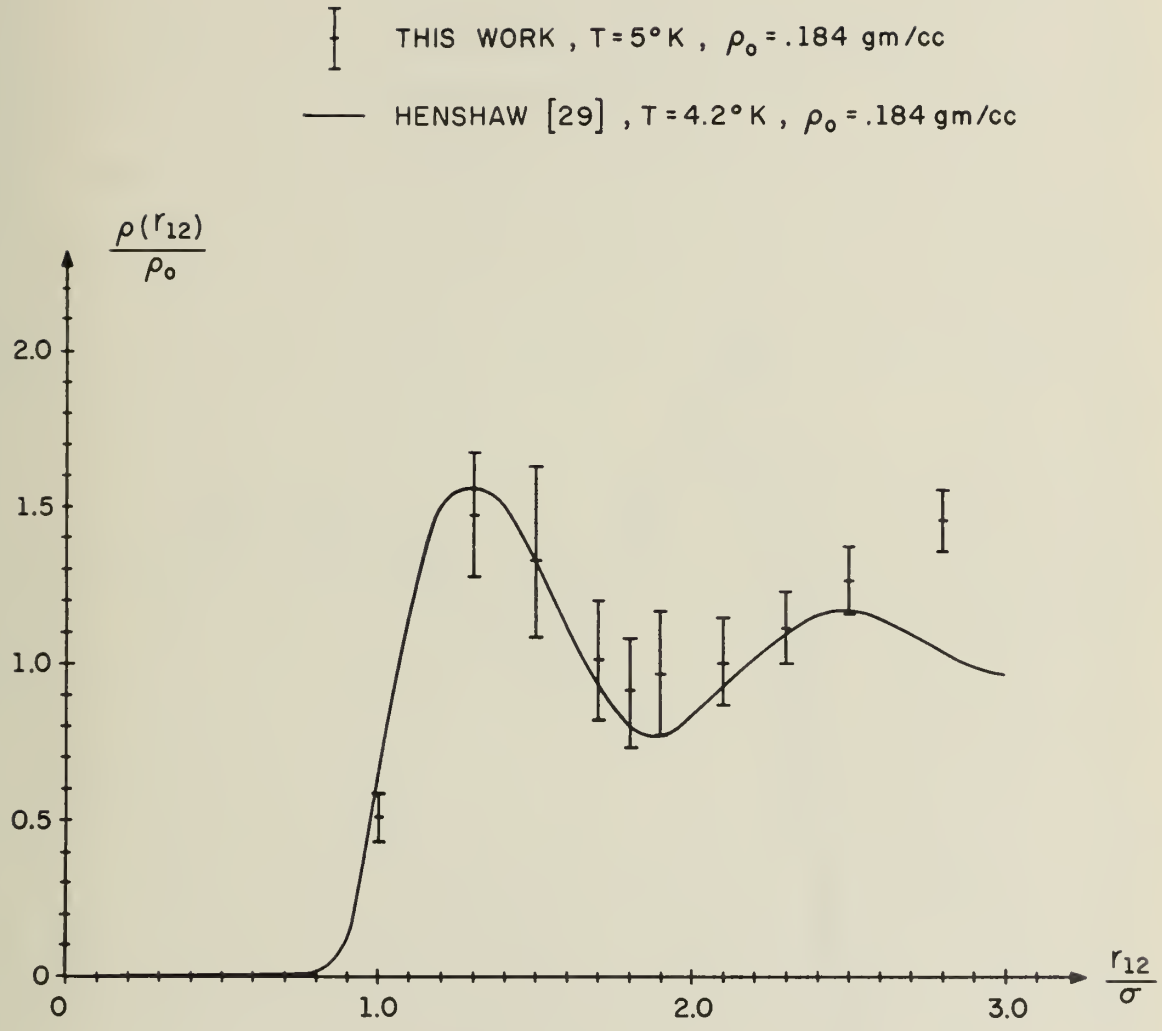

FIGURE 14. THE PAIR DISTRIBUTION FUNCTION FOR AVERAGE DENSITY ρ_0 = .184 gm/cc.

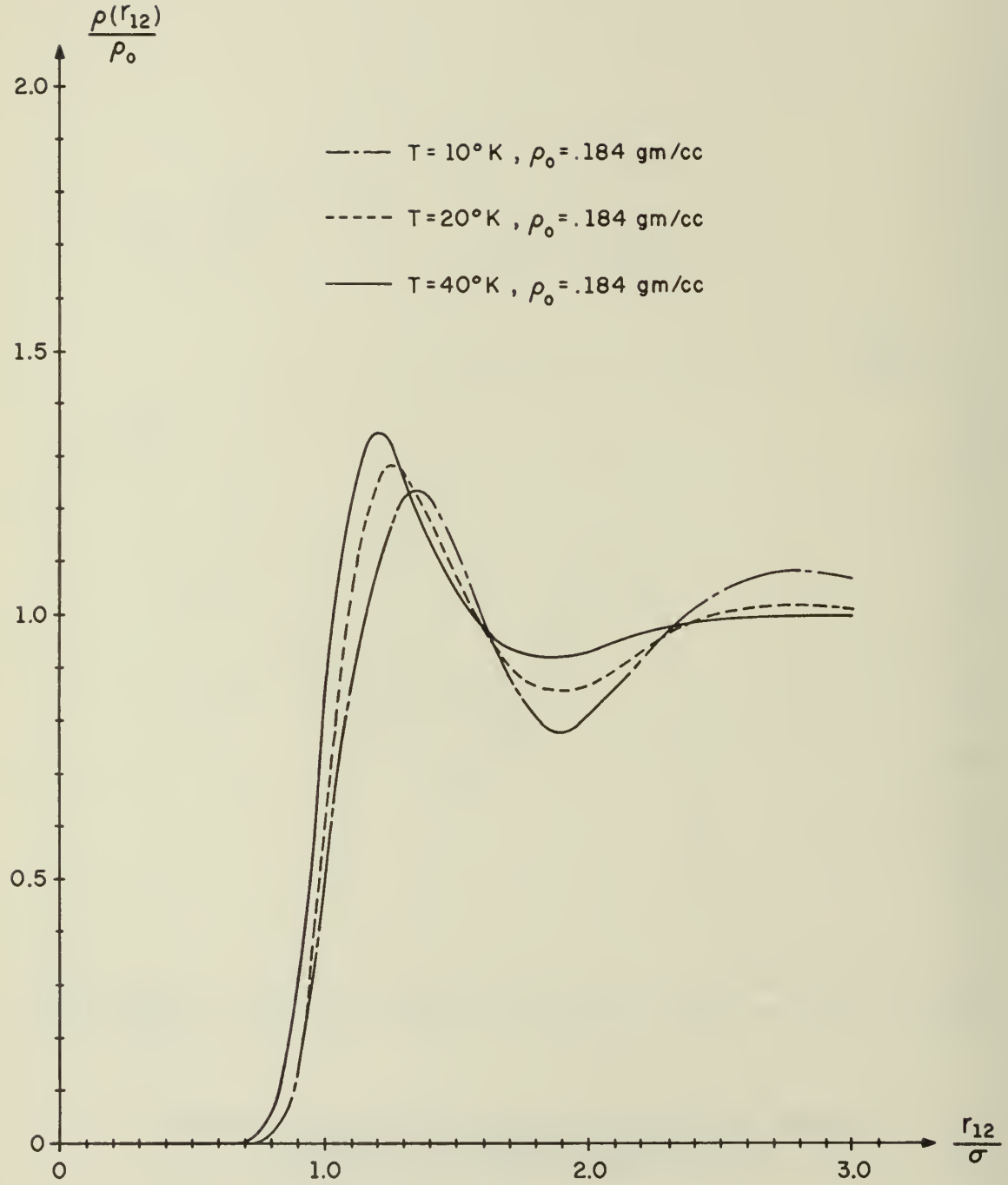

FIGURE 15. THE PAIR DISTRIBUTION FUNCTION AS A FUNCTION OF TEMPERATURE FOR ρ_0 = .184 gm/cc.

Two factors influence the comparison between Henshaw's neutron diffraction data for liquid He^4 and the numerical results of this work. The first is the choice of the Lennard-Jones (12-6) potential, Eq. (2.1.2), as the correct intermolecular potential for helium. The second is the validity of the cluster expansion for temperatures and densities at which helium is a liquid. The influence due to each of these factors cannot be separated without recomputing $W_2(r_{12})$ and $g_1(r_{12})$ for a different intermolecular potential. However, barring compensating errors in these two approximations, Figures 13 and 14 indicate that both approximations are fairly good for the pair distribution of liquid He^4 at $5^\circ K$.

Using Eq. (2.3.20) the third virial coefficient C(T) was evaluated for all temperatures at which $g_1(r_{12})$ was calculated except for $5^\circ K$. $C(5^\circ K)$ was not calculated partly due to the large sampling errors in $g_1(r_{12})$ at $5^\circ K$ but primarily due to the fact that values of $g_1(r_{12})$ for $r_{12} > 2.8\sigma$ give a large contribution to the integral for $C(5^\circ K)$ and no numerical results were obtained for this range of r_{12}. Figure 16 shows the numerical results for C(T) compared to the values adopted by Keesom [30] for the experimental third virial coefficient and the values calculated classically from the Lennard-Jones (12-6) potential (Hirschfelder [1]).

Over almost all of the temperature range the computed values fall consistently below the experimental results. Since Eq. (2.3.20) does not depend on the neglect of higher order terms in the cluster

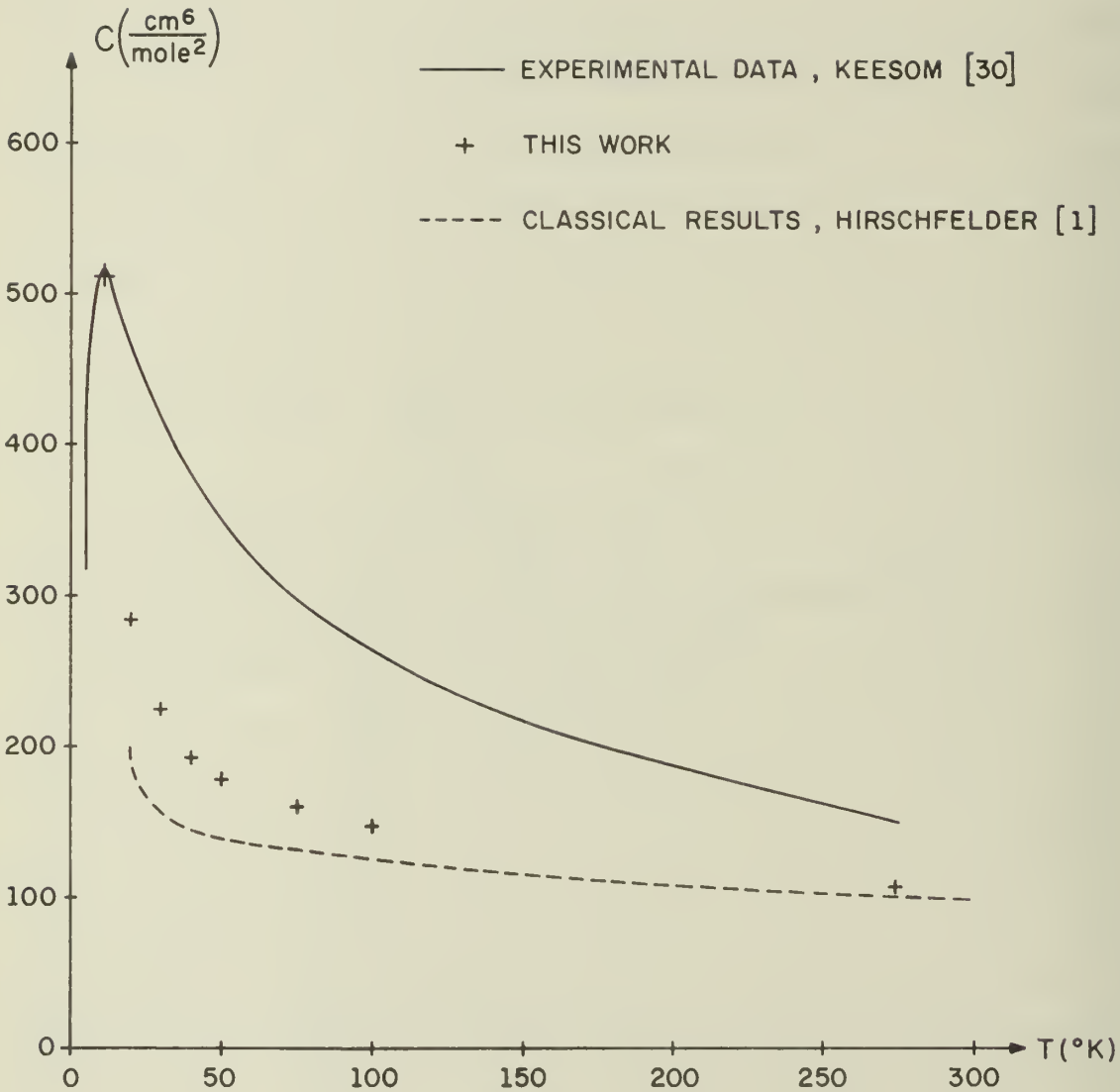

FIGURE 16. COMPARISON OF CALCULATED THIRD VIRIAL COEFFICIENT WITH CLASSICAL AND EXPERIMENTAL VALUES.

expansion the cause of this difference is evidently the choice of the pairwise additive Lennard-Jones (12-6) potential as the correct 3-particle potential for helium. Some recent calculations by Sherwood, De Rocco, and Mason [31] indicate that nonadditive 3-body forces have a sizeable effect on the third virial coefficient. The ways in which $g_1(r_{12})$ and C(T) differ from the experimental values can be reconciled qualitatively. Figures 13 and 14 indicate that the calculated $g_1(r_{12})$ is fairly consistently larger than the experimental $g_1(r_{12})$. On performing the integration over r_{12} in Eq. (2.3.20) this would lead to a C(T) which would be smaller than its experimental values as is verified in Figure 16.

5.3 Conclusion

The comparisons of Section 5.2 point to two conclusions regarding the physics of the He^4 system. The first is that quantum mechanical calculations based on the cluster expansion and assuming a pairwise additive Lennard-Jones (12-6) potential can produce a reasonable qualitative fit to the pair distribution function in liquid He^4. Secondly, the consistent deviation of the calculated third virial coefficient from the experimental values over the full temperature range indicates that the choice of the latter potential for the 3-body interaction in He^4 is not good enough to yield quantitative agreement with experiment.

From the mathematical viewpoint it has been shown that the Wiener integral may be a useful computational tool. The upper bounds of Section 3.2 indicate that the expression of a quantity in terms of Wiener integrals can yield qualitative and semiquantitative information on the size and behavior of that quantity. Finally, the numerical evaluation of a Wiener integral expression has been shown to be computationally feasible in a situation where the amount of computation involved in integrating the original partial differential equation giving rise to the Wiener integral would be prohibitive.

With the numerical techniques developed it would be interesting to investigate the effect on the third virial coefficient of a change in the intermolecular potential. A quantum mechanical calculation of the third virial coefficient might offer a way of comparing the potentials which are indistinguishable with respect to the second virial coefficient. Another possible extension of this work would be an investigation of the behavior of the exchange terms in the 3-particle density matrix. Of course, both direct and exchange terms can be computed for systems of more than three particles using the same formulation, but indications are that the necessary computation increases greatly with each added particle.

LIST OF REFERENCES

[1] J. O. Hirschfelder, C. F. Curtis, and R. B. Bird, Molecular Theory of Gases and Liquids, Chap. 6, John Wiley and Sons; 1954.

[2] S. Y. Larsen, "Quantum Mechanical Calculation of the Third Virial Coefficient of He^4," The Physical Review, Vol. 130, No. 4, pp. 1426-1440; May 1963.

[3] A. Pais, and G. E. Uhlenbeck, "On the Quantum Theory of the Third Virial Coefficient," The Physical Review, Vol. 116, No. 2, pp. 250-269; October 1959.

[4] C. N. Yang, and T. D. Lee, "Many-Body Problem in Quantum Statistical Mechanics. I. General Formulation," The Physical Review, Vol. 113, No. 5, pp. 1165-1177; March 1959.

[5] S. Y. Larsen, K. Witte, and J. E. Kilpatrick, "On the Quantum-Mechanical Pair-Correlation Function of ^4He Gas at Low Temperatures," Journal of Chemical Physics, Vol. 44, No. 1, pp. 213-220; January 1966.

[6] L. D. Fosdick, and H. F. Jordan, "Path Integral Calculation of the Two Particle Slater Sum for He^4," The Physical Review, Vol. 143, No. 1, pp. 58-66; March 1966.

[7] J. de Boer, and A. Michels, "Quantum-Mechanical Calculation of the Second Virial-coefficient of Helium at Low Temperatures," Physica, Vol 6, No. 5, pp. 409-420; March 1939.

[8] J. de Boer, "Molecular Distribution and Equation of State of Gases," Reports on Progress in Physics, Vol. 12, pp. 305-374; 1949.

[9] B. Kahn, and G. E. Uhlenbeck, "Theory of Condensation," Physica, Vol. 5, pp. 399-416, May 1938.

[10] K. Huang, Statistical Mechanics, Chap. 14, Sects. 14.1 and 14.2, John Wiley and Sons; 1963.

[11] S. G. Brush, "Functional Integrals and Statistical Physics," Reviews of Modern Physics, Vol. 33, No. 1, pp. 79-92; January 1961.

[12] I. M. Gel'fand, and A. M. Yaglom, "Integration in Functional Space and its Applications in Quantum Physics," Journal of Mathematical Physics, Vol. 1, No. 1, pp. 48-69; January-February 1960.

[13] M. Kac, Lectures in Applied Mathematics, Vol. I, Proceedings of the Summer Seminar, Boulder, Colorado, 1957, Chap. IV, Interscience Publishers, Inc.; 1958.

[14] J. Neyman, Editor, Proceedings of the Second Berkeley Symposium on Mathematical Statistics and Probability, Berkeley, University of California Press; 1951.

[15] R. P. Feynman, and A. R. Hibbs, Quantum Mechanics and Path Integrals, Chap. 10, McGraw-Hill, Inc.; 1965.

[16] P. Levy, "Le Mouvement Brownien," Memorial des Sciences Mathematiques, Fascicule 126, Gauthier-Villars, Paris; 1954.

[17] S. Y. Larsen, J. E. Kilpatrick, E. H. Lieb, and H. F. Jordan, "Suppression at High Temperatures of Effects Due to Statistics in the Second Virial Coefficient of a Real Gas," The Physical Review, Vol. 140, No. 1A, pp. 129-130; October 1965.

[18] E. H. Lieb, "Calculation of Exchange Second Virial Coefficient of a Hard-Sphere Gas by Path Integrals," Journal of Mathematical Physics, Vol. 8, No. 1, pp. 43-52; January 1967.

[19] R. H. Cameron, "A Simpson's Rule for the Evaluation of Wiener's Integrals in Function Space," Duke Mathematical Journal, Vol. 18, pp. 111-130; 1951.

[20] L. D. Fosdick, "Numerical Estimation of the Partition Function in Quantum Statistics," Journal of Mathematical Physics, Vol. 3, No. 2, pp. 1251-1264; November-December 1962.

[21] L. D. Fosdick, "Approximation of a Class of Wiener Integrals," Mathematics of Computation, Vol. 19, pp. 225-233; 1965.

[22] I. M. Gel'fand, and N. N. Chentsov, "The Numerical Calculation of Path Integrals," J. Exptl. Theoret. Phys. (U.S.S.R.), Vol. 31, pp. 1106-1107; December 1956.

[23] A. G. Konheim, and W. L. Miranker, "Numerical Evaluation of Wiener Integrals," I.B.M. Research Report, RC-1540; January 1966.

[24] T. Kihara, Y. Midzuno, and T Shizume, "Virial Coefficients and Intermolecular Potential of Helium," Journal of the Physical Society of Japan, Vol. 10, No. 4; April 1955.

[25] N. Metropolis, A. W. Rosenbluth, M. N. Rosenbluth, A. H. Teller, and E. Teller, "Equation of State Calculations by Fast Computing Machines," The Journal of Chemical Physics, Vol. 21, No. 6, pp. 1087-1092; June 1953.

[26] J. M. Hammersly, and D. C. Handscomb, Monte Carlo Methods, John Wiley and Sons; 1954.

[27] J. L. Doob, Stochastic Processes, Chap. 5, John Wiley and Sons; 1953.

[28] D. Henderson, "Exact and Approximate Values for the Radial Distribution Function at Low Densities for the 6:12 Potential," Molecular Physics, Vol. 10, No. 1, p. 73; 1965.

[29] D. G. Henshaw, "Pressure Effect in the Atomic Distribution in Liquid Helium by Neutron Diffraction," The Physical Review, Vol. 119, No. 1, pp. 14-21; July 1960.

[30] W. H. Keesom, Helium, Chap. 2, Elsevier; 1942.

[31] A. E. Sherwood, A. G. DeRocco, and E. A. Mason, "Nonadditivity of Intermolecular Forces: Effects on the Third Virial Coefficient," Journal of Chemical Physics, Vol. 44, No. 8, pp. 2984-2994; April 1966.

APPENDIX A

LEMMA FOR THE PROOF OF Eq. (4.2.21)

Lemma: $$p^*(\underset{\sim}{x}'|\underset{\sim}{x})w(\underset{\sim}{x}) = p^*(\underset{\sim}{x}^T|\underset{\sim}{x}'^T)w(\underset{\sim}{x}'^T) \tag{4.2.20}$$

Proof: From Eqs. (4.2.11) and (4.2.13) it follows that

$$p^*(\underset{\sim}{x}^T|\underset{\sim}{x}'^T)w(\underset{\sim}{x}'^T)$$

$$= \left(\frac{k}{\pi}\right)^{\frac{k-1}{2}} (2\pi)^{\frac{1}{2}} \left(\frac{k}{2\pi}\right)^{\frac{k}{2}} \exp\left[-k \sum_{i=1}^{k-1} \left(x_i^T - \frac{x_{i-1}^T + x_{i+1}'^T}{2}\right)^2\right.$$

$$\left. - \frac{k}{2} \sum_{i=1}^{k} (x_i'^T - x_{i-1}'^T)^2\right] . \tag{A.1}$$

By the definition of $\underset{\sim}{x}^T$, $x_i^T = x_{k-i}$, i=0,1,...,k, so Eq. (A.1) becomes

$$p^*(\underset{\sim}{x}^T|\underset{\sim}{x}'^T)w(\underset{\sim}{x}'^T)$$

$$= \left(\frac{k}{\pi}\right)^{\frac{k-1}{2}} (2\pi)^{\frac{1}{2}} \left(\frac{k}{2\pi}\right)^{\frac{k}{2}} \exp\left[-k \sum_{i=1}^{k-1} \left(x_{k-i} - \frac{x_{k-i+1} + x'_{k-i-1}}{2}\right)^2\right.$$

$$\left. - \frac{k}{2} \sum_{i=1}^{k} (x'_{k-i} - x'_{k-i+1})^2\right] . \tag{A.2}$$

Setting $\ell = k-i$, one finds that

$$p^*(\underset{\sim}{x}^T|\underset{\sim}{x}'^T)w(\underset{\sim}{x}'^T)$$

$$= \left(\frac{k}{\pi}\right)^{\frac{k-1}{2}} (2\pi)^{\frac{1}{2}} \left(\frac{k}{2\pi}\right)^{\frac{k}{2}} \exp\left[-k \sum_{\ell=1}^{k-1} x_\ell^2 + k \sum_{\ell=1}^{k-1} x_\ell x_{\ell+1}\right.$$

$$+ k \sum_{\ell=2}^{k-1} x_\ell x'_{\ell-1} - k \sum_{\ell=1}^{k-1} \frac{(x_{\ell+1} + x'_{\ell-1})^2}{4} - \frac{k}{2} \sum_{\ell=0}^{k-1} (x'_\ell)^2$$

$$\left. + k \sum_{\ell=1}^{k} x'_\ell x'_{\ell+1} - \frac{k}{2} \sum_{\ell=1}^{k} (x'_\ell)^2\right] , \qquad (A.3)$$

and making use of the fact that $x_o = x_k = x'_o = x'_k = 0$, this becomes

$$p^*(\underset{\sim}{x}^T|\underset{\sim}{x}'^T)w(\underset{\sim}{x}'^T)$$

$$= \left(\frac{k}{\pi}\right)^{\frac{k-1}{2}} (2\pi)^{\frac{1}{2}} \left(\frac{k}{2\pi}\right)^{\frac{k}{2}} \exp\left[-k \sum_{\ell=1}^{k-1} (x'_\ell)^2 + k \sum_{j=1}^{k-1} x'_j x'_{j-1}\right.$$

$$+ k \sum_{j=1}^{k-1} x'_j x_{j+1} - k \sum_{\ell=1}^{k-1} \frac{(x_{\ell+1} + x'_{\ell-1})^2}{4}$$

$$\left. - k \sum_{\ell=1}^{k-1} x_\ell^2 + \sum_{j=1}^{k} x_j x_{j-1}\right] , \qquad (A.4)$$

where $j = \ell+1$. Equating the dummy subscripts and combining the sums, one obtains

$$p^*(\underset{\sim}{x}^T|\underset{\sim}{x}'^T)w(\underset{\sim}{x}'^T)$$

$$= \left(\frac{k}{\pi}\right)^{\frac{k-1}{2}} (2\pi)^{\frac{1}{2}} \left(\frac{k}{2\pi}\right)^{\frac{k}{2}} \exp\left[-k \sum_{\ell=1}^{k-1} \left(x'_\ell - \frac{x_{\ell+1} + x'_{\ell-1}}{2}\right)^2\right.$$

$$\left. - \frac{k}{2} \sum_{\ell=1}^{k} (x_\ell - x_{\ell-1})^2\right] ,$$

$$= p^*(\underset{\sim}{x}'|\underset{\sim}{x})w(\underset{\sim}{x}) , \qquad (A.5)$$

which completes the proof.

APPENDIX B

DETAILED COMPUTATIONAL PROCEDURE AND NUMERICAL RESULTS FOR $g_c(r_{12};M)$, $g_e(r_{12};M)$ and $C(T)$

The step by step procedure for computing the approximation $g_c(r_{12};M)$ to $g_c(r_{12})$ is as follows:

1. Generate M independent Wiener path approximations consisting of 3k-dimensional vectors $\underset{\sim}{q}_t^{(k)}$, t = 1,2,...,M, drawn from a probability distribution $d\mu_{qk}$ by Eq. (4.2.2), $\underset{\sim}{q}_o = \underset{\sim}{q}_k = 0$,

$$\underset{\sim}{q}_i = \frac{\underset{\sim}{q}_{i-1}\left(1 - \frac{i}{k}\right)}{1 - \frac{i-1}{k}} + \underset{\sim}{\xi}_i \left[\frac{\frac{1}{k}\left(1 - \frac{i}{k}\right)}{1 - \frac{i-1}{k}}\right]^{\frac{1}{2}}, \quad i = 1,2,\ldots,k-1 \quad , \tag{B.1}$$

where the $\underset{\sim}{\xi}_i$ are 3-dimensional random variables, the coordinate variables of which are independent and normally distributed with mean 0 and variance 1.

2. Generate an M step Markov chain $\{\underset{\sim}{r}_t^{(k)} | t=1,2,\ldots,M\}$ having the stationary probability

$$\frac{D_{12}(\underset{\sim}{r}^{(k)})}{W_2(\underset{\sim}{1},\underset{\sim}{2})} \; d\mu_{rk}$$

by first generating $\underset{\sim}{r}_t^{-(k)}$ using the procedure described by Eq. (4.2.28)

and setting $\underset{\sim}{r}_t^{(k)} = \underset{\sim}{\bar{r}}_t^{(k)}$ if $D_{12}(\underset{\sim}{\bar{r}}_t^{(k)}) \geq D_{12}(\underset{\sim}{r}_{t-1}^{(k)})$ while if $D_{12}(\underset{\sim}{\bar{r}}_t^{(k)}) < D_{12}(\underset{\sim}{r}_{t-1}^{(k)})$ set

$$\underset{\sim}{r}_t^{(k)} = \underset{\sim}{\bar{r}}_t^{(k)} \text{ with probability } \frac{D_{12}(\underset{\sim}{\bar{r}}_t^{(k)})}{D_{12}(\underset{\sim}{r}_{t-1}^{(k)})}$$

and

$$\underset{\sim}{r}_t^{(k)} = \underset{\sim}{r}_{t-1}^{(k)} \text{ with probability } 1 - \frac{D_{12}(\underset{\sim}{r}_t^{(k)})}{D_{12}(\underset{\sim}{r}_{t-1}^{(k)})} \quad .$$

3. Generate M independent random vectors $\underset{\sim}{Q}_t = (Q_x, Q_y, 0)_t$, $t = 1,2,\ldots,M$, according to the probability $\Gamma_c(\underset{\sim}{Q})d^2\underset{\sim}{Q}$.

4. Form the average

$$g_c(r_{12};M) = \frac{1}{M} \sum_{t=1}^{M} L_c(\underset{\sim}{r}_t^{(k)}, \underset{\sim}{q}_t^{(k)}, \underset{\sim}{Q}_t)\, \Gamma_c^{-1}(\underset{\sim}{Q}_t) \quad . \tag{B.2}$$

The equations pertinent to the above procedure are

$$L_c(\underset{\sim}{r}^{(k)}, \underset{\sim}{q}^{(k)}, \underset{\sim}{Q}) = \left[D_{13}\left(\frac{\sqrt{3}}{2}\,\underset{\sim}{q}^{(k)} + \frac{1}{2}\,\underset{\sim}{r}^{(k)}\right) - 1\right] \times \left[D_{23}\left(\frac{\sqrt{3}}{2}\,\underset{\sim}{q}^{(k)} - \frac{1}{2}\,\underset{\sim}{r}^{(k)}\right) - 1\right] , \tag{4.3.5}$$

$$D_{12}(\underset{\sim}{r}^{(k)}) = \exp\left\{-\frac{\beta}{6k}\sum_{i=1}^{k}\left[V\left(\frac{\lambda}{\sqrt{\pi}}\,\underset{\sim}{r}_{i-1} + \underset{\sim}{r}_{12}\right) + 4V\left(\frac{\lambda}{\sqrt{\pi}}\left(\frac{\underset{\sim}{r}_i + \underset{\sim}{r}_{i-1}}{2}\right) + \underset{\sim}{r}_{12}\right)\right.\right.$$

$$\left.\left. + V\left(\frac{\lambda}{\sqrt{\pi}}\,\underset{\sim}{r}_i + \underset{\sim}{r}_{12}\right) + \frac{\lambda^2}{2\pi k}V''\left(\frac{\lambda}{\sqrt{\pi}}\left(\frac{\underset{\sim}{r}_i + \underset{\sim}{r}_{i-1}}{2}\right) + \underset{\sim}{r}_{12}\right)\right]\right\} ,$$

$$D\begin{Bmatrix}13\\23\end{Bmatrix}(\underset{\sim}{q}^{(k)}) = \exp\left\{-\frac{\beta}{6k}\sum_{i=1}^{k}\left[V\left(\frac{\lambda}{\sqrt{\pi}}\,\underset{\sim}{q}_{i-1} + \underset{\sim}{Q} \pm \frac{\underset{\sim}{r}_{12}}{2}\right)\right.\right.$$

$$+ 4V\left(\frac{\lambda}{\sqrt{\pi}}\left(\frac{\underset{\sim}{q}_i + \underset{\sim}{q}_{i-1}}{2}\right) + \underset{\sim}{Q} \pm \frac{\underset{\sim}{r}_{12}}{2}\right) + V\left(\frac{\lambda}{\sqrt{\pi}}\,\underset{\sim}{q}_i + \underset{\sim}{Q} \pm \frac{\underset{\sim}{r}_{12}}{2}\right)$$

$$\left.\left. + \frac{\lambda^2}{2\pi k}V''\left(\frac{\lambda}{\sqrt{\pi}}\left(\frac{\underset{\sim}{q}_i + \underset{\sim}{q}_{i-1}}{2}\right) + \underset{\sim}{Q} \pm \frac{\underset{\sim}{r}_{12}}{2}\right)\right]\right\} , \qquad (4.1.29)$$

$$V(r) = 4\kappa\left[\left(\frac{\sigma}{r}\right)^{12} - \left(\frac{\sigma}{r}\right)^{6}\right], \quad \kappa = 14.04 \times 10^{-16} \text{ erg}, \quad \sigma = 2.56 \times 10^{-8} \text{ cm} , \qquad (2.1.2)$$

and

$$\Gamma_c(\underset{\sim}{Q})d^2\underset{\sim}{Q} = \frac{1}{\sqrt{2\pi}\gamma_x}\exp\left(-\frac{Q_x^2}{2\gamma_x^2}\right)\frac{1}{\sqrt{2\pi}\gamma_y}\exp\left(-\frac{Q_y^2}{2\gamma_y^2}\right)dQ_x dQ_y \quad . \qquad (4.3.9)$$

The procedure for computing the approximation $g_e(r_{12};M)$ to $g_e(r_{12})$ is the same as that for $g_c(r_{12};M)$ except that steps 3 and 4 are modified.

3. Generate M independent random vectors $\underset{\sim}{Q}_t = (\rho_Q, \theta_Q, 0)_t$, $t = 1,2,\ldots,M$, according to a probability $\Gamma_e(\underset{\sim}{Q})d^2\underset{\sim}{Q}$.

4. Form the average

$$g_e(r_{12};M) = \frac{1}{M} \sum_{t=1}^{M} A(\underset{\sim}{r}_t^{(k)}, \underset{\sim}{q}_t^{(k)}, \underset{\sim}{Q}_t)\, \Gamma_e^{-1}(\underset{\sim}{Q}_t) \quad . \tag{B.3}$$

The additional equations needed for the computation of $g_e(r_{12};M)$ are

$$A(\underset{\sim}{r}^{(k)}, \underset{\sim}{q}^{(k)}, \underset{\sim}{Q}) = \frac{1}{2}\Big[L_e(\underset{\sim}{r}^{(k)}, \underset{\sim}{q}^{(k)}, \underset{\sim}{Q}) + L_e(\underset{\sim}{r}^{(k)}, \underset{\sim}{q}^{(k)}, -\underset{\sim}{Q})$$

$$+ L_e(\underset{\sim}{r}^{(k)}, -\underset{\sim}{q}^{(k)}, \underset{\sim}{Q}) + L_e(\underset{\sim}{r}^{(k)}, -\underset{\sim}{q}^{(k)}, -\underset{\sim}{Q})\Big], \tag{4.3.24}$$

$$L_e(\underset{\sim}{r}^{(k)}, \underset{\sim}{q}^{(k)}, \underset{\sim}{Q}) = 2\left[D_{13}\left(\underset{\sim}{Q}, \frac{\sqrt{3}}{2}\underset{\sim}{q}^{(k)} + \frac{1}{2}\underset{\sim}{r}^{(k)}\right) - D_{13}(\underset{\sim}{Q}, \underset{\sim}{q}^{(k)})\right], \tag{4.3.21}$$

$$D_{13}(\underset{\sim}{Q},\underset{\sim}{q}^{(k)}) = \exp\left\{-\frac{\beta}{6k}\sum_{i=1}^{k}\left[V\left(\frac{\lambda}{\sqrt{\pi}}\underset{\sim}{q}_{i-1} + \underset{\sim}{Q}\right) + 4V\left(\frac{\lambda}{\sqrt{\pi}}\left(\frac{\underset{\sim}{q}_i + \underset{\sim}{q}_{i-1}}{2}\right) + \underset{\sim}{Q}\right)\right.\right.$$

$$\left.\left. + V\left(\frac{\lambda}{\sqrt{\pi}}\underset{\sim}{q}_i + \underset{\sim}{Q}\right) + \frac{\lambda^2}{2\pi k}V''\left(\frac{\lambda}{\sqrt{\pi}}\left(\frac{\underset{\sim}{q}_i + \underset{\sim}{q}_{i-1}}{2}\right) + \underset{\sim}{Q}\right)\right]\right\}, \tag{4.3.22}$$

and

$$\Gamma_e(\underset{\sim}{Q})d^2\underset{\sim}{Q} = \frac{\rho_Q^5}{6!\gamma_\rho^2}\exp\left(-\frac{\rho_Q}{\gamma_\rho}\right)d\rho_Q\, d\xi_Q \;,\; 0 \le \xi_Q = \cos\theta_Q \le 1 \quad . \tag{4.3.19}$$

Table 1 gives the results of the calculations of $\lambda^{-3}g_c(r_{12};20,000)$ and $\lambda^{-3}g_e(r_{12};20,000)$ along with the values of $W_2(r_{12})$ computed in [6]. The quantity $\lambda^{-3}g_1(r_{12};20,000) = \lambda^{-3}g_c(r_{12};20,000) + \lambda^{-3}g_e(r_{12};20,000)$ is shown graphically as a function of r_{12} in Figures 17 through 25. The lengths of the error bars in these figures are twice the sum of the standard deviations in $\lambda^{-3}g_c(r_{12};20,000)$ and $\lambda^{-3}g_e(r_{12};20,000)$.

Table 2 presents the values for the third virial coefficient calculated from the formula

$$C = -\frac{N_0^2}{3}\left[\int g_1(r_{12})\, W_2(r_{12})\, d^3\underset{\sim}{r}_2 - 4b_2^2\right]. \qquad (2.3.20)$$

The integration over r_{12} was performed by Simpson's rule using $g_1(r_{12};20,000)$ for $g_1(r_{12})$ and taking the values of $W_2(r_{12})$ and b_2 calculated in [6].

Table 1.1. NUMERICAL VALUES OF $\lambda^{-3}g_c(r_{12};20,000)$, $\lambda^{-3}g_e(r_{12};20,000)$, AND $W_2(r_{12})$ FOR T = 5°K.

$\frac{r_{12}}{\sigma}$	$\frac{1}{\lambda^3} g_c(r_{12};M)$	Std. Dev.	$\frac{1}{\lambda^3} g_e(r_{12};M)$	Std. Dev.	$W_2(r_{12})$
1.0	0.11161	0.05433	0.01593	0.05076	0.41620
1.3	+0.00768	0.05091	0.02307	0.03620	1.39898
1.5	-0.09163	0.04704	+0.02604	0.05486	1.52524
1.7	-0.15542	0.04174	-0.00652	0.03842	1.41138
1.8	-0.16863	0.03699	-0.02636	0.03781	1.33505
1.9	-0.10887	0.03502	-0.03488	0.05512	1.26486
2.1	-0.10791	0.03155	+0.02816	0.04026	1.15433
2.3	+0.06428	0.02298	-0.04913	0.03940	1.08719
2.5	0.15227	0.01892	-0.02889	0.04606	1.04950
2.8	0.20509	0.01092	+0.04914	0.04430	1.02273

Table 1.2. NUMERICAL VALUES OF $\lambda^{-3} g_c(r_{12};20,000)$, $\lambda^{-3} g_e(r_{12};20,000)$, AND $W_2(r_{12})$ FOR T = 10°K.

$\frac{r_{12}}{\sigma}$	$\frac{1}{\lambda^3} g_c(r_{12};M)$	Std. Dev.	$\frac{1}{\lambda^3} g_e(r_{12};M)$	Std. Dev.	$W_2(r_{12})$
0.6	0.30204	0.05718	-0.10363	0.05672	0.00000
0.7	0.43065	0.05918			0.00001
0.8	0.22653	0.05944	-0.11826	0.04663	0.00845
0.9	0.20432	0.05659			0.11992
1.0	0.21626	0.05623	+0.02633	0.03522	0.43502
1.1	+0.00022	0.05535			0.84777
1.2	-0.09561	0.05339	0.11547	0.03143	1.17350
1.3	-0.13564	0.05041	0.00588	0.03157	1.33885
1.4	-0.26533	0.04638	0.02020	0.03433	1.38106
1.5	-0.31497	0.04414	0.03717	0.03018	1.34965
1.6	-0.43696	0.03915	0.00436	0.03249	1.28194
1.7	-0.43063	0.03585	+0.03937	0.06796	1.21369
1.8	-0.48012	0.03213	-0.12736	0.03236	1.15856
1.9	-0.45266	0.02916			1.11587
2.0	-0.41747	0.02496	+0.01061	0.03334	1.08438
2.1	-0.25859	0.02162			1.06163
2.2	-0.18780	0.01845	+0.04063	0.03334	1.04551
2.3	-0.09946	0.01625	-0.01458	0.03264	1.03408
2.4	+0.00139	0.01320	+0.02194	0.03164	1.02588
2.5	0.07724	0.01100	+0.05166	0.03082	1.01991
2.6	0.10874	0.00953	-0.03222	0.03318	1.01550
2.7	0.14166	0.00755	+0.00224	0.03226	1.01220
2.8	0.13137	0.00595	+0.00217	0.03217	1.00970
2.9	0.14632	0.00471			1.00778
3.0	0.11885	0.00367	-0.00508	0.03348	1.00629
3.2	0.08919	0.00214			1.00420
3.4	0.06674	0.00149			1.00289
3.6	0.04890	0.00099			1.00203
3.8	0.03304	0.00072			1.00145
4.0	0.02155	0.00047			1.00106

Table 1.3. NUMERICAL VALUES OF $\lambda^{-3}g_c(r_{12};20,000)$, $\lambda^{-3}g_e(r_{12};20,000)$, AND $W_2(r_{12})$ FOR T = 20°K.

$\frac{r_{12}}{\sigma}$	$\frac{1}{\lambda^3} g_c(r_{12};M)$	Std. Dev.	$\frac{1}{\lambda^3} g_e(r_{12};M)$	Std. Dev.	$W_2(r_{12})$
0.6	1.7702	0.08450	-0.62796	0.07301	0.00000
0.7	1.5075	0.08448	-0.21953	0.05161	0.00000
0.8	1.4115	0.08353	-0.11030	0.04157	0.00827
0.9	1.1673	0.08096	-0.08044	0.03704	0.14649
1.0	0.78071	0.07988	+0.02763	0.03097	0.52629
1.1	0.53478	0.07558	0.02948	0.03080	0.94670
1.2	+0.21673	0.07107	0.08262	0.02909	1.19770
1.3	-0.01346	0.06457	0.03672	0.03007	1.26763
1.4	-0.31430	0.05738	0.01662	0.03105	1.24238
1.5	-0.48981	0.05180	+0.03585	0.02992	1.18817
1.6	-0.76050	0.04506	-0.02124	0.03089	1.13647
1.7	-0.85461	0.03851	+0.05727	0.02978	1.09690
1.8	-0.90454	0.03174	-0.02649	0.03009	1.06884
1.9	-0.84328	0.02588	-0.02634	0.03156	1.04937
2.0	-0.72240	0.02248	-0.03736	0.03103	1.03591
2.1	-0.58432	0.01759	-0.06747	0.03031	1.02652
2.2	-0.38289	0.01473	-0.01376	0.03141	1.01986
2.3	-0.23783	0.01188	-0.01845	0.02985	1.01508
2.4	-0.08979	0.00993	-0.01048	0.03039	1.01159
2.5	-0.01504	0.00764	+0.01846	0.03114	1.00901
2.6	+0.03631	0.00593	-0.04298	0.03033	1.00708
2.7	0.06169	0.00461	-0.01156	0.02973	1.00561
2.8	0.06026	0.00369	+0.03174	0.02972	1.00449
2.9	0.05736	0.00298	+0.02549	0.03214	1.00362
3.0	0.05746	0.00232	-0.00994	0.03077	1.00294
3.2	0.04262	0.00149			1.00199
3.4	0.03200	0.00101			1.00137
3.6	0.02172	0.00069			1.00097
3.8	0.01541	0.00051			1.00070
4.0	0.01030	0.00038			1.00051

Table I.4. NUMERICAL VALUES OF $\lambda^{-3}g_c(r_{12};20,000)$, $\lambda^{-3}g_e(r_{12};20,000)$, AND $W_2(r_{12})$ FOR T = 30°K.

$\frac{r_{12}}{\sigma}$	$\frac{1}{\lambda^3}g_c(r_{12};M)$	Std. Dev.	$\frac{1}{\lambda^3}g_e(r_{12};M)$	Std. Dev.	$W_2(r_{12})$
0.6	3.7089	0.12325	-0.55485	0.07420	0.00000
0.7	3.1127	0.11960	-0.33827	0.05606	0.00001
0.8	2.9934	0.11860	-0.06397	0.04174	0.01251
0.9	2.6277	0.11824	-0.08559	0.03514	0.17920
1.0	2.0920	0.11073	-0.01259	0.03071	0.58907
1.1	1.6787	0.10490	+0.00403	0.03031	0.98567
1.2	1.0346	0.09486	-0.01300	0.03004	1.18254
1.3	+0.50982	0.08690	+0.06148	0.03104	1.21059
1.4	-0.12908	0.07376	0.01243	0.03083	1.17199
1.5	-0.62747	0.06234	0.01058	0.03122	1.12496
1.6	-1.0382	0.05072	+0.03607	0.03135	1.08763
1.7	-1.1272	0.04181	-0.01810	0.02952	1.06141
1.8	-1.2507	0.03376	-0.03943	0.03061	1.04354
1.9	-1.1691	0.02662	-0.00269	0.03143	1.03135
2.0	-0.96546	0.02114	+0.06968	0.03079	1.02292
2.1	-0.71601	0.01693	0.03424	0.03105	1.01701
2.2	-0.46636	0.01305	+0.00379	0.03116	1.01280
2.3	-0.28688	0.01032	-0.00871	0.03214	1.00976
2.4	-0.15784	0.00818	-0.00372	0.03316	1.00752
2.5	-0.07918	0.00650	-0.00138	0.03094	1.00586
2.6	-0.03204	0.00505	+0.02841	0.03255	1.00462
2.7	+0.01384	0.00396	-0.03363	0.03069	1.00367
2.8	0.01602	0.00310	+0.03446	0.03112	1.00294
2.9	0.02666	0.00248	-0.01367	0.03129	1.00238
3.0	0.01990	0.00198	-0.03350	0.03093	1.00193
3.2	0.01861	0.00131			1.00131
3.4	0.01426	0.00089			1.00090
3.6	0.00919	0.00064			1.00064
3.8	0.00681	0.00048			1.00046
4.0	0.00479	0.00037			1.00034

Table 1.5. NUMERICAL VALUES OF $\lambda^{-3}g_c(r_{12};20,000)$, $\lambda^{-3}g_e(r_{12};20,000)$, AND $W_2(r_{12})$ FOR T = 40°K.

$\frac{r_{12}}{\sigma}$	$\frac{1}{\lambda^3} g_c(r_{12};M)$	Std. Dev.	$\frac{1}{\lambda^3} g_e(r_{12};M)$	Std. Dev.	$W_2(r_{12})$
0.6	6.5168	0.16779	-1.34129	0.09346	0.00000
0.7	5.8136	0.16632	-0.30960	0.05813	0.00002
0.8	5.2420	0.16122	-0.12666	0.04290	0.01505
0.9	4.6279	0.15673	-0.06758	0.03598	0.21818
1.0	3.7103	0.14460	+0.05650	0.03208	0.66868
1.1	2.8058	0.13353	0.05465	0.03152	1.03258
1.2	2.0697	0.12226	0.03208	0.03006	1.16868
1.3	1.1047	0.10556	+0.02770	0.03180	1.16784
1.4	+0.10555	0.08817	-0.02226	0.03205	1.12805
1.5	-0.51087	0.07306	-0.00293	0.03048	1.09045
1.6	-1.0742	0.05946	-0.05644	0.03306	1.06301
1.7	-1.3525	0.04512	+0.03024	0.03016	1.04421
1.8	-1.4343	0.03477	0.01522	0.03201	1.03146
1.9	-1.3756	0.02575	0.01866	0.03218	1.02273
2.0	-1.1223	0.02022	0.00651	0.03113	1.01667
2.1	-0.81214	0.01576	0.03297	0.03173	1.01241
2.2	-0.56541	0.01234	0.02112	0.03182	1.00936
2.3	-0.34673	0.00976	+0.00832	0.03198	1.00715
2.4	-0.20666	0.00754	-0.03604	0.03083	1.00552
2.5	-0.12062	0.00592	+0.00146	0.03188	1.00431
2.6	-0.06254	0.00459	-0.04644	0.03171	1.00340
2.7	-0.03496	0.00363	+0.04956	0.03278	1.00270
2.8	-0.01160	0.00289	0.00766	0.03141	1.00217
2.9	-0.00110	0.00231	+0.02028	0.03253	1.00176
3.0	-0.00212	0.00189	-0.06352	0.03143	1.00143
3.2	+0.00275	0.00127			1.00097
3.4	0.00410	0.00087			1.00067
3.6	0.00224	0.00065			1.00048
3.8	0.00191	0.00048			1.00034
4.0	0.00125	0.00038			1.00025

Table 1.6. NUMERICAL VALUES OF $\lambda^{-3} g_c(r_{12};20,000)$, $\lambda^{-3} g_e(r_{12};20,000)$, AND $W_2(r_{12})$ FOR T = 50°K.

$\frac{r_{12}}{\sigma}$	$\frac{1}{\lambda^3} g_c(r_{12};M)$	Std. Dev.	$\frac{1}{\lambda^3} g_e(r_{12};M)$	Std. Dev.	$W_2(r_{12})$
0.6	9.5664	0.21727	-0.83890	0.08907	0.00000
0.7	8.7736	0.21338	-0.41851	0.06036	0.00001
0.8	7.3618	0.20678	-0.22029	0.04423	0.01763
0.9	6.6846	0.19733	-0.02030	0.03489	0.24798
1.0	5.5319	0.18309	+0.02428	0.03138	0.71891
1.1	4.4098	0.16844	0.01908	0.03063	1.05350
1.2	2.8499	0.14929	0.02397	0.03038	1.15232
1.3	1.5876	0.12432	0.00415	0.03142	1.13778
1.4	+0.33265	0.10413	+0.04323	0.03178	1.10136
1.5	-0.48695	0.08494	-0.00670	0.03169	1.07088
1.6	-1.1023	0.06671	+0.01203	0.03228	1.04933
1.7	-1.6007	0.04780	-0.03959	0.03172	1.03467
1.8	-1.6056	0.03575	+0.03151	0.03119	1.02472
1.9	-1.5481	0.02594	0.00077	0.03222	1.01789
2.0	-1.2836	0.01960	+0.02970	0.03230	1.01315
2.1	-0.91036	0.01526	-0.01185	0.03153	1.00980
2.2	-0.60499	0.01184	-0.00923	0.03129	1.00740
2.3	-0.40800	0.00940	-0.05462	0.03129	1.00566
2.4	-0.24114	0.00717	+0.02053	0.03092	1.00438
2.5	-0.14169	0.00561	+0.00280	0.03235	1.00342
2.6	-0.09400	0.00442	-0.00663	0.03239	1.00270
2.7	-0.05507	0.00350	-0.01496	0.03231	1.00215
2.8	-0.03636	0.00276	+0.03584	0.03251	1.00172
2.9	-0.02176	0.00221	+0.03949	0.03107	1.00140
3.0	-0.01912	0.00182	-0.06284	0.03284	1.00114
3.2	-0.00742	0.00124			1.00077
3.4	-0.00353	0.00088			1.00053
3.6	-0.00189	0.00065			1.00038
3.8	-0.00182	0.00050			1.00027
4.0	-0.00144	0.00039			1.00020

Table 1.7. NUMERICAL VALUES OF $\lambda^{-3}g_c(r_{12};20,000)$, $\lambda^{-3}g_e(r_{12};20,000)$, AND $W_2(r_{12})$ FOR T = 75°K.

$\frac{r_{12}}{\sigma}$	$\frac{1}{\lambda^3} g_c(r_{12};M)$	Std. Dev.	$\frac{1}{\lambda^3} g_e(r_{12};M)$	Std. Dev.	$W_2(r_{12})$
0.6					0.00000
0.7	17.099	0.35252	-0.57189	0.06499	0.00005
0.8	14.592	0.33201	-0.08237	0.04288	0.03028
0.9	13.849	0.32565	-0.03102	0.03544	0.34036
1.0	9.9851	0.28127	+0.01446	0.03462	0.82732
1.1	8.1720	0.25669	+0.07193	0.03240	1.07206
1.2	5.6260	0.22191	-0.02478	0.03356	1.11255
1.3	3.4497	0.18889	-0.05651	0.03344	1.09178
1.4	+1.3873	0.14718	+0.02364	0.03500	1.06573
1.5	-0.29434	0.11083	0.05378	0.03440	1.04574
1.6	-1.2900	0.08048	+0.04425	0.03376	1.03187
1.7	-1.9094	0.05446	-0.01024	0.03336	1.02246
1.8	-2.0339	0.03728	-0.01130	0.03456	1.01606
1.9	-1.8976	0.02542	+0.04435	0.03305	1.01166
2.0	-1.5165	0.01976	-0.00107	0.03400	1.00858
2.1	-1.0853	0.01530	+0.04414	0.03454	1.00641
2.2	-0.71191	0.01158	-0.00974	0.03395	1.00485
2.3	-0.48689	0.00897	+0.00430	0.03431	1.00371
2.4	-0.33031	0.00688	0.00171	0.03486	1.00288
2.5	-0.22195	0.00540	0.02422	0.03323	1.00225
2.6	-0.15578	0.00422	+0.01697	0.03309	1.00178
2.7	-0.11421	0.00340	-0.00746	0.03451	1.00142
2.8	-0.07068	0.00268	-0.00444	0.03284	1.00114
2.9	-0.05547	0.00218	-0.04366	0.03403	1.00092
3.0	-0.04714	0.00182	-0.05734	0.03413	1.00075
3.2	-0.02699	0.00124			1.00051
3.4	-0.01723	0.00089			1.00035
3.6	-0.01146	0.00069			1.00025
3.8	-0.00782	0.00051			1.00018
4.0	-0.00605	0.00041			1.00013

Table 1.8. NUMERICAL VALUES OF $\lambda^{-3} g_c(r_{12};20,000)$, $\lambda^{-3} g_e(r_{12};20,000)$, AND $W_2(r_{12})$ FOR T = 100°K.

$\frac{r_{12}}{\sigma}$	$\frac{1}{\lambda^3} g_c(r_{12};M)$	Std. Dev.	$\frac{1}{\lambda^3} g_e(r_{12};M)$	Std. Dev.	$W_2(r_{12})$
0.6	28.866	0.52539	-1.42417	0.11788	0.00000
0.7	26.301	0.50866	-0.78737	0.06773	0.00005
0.8	23.154	0.47882	-0.18906	0.04141	0.04034
0.9	20.788	0.45434	-0.01739	0.03523	0.40579
1.0	16.211	0.39965	+0.04359	0.03273	0.87784
1.1	12.226	0.35103	+0.00389	0.03494	1.06646
1.2	8.7524	0.30203	-0.02168	0.03340	1.08760
1.3	4.9980	0.23690	+0.05336	0.03437	1.06906
1.4	2.5440	0.19197	+0.01317	0.03412	1.04907
1.5	+0.15175	0.14091	-0.03295	0.03369	1.03411
1.6	-1.2950	0.09839	-0.02260	0.03360	1.02378
1.7	-2.2048	0.05886	-0.07566	0.03561	1.01678
1.8	-2.4492	0.03686	+0.06214	0.03393	1.01201
1.9	-2.1632	0.02597	-0.01889	0.03417	1.00872
2.0	-1.6750	0.02022	-0.01509	0.03374	1.00643
2.1	-1.1995	0.01549	-0.06320	0.03469	1.00480
2.2	-0.80334	0.01158	-0.06583	0.03448	1.00364
2.3	-0.57866	0.00898	+0.02067	0.03428	1.00278
2.4	-0.40427	0.00698	-0.00948	0.03366	1.00216
2.5	-0.27668	0.00539	+0.01531	0.03375	1.00169
2.6	-0.19290	0.00426	-0.00674	0.03428	1.00133
2.7	-0.14304	0.00341	-0.02822	0.03388	1.00106
2.8	-0.10312	0.00272	-0.00883	0.03550	1.00085
2.9	-0.08112	0.00223	-0.03814	0.03436	1.00069
3.0	-0.06210	0.00182	+0.03840	0.03423	1.00056
3.2	-0.04163	0.00128			1.00038
3.4	-0.02636	0.00092			1.00026
3.6	-0.01764	0.00069			1.00019
3.8	-0.01212	0.00054			1.00014
4.0	-0.00962	0.00043			1.00010

Table 1.9. NUMERICAL VALUES OF $\lambda^{-3}g_c(r_{12};20,000)$, $\lambda^{-3}g_e(r_{12};20,000)$, AND $W_2(r_{12})$ FOR T = 273.18°K.

$\frac{r_{12}}{\sigma}$	$\frac{1}{\lambda^3} g_c(r_{12};M)$	Std. Dev.	$\frac{1}{\lambda^3} g_e(r_{12};M)$	Std. Dev.	$W_2(r_{12})$
0.6	125.44	2.0011	-1.81087	0.11496	0.00000
0.7	115.17	1.9319	-0.58497	0.06149	0.00119
0.8	96.324	1.7268	-0.04505	0.04281	0.18533
0.9	81.748	1.5693	-0.04151	0.03984	0.72582
1.0	61.584	1.3248	-0.03488	0.04038	0.98181
1.1	45.317	1.0947	-0.04590	0.04040	1.03326
1.2	31.259	0.89040	+0.01854	0.04181	1.03307
1.3	19.126	0.66217	+0.06585	0.04014	1.02481
1.4	9.6566	0.47061	-0.02573	0.04132	1.01745
1.5	+2.3783	0.28913	+0.07952	0.04200	1.01213
1.6	-2.0686	0.14422	+0.02492	0.03909	1.00848
1.7	-3.8415	0.07019	-0.04085	0.04049	1.00600
1.8	-3.7872	0.04234	+0.00200	0.04228	1.00430
1.9	-3.1047	0.03182	-0.02403	0.04070	1.00313
2.0	-2.2944	0.02359	+0.00917	0.04094	1.00231
2.1	-1.6418	0.01739	+0.03585	0.04239	1.00173
2.2	-1.1848	0.01324	-0.00987	0.04263	1.00131
2.3	-0.84689	0.01005	+0.11174	0.04141	1.00101
2.4	-0.60708	0.00770	-0.00914	0.03990	1.00078
2.5	-0.45287	0.00605	+0.01644	0.04090	1.00061
2.6	-0.35206	0.00483	0.05927	0.04145	1.00048
2.7	-0.26398	0.00389	0.00352	0.04258	1.00038
2.8	-0.20450	0.00315	+0.00066	0.04304	1.00031
2.9	-0.15736	0.00256	-0.02901	0.04089	1.00025
3.0	-0.12176	0.00213	+0.01181	0.04266	1.00020
3.2	-0.08107	0.00153			1.00014
3.4	-0.05550	0.00113			1.00010
3.6	-0.03776	0.00085			1.00007
3.8	-0.02727	0.00068			1.00005
4.0	-0.02110	0.00056			1.00004

Table 2. NUMERICAL VALUES OF THE THIRD VIRIAL COEFFICIENT C(T) AND THE CLUSTER INTEGRAL b_2.

$T(^{o}K)$	$C\left(\frac{cm^6}{mole^2}\right)$	$b_2(cm^3)$
10	515	1.68
20	286	+.55
30	226	-1.50
40	195	-4.15
50	178	-7.27
75	162	-16.62
100	150	-27.58
273.18	107	-130.87

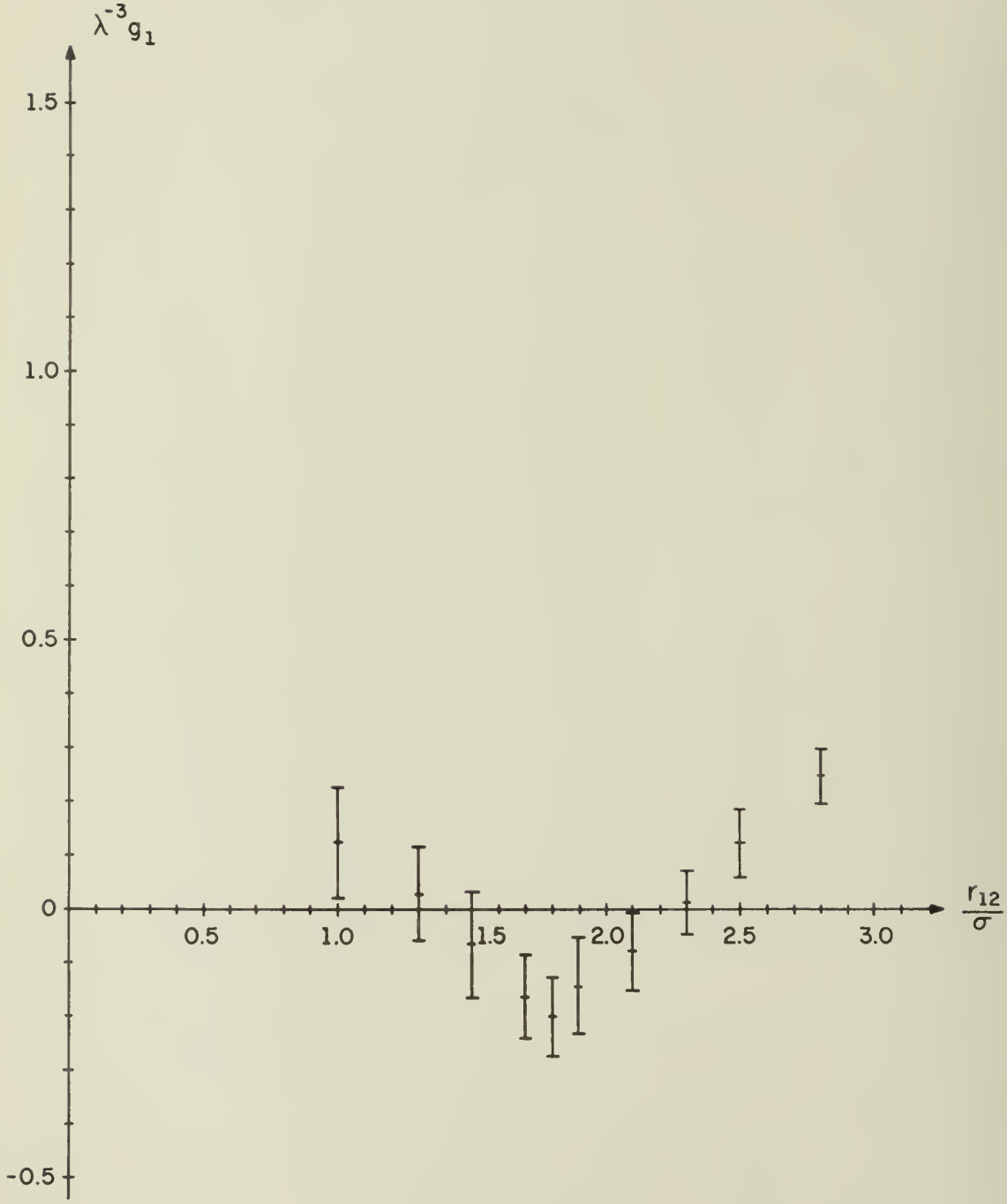

FIGURE 17. $\lambda^{-3} g_1$ AND SAMPLING ERROR FOR T=5°K.

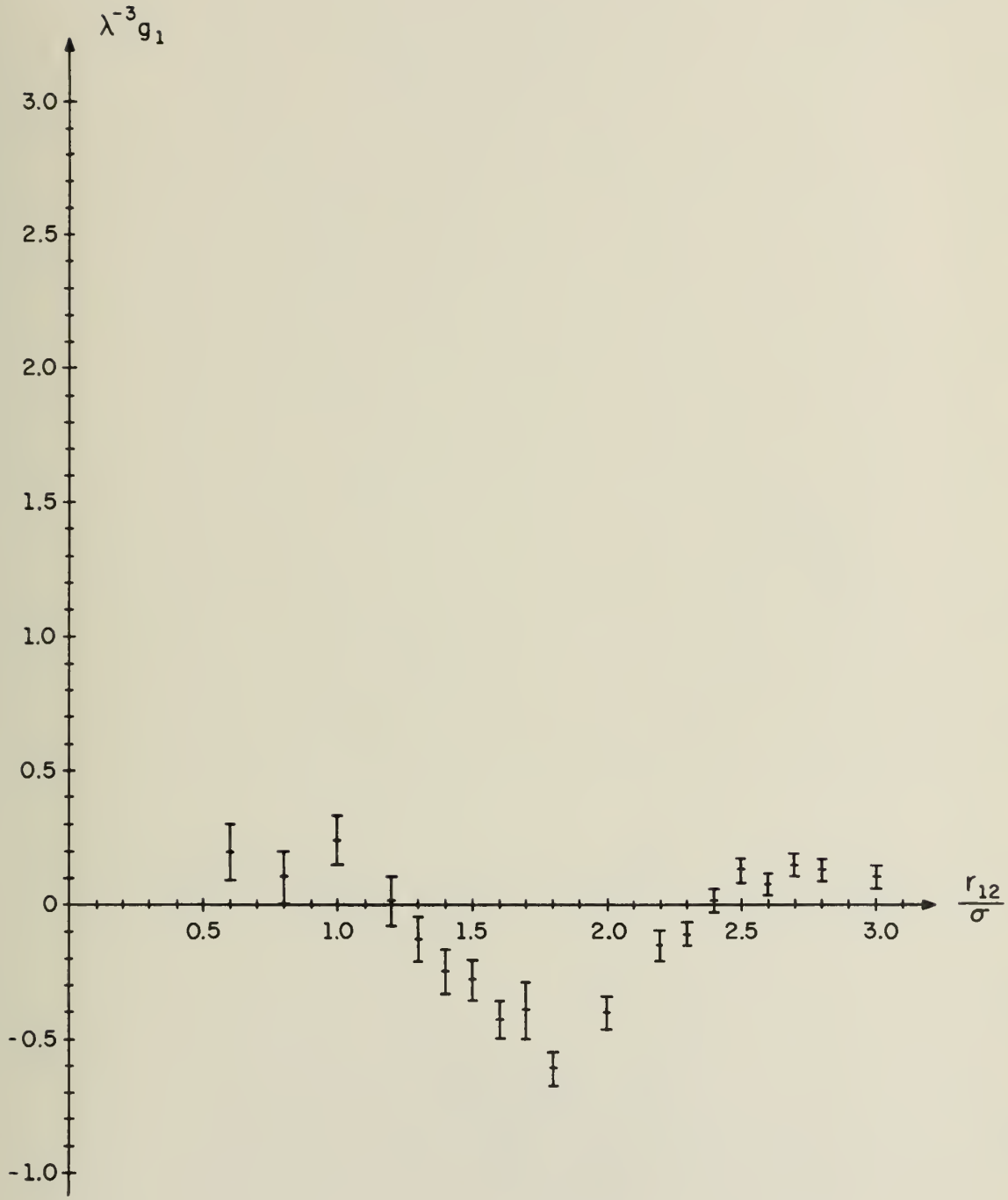

FIGURE 18. $\lambda^{-3}g_1$ AND SAMPLING ERROR FOR T=10°K.

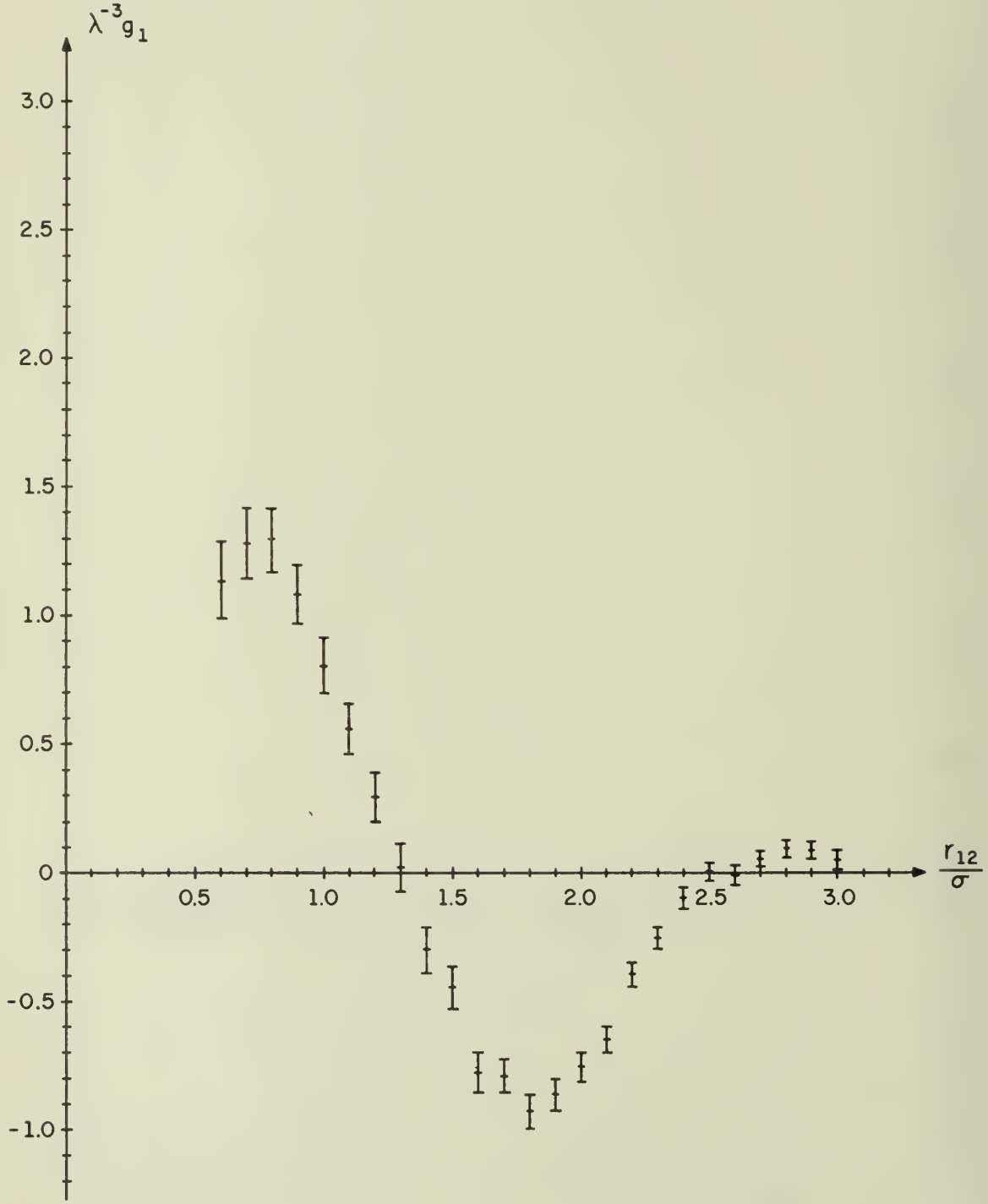

FIGURE 19. $\lambda^{-3}g_1$ AND SAMPLING ERROR FOR T=20°K.

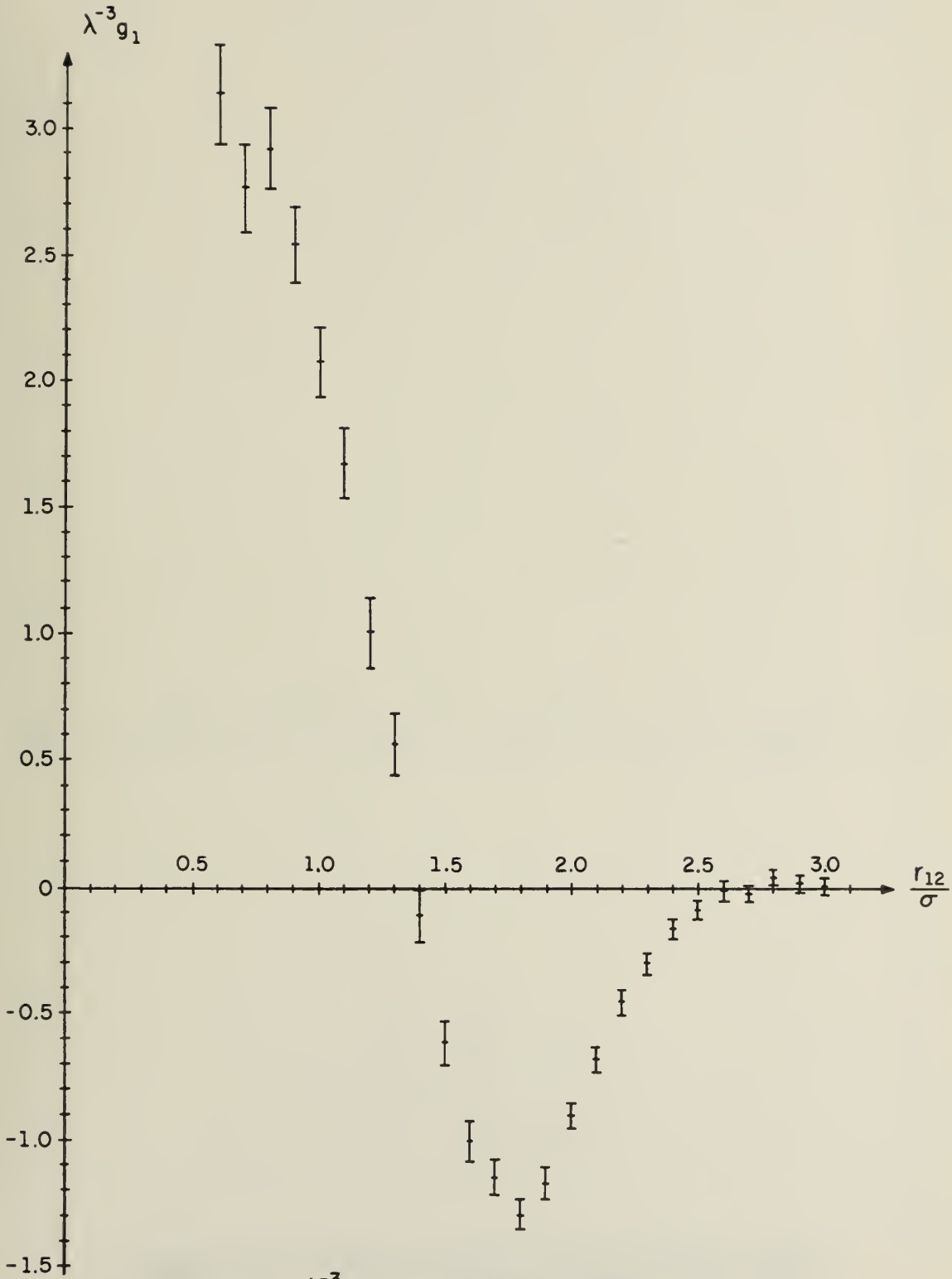

FIGURE 20. $\lambda^{-3}g_1$ AND SAMPLING ERROR FOR T=30°K.

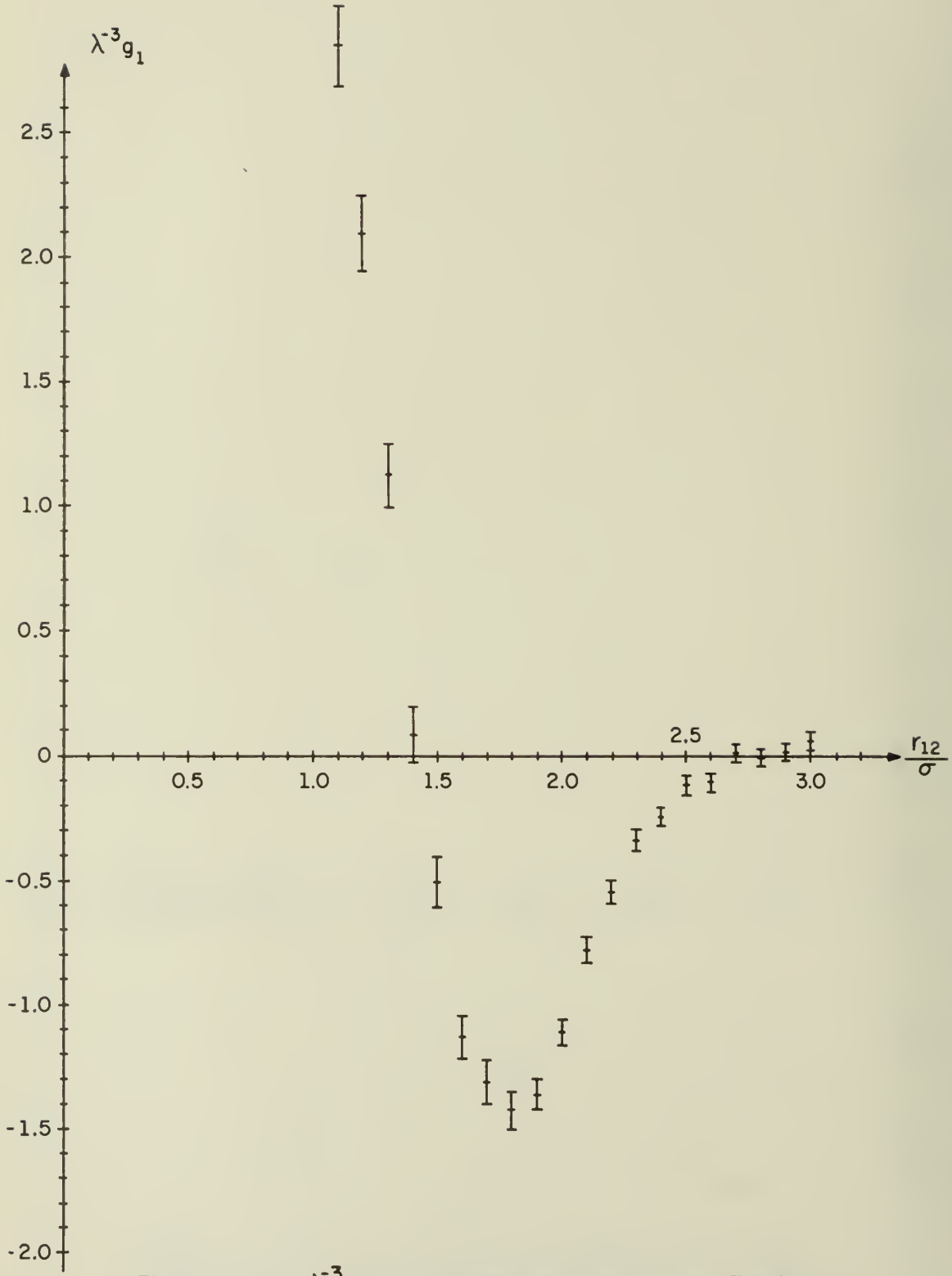

FIGURE 21. $\lambda^{-3}g_1$ AND SAMPLING ERROR FOR T=40°K.

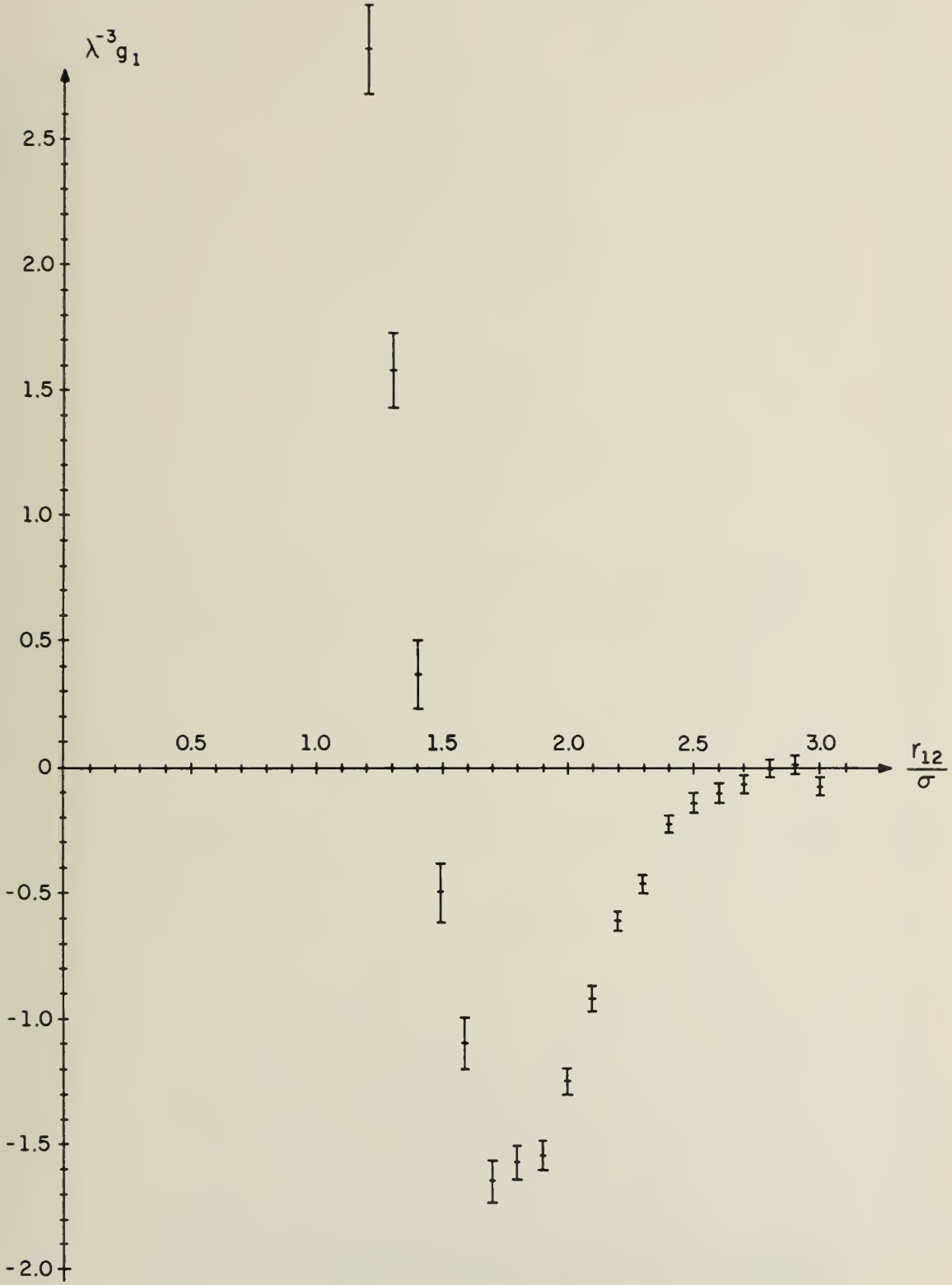

FIGURE 22. $\lambda^{-3}g_1$ AND SAMPLING ERROR FOR T=50°K.

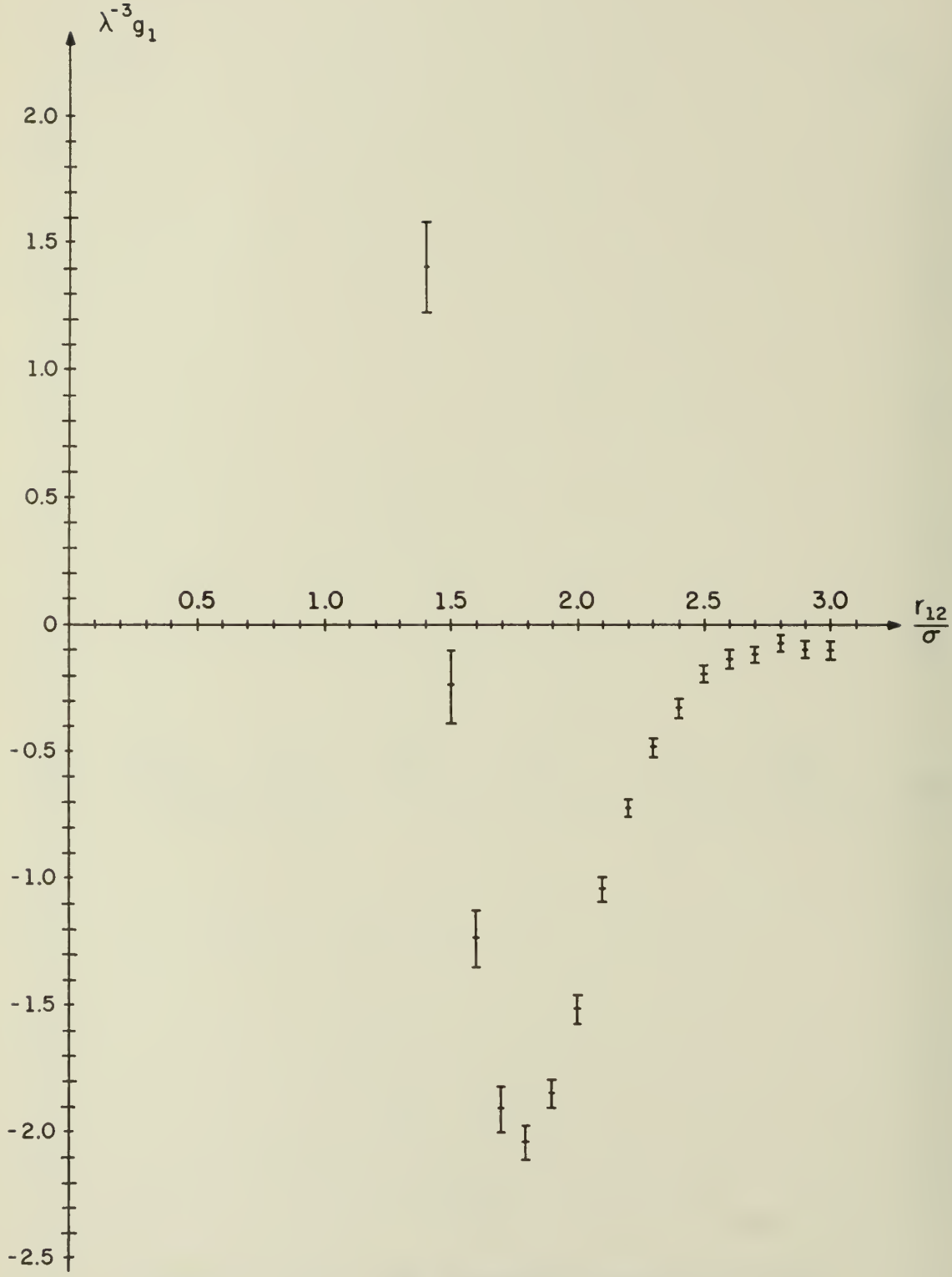

FIGURE 23. $\lambda^{-3}g_1$ AND SAMPLING ERROR FOR T=75°K

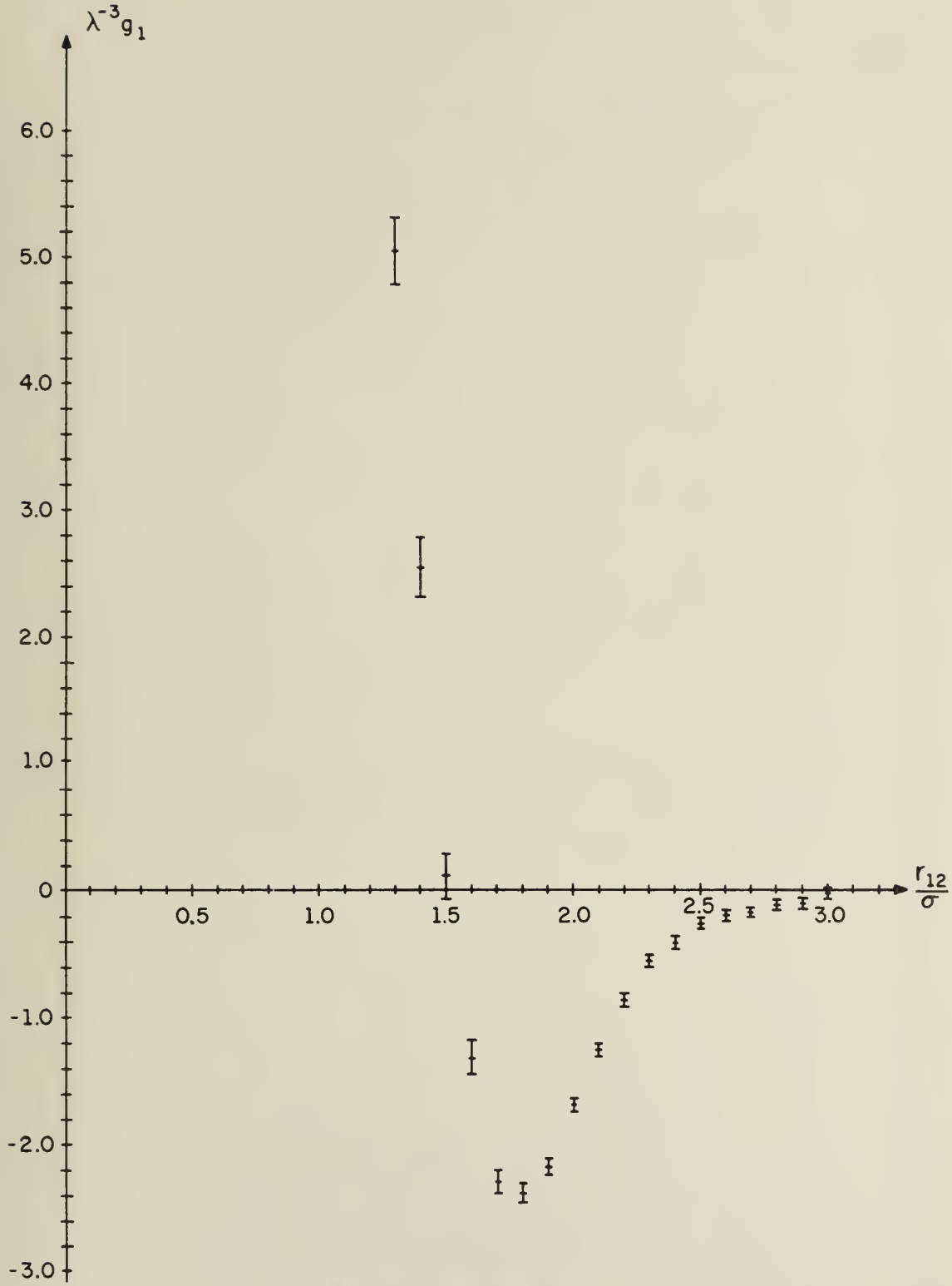

FIGURE 24. $\lambda^{-3}g_1$ AND SAMPLING ERROR FOR T=100°K

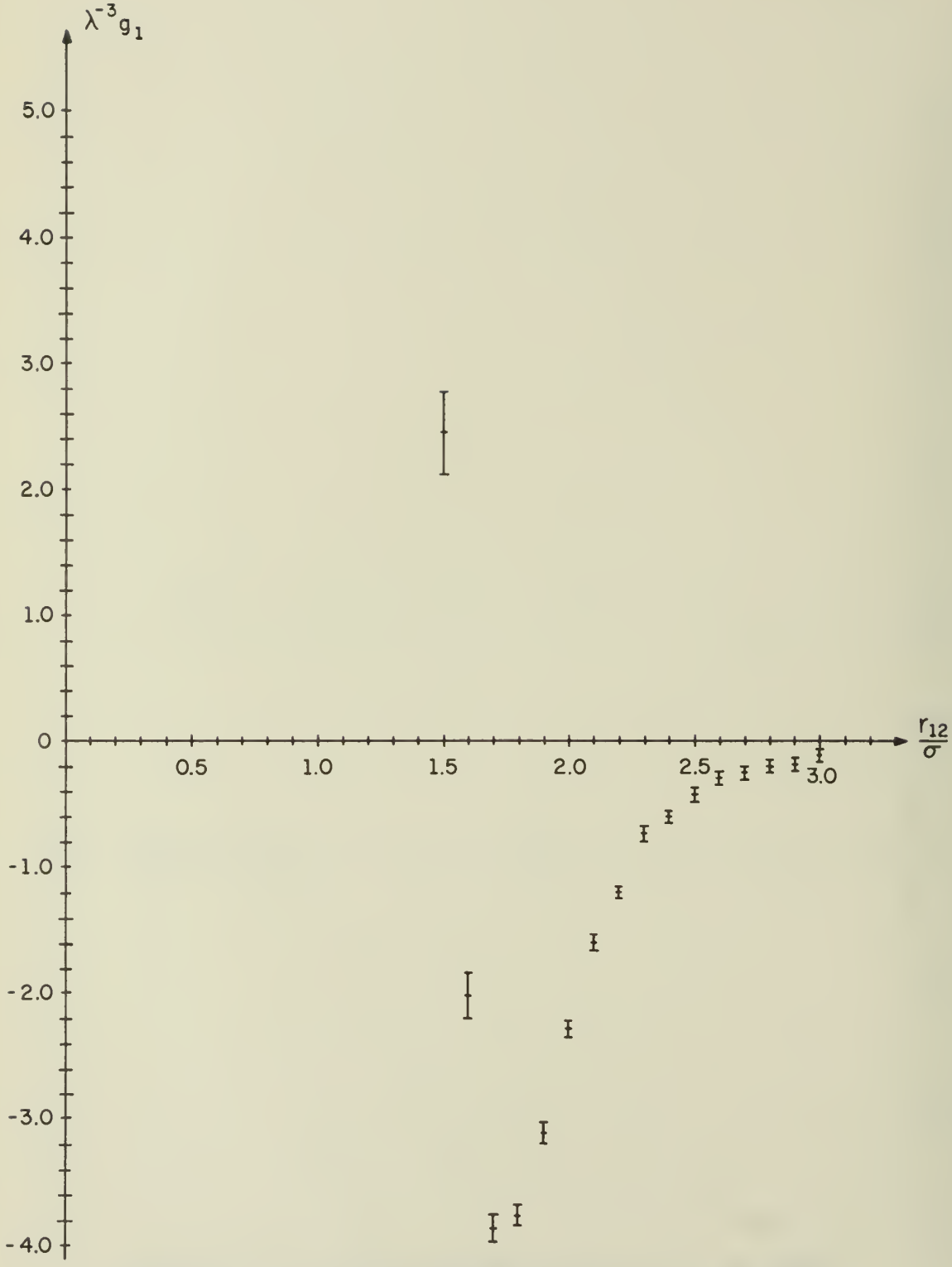

FIGURE 25. $\lambda^{-3}g_1$ AND SAMPLING ERROR FOR T=273.18°K

VITA

Harry Frederick Jordan was born in Takoma Park, Maryland on March 6, 1940. He received the B.A. degree in physics and mathematics Cum Laude from Rice University in 1961 and the M.S. degree in physics from the University of Illinois in 1963. During the period June 1962 through August 1966, he was a research assistant in the Department of Computer Science at the University of Illinois with the exception of the summer of 1964 during which he served as a research assistant at the Los Alamos Scientific Laboratory of the University of California. He is currently an assistant professor of electrical engineering at the University of Colorado. Mr. Jordan is a member of Sigma Xi, the American Physical Society, and the Association for Computing Machinery.

AUG 16 1968

UNIVERSITY OF ILLINOIS-URBANA
3 0112 004249840